JUSTUS-LIEBIG-
UNIVERSITÄT
GIESSEN

Tho1 is necessary for recruitment of transcription elongation factors and nuclear mRNP assembly

Dissertation zur Erlangung des Doktorgrades
am Fachbereich 08 für Biologie und Chemie
der Justus-Liebig-Universität Gießen

Birte Keil

2021

Die vorliegende Arbeit am Institut für Biochemie (Fachbereich 08) der Justus-Liebig-Universität Gießen, unter Leitung von Prof. Dr. Katja Sträßer, erstellt.

Dissertation eingereicht am: 12.10.2021

Erstgutachter: Prof. Dr. Katja Sträßer
Fachbereich 08: Biologie und Chemie
Institut für Biochemie
Justus-Liebig-Universität Gießen

Zweitgutachter: Prof. Dr. Albrecht Bindereif
Fachbereich 08: Biologie und Chemie
Institut für Biochemie
Justus-Liebig-Universität Gießen

List of content

1 Zusammenfassung

Die Bildung von Boten-Ribonukleinsäurepartikeln (*messenger ribonucleoprotein particles*; mRNPs) ist ein essentieller Schritt in der Genexpression. Bereits während der Transkription werden RNA-Bindungsproteine (RBP) zur pre-mRNA rekrutiert und bilden zusammen mit der RNA das mRNP. RBPs sind in der Vermittlung aller wichtigen Schritte der mRNA-Prozessierung beteiligt. Außerdem sind sie für die Stabilität, den mRNA-Export und die Translation notwendig. Der TREX-Komplex besteht insgesamt aus neun Untereinheiten: Der fünfteilige THO-Komplex (Tho2, Hpr1, Mft1, Thp1 und Tex1), den SR-ähnlichen Proteinen Gbp2 und Hrb1, der RNA Helikase Sub2 und das Export-Adapterprotein Yra1. Das nukleäre mRNA-Bindeprotein Tho1 wurde entdeckt, da es mittels Überexpression die Phänotypen der THO-Komplex-Mutanten unterdrücken kann. Tho1 bindet mRNA und wird zum transkribierten Gen mittels mRNA und dem THO-Komplex rekrutiert. Das menschliche Ortholog CIP29 lässt sich in Gegenwart von ATP über TREX aufreinigen. Trotz all dieser Informationen ist die Rolle von Tho1 in der mRNP-Bildung noch größtenteils unbekannt und es konnte noch kein Phänotyp für Δ*tho1* in *S. cerevisiae* detektiert werden. In einer früheren Studie konnte gezeigt werden, dass die Phosphorylierung der C-terminalen Region (CTR) von Spt5 eine entscheidende Rolle bei der Rekrutierung von Tho1, Hpr1 und Paf1 spielt. Paf1 ist eine Untereinheit des PAF-Komplexes und übernimmt Aufgaben in der Elongation der Transkription. Die Rekrutierung von Tho1 in CTR-Mutanten ähnelt eher Paf1 und ist gegensätzlich zu Hpr1 (Meinel, 2013).

In der vorliegenden Arbeit war ich am Zusammenspiel zwischen Tho1, Hpr1 und Paf1 interessiert. Zunächst wurde eine Wachstumsuntersuchung durchgeführt bei der sowohl Einzel- als auch Doppelmutanten betrachtet wurden. Δ*tho1* supprimiert den kältesensitiven Wachstumsphänotyp von Δ*hpr1* und Δ*paf1.* Durch Chromatin-Immunpräzipitations- (ChIP) Experimente konnte gezeigt werden, dass Tho1 auf negative Weise die Rekrutierung von Hpr1 an das transkribierte Gen beeinflusst. Zur gleichen Zeit hat es eine positive Wirkung auf die Rekrutierung von Paf1. Des Weiteren konnte gezeigt werden, dass sich Tho1 RNA-unabhängig sowohl mit dem TREX/THO-Komplex als auch dem PAF-Komplex aufreinigen lässt. Zusätzlich konnte nachgewiesen werden, dass bei fehlendem Hpr1 mehr Paf1 mit Tho1 aufgereinigt wird. Für die korrekte Bildung des nukleären mRNPs spielt Tho1 eine Rolle, da gezeigt werden konnte, dass sich die Zusammensetzung des mRNPs ändert, sobald sich das Level an Tho1 ändert. Ein mRNA-Export-Defekt konnte weder in der Überexpression noch der Deletionsmutante von Tho1 festgestellt werden.

Zusammenfassend konnte gezeigt werden, dass Tho1 den Elongationsfaktor Paf1 rekrutiert und die Anwesenheit von Hpr1 am transkribierten Gen reguliert. Außerdem führt eine Änderung des intrazellulären Tho1 Levels zu einer veränderten mRNP Bildung.

2 Summary

The formation of messenger ribonucleoprotein particles (mRNPs) is an essential step in gene expression. Already during transcription, RNA-binding proteins (RBPs) are recruited to the emerging mRNA; together they form the mRNP. RBPs orchestrate all important steps in the processing of mRNA. Additionally, they are necessary for mRNA stability, nuclear export and translation. The heterononameric TREX complex couples **tr**anscription to mRNA **ex**port. It consists of the pentameric THO sub-complex (Tho2, Hpr1, Mft1, Thp1 and Tex1), the SR-like proteins Gbp2 and Hrb1, the RNA helicase Sub2 and the export adaptor protein Yra1. The nuclear mRNA-binding protein Tho1 was identified based on its ability to supress the phenotype of THO mutants when overexpressed. Tho1 can bind RNA and its recruitment to the transcribed gene depends on the mRNA and the THO complex. The human orthologue of Tho1, CIP29, co-purifies with the TREX complex in the presence of ATP. The role of Tho1 in mRNP formation is still mainly unknown and a Δ*tho1* strain has no known phenotype in *S. cerevisiae*. In a previous study, it could be shown that the phosphorylation of the C-terminal region (CTR) of Spt5 is important for the recruitment of Hpr1, Tho1 and Paf1. Paf1 is part of the PAF complex and functions in transcription elongation. The recruitment of Paf1 depends on the correct phosphorylation of the CTR. In CTR phosphorylation mutants, the recruitment of Tho1 resembles that of Paf1 and is anticorrelated with Hpr1 recruitment (Meinel, 2013).

In this study, I was interested in the interplay between Tho1, Hpr1 and Paf1. First, growth assays with single and double mutants were performed. Δ*tho1* suppresses the cold-sensitive growth defect of Δ*hpr1* and Δ*paf1.* ChIP experiments showed that Tho1 regulates the recruitment of TREX to the transcribed gene in a negative manner. In contrast, Tho1 influences the recruitment of the PAF complex positively. Furthermore, we could show that Tho1 co-purifies with both the TREX/THO complex and the PAF-complex. Additionally, the deletion of *hpr1* enhances the co-purification of Paf1 with Tho1. Tho1 is necessary for the correct assembly of nuclear mRNPs; changes in the level of Tho1 lead to changes in mRNP composition. No mRNA export defect was observed in cells where Tho1 was overexpressed or deleted.

In sum, Tho1 is relevant for the recruitment of the elongation factor Paf1 and regulates the occupancy of Hpr1 at the transcribed gene. Moreover, changed intracellular Tho1 level leads to an altered mRNP assembly.

3 Introduction

3.1 Gene expression

Gene expression is an essential process in all living cells. The information of the DNA is transcribed into mRNA by RNA polymerase II (RNAPII) and translated into proteins at the ribosomes. While the DNA is located in the nucleus, the translation of the mRNA into proteins takes place in the cytoplasm of eukaryotic cells. Already during transcription, the synthesized pre-mRNA is bound by RNA-binding proteins (RBPs) and packaged into a messenger ribonucleoprotein particle (mRNP). These proteins orchestrate the processing of the mRNA. Only correctly processed and packaged mRNPs are exported into the cytoplasm through the nuclear pore complexes (Figure 1).

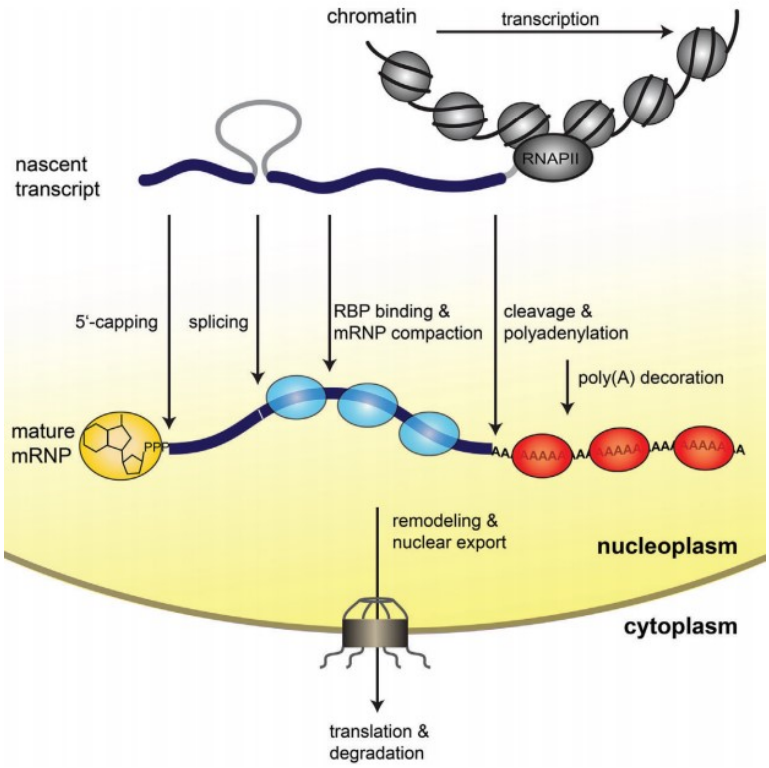

Figure 1: Gene expression. RNAPII transcribes protein-coding genes. The emerging pre-mRNA is immediately bound by RNA-binding proteins (RBPs) and protein complexes, which regulate the processing of the mRNA (5´capping, splicing and 3´ end formation). The composition of the messenger ribonucleoprotein particle (mRNP) changes along the way to an export-competent mRNP that is exported through the nuclear pores into the cytoplasm. In the cytoplasm, the mRNA is translated into proteins and degraded. Blue and red circles represent different RBPs (Meinel and Sträßer, 2015).

3.1.1 Transcription

The first step of gene expression is transcription. Eukaryotic cells have three structurally related RNA polymerases that copy DNA into RNA. RNAPI transcribes the genes coding for 5.8S, 18S and 28S rRNA, while RNAPIII transcribes tRNAs and the 5S rRNA (Dieci *et al.*, 2007; Grummt, 2003; Russell and Zomerdijk, 2005). RNAPII transcribes messenger RNAs (mRNAs), but also microRNAs (miRNA), small nuclear RNAs (snRNAs), and small nucleolar RNAs (snoRNAs) (Davis and Ares, 2006; Faller and Guo, 2008; Guttman *et al.*, 2009; Lykke-Andersen and Jensen, 2007; Wyers *et al.*, 2005). Transcription itself is divided into three major phases: initiation, the elongation and termination.

Initiation is a highly regulated process in which RNAPII first has to find the transcription start site (TSS), open the DNA for transcription, and start RNA synthesis (Hantsche and Cramer, 2016). First, the general transcription factor TFIID (transcription factor II D) recognizes the promotor region, and can be stabilized through TFIIA. TFIIB recognizes the DNA backbone, and TFIID then recruits RNAPII (Buratowski *et al.*, 1989). Next, TFIIE and TFIIH bind to the assembly to form the so-called pre-initiation complex (PIC). PIC architecture seems to be consistent between yeast and humans (Chen *et al.*, 2007; Grünberg *et al.*, 2012; Mühlbacher *et al.*, 2014). Structural approaches show that the position of TFIIE in the complex changes depending on whether the promotor region is open or closed. This indicates that TFIIE is involved either in opening of the DNA or the stabilization of open DNA. TFIIH contains a DNA translocase that functions in promotor opening (Hantsche and Cramer, 2016). The mediator complex is a central co-activator and regulates the initiation of most protein-coding genes by bridging distant activators and RNAPII (Conaway and Conaway, 2011; Kornberg, 2005; Malik and Roeder, 2010).

During elongation, RNAPII selects and binds an RNA nucleoside triphosphate (NTP) that is complementary to the presented template DNA base. Through catalysis of a phosphodiester bond, a nucleotide is added to the growing RNA chain (Cheung and Cramer, 2012; Martinez-Rucobo and Cramer, 2013). Elongation often faces obstacles and is prone to errors. The accuracy of RNAPII is improved through a “proofreading” mechanism (Martinez-Rucobo and Cramer, 2013; Sydow *et al.*, 2009; Wang *et al.*, 2006). A mismatched base pair distorts the active site, causing RNAPII to pause and backtrack to the mismatch. At the proofreading site, the intrinsic endonuclease cleaves the RNA dinucleotide and transcription can resume (Sydow *et al.*, 2009; Zenkin *et al.*, 2006). Transcribing DNA is difficult because DNA is packaged into chromatin. Transcription

elongation factors like Spt4/5, the PAF complex, Elf1 and TFIIS enable RNAPII to read through blocks of elongation (Mayer *et al.*, 2010).

At the end of the transcription cycle, the termination takes place. This step is important to recycle RNAPII and to prevent transcriptional interference with downstream genes (Kuehner *et al.*, 2011; Mischo and Proudfoot, 2013; Proudfoot, 2016). The end is marked when the polymerase reads past the polyadenylation (poly(A)) signal. The nascent RNA is cleaved and a poly(A) tail is added. RNAPII terminates further downstream (Schwalb *et al.*, 2016). For the termination, two different models have been suggested. The allosteric model assumes that the binding of RNA 3´ end processing factors induces structural rearrangements that lead to termination (Logan *et al.*, 1987). In the torpedo model, the (yeast) nuclease Rat1 degrades the newly synthesized RNA. When the nuclease reaches the elongating RNAPII, it will be taken off the DNA (Connelly and Manley, 1988; Proudfoot, 1989).

3.1.2 mRNP formation

As soon as the nascent mRNA appears, the process to form a mature mRNP that can be transported into the cytoplasm starts. First, the emerging mRNA is capped at the 5´end by capping enzymes to protect the mRNA from exonucleolytic degradation. The 5´cap is bound by the cap-binding complex (composed of Cbp80 and Cbp20 in yeast), which promotes further steps in mRNA processing (Topisirovic *et al.*, 2011). If the growing mRNA contains introns, the mRNA is spliced by the spliceosome to remove introns and ligate the exons (Will and Lührmann, 2011). The TREX complex, which couples **tr**anscription to **ex**port, is among the RBPs that bind along the mRNA to form an export-competent mRNP (Chávez *et al.*, 2000; Hurt *et al.*, 2004; Strässer *et al.*, 2002). Other proteins such as Nab2 and Npl3 also belong to the RBPs. Nab2 controls poly(A) length (Batisse *et al.*, 2009; Green *et al.*, 2002; Hector *et al.*, 2002), and the SR-like protein Npl3 regulates termination by antagonizing premature 3´end processing (Bucheli and Buratowski, 2005; Deka *et al.*, 2008). At the poly(A) site, the last co-transcriptional step takes place, the release of the mRNA by cleavage at its 3´end (Mandel *et al.*, 2008). The process of mRNP formation is highly connected, and three platforms that recruit RNA-binding proteins to the (pre-)mRNA orchestrate all these processes at the level of transcription. The first recruitment platform is the carboxy-terminal domain (CTD) of Rpb1, the largest subunit of RNAPII. The second is the C-terminal region (CTR) of Spt5. Then, last but not least, there is the mRNA itself (Figure 2).

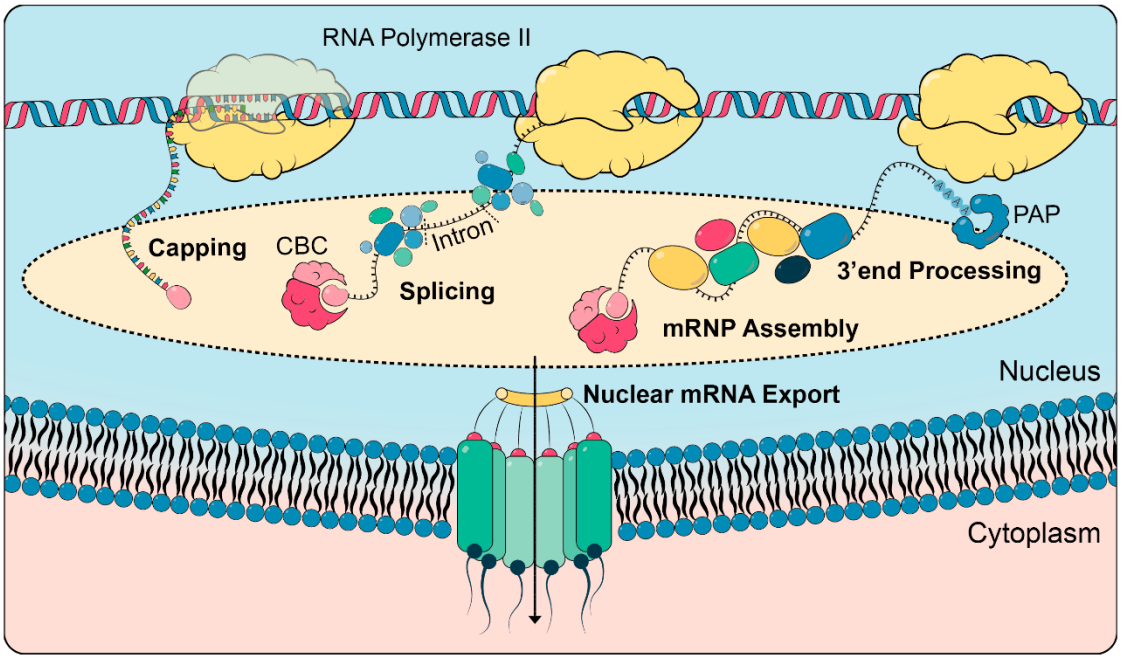

Figure 2: mRNP formation. As soon as the pre-mRNA emerges, it is capped at the 5´end. The cap is bound by the cap-binding complex (CBC), which orchestrates further processing steps such as splicing of possible introns and 3´ end processing. During all processing steps, the mRNA is bound by RNA-binding proteins (RBPs) to form an mRNP. In the end, the export-competent mRNP is transported through the nuclear pore into the cytoplasm (Zarnack *et al.*, 2020).

3.1.2.1 CTD of RNAPII as recruitment platform

The CTD of Rpb1 is a unique feature of RNAPII that consists of 26 conserved repetitive heptapeptides ($Y_1S_2P_3T_4S_5P_6S_7$) in *S. cerevisiae* and 52 in humans (Corden *et al.*, 1985; Liu *et al.*, 2010). During the different steps of transcription, the CTD is intensely and reversible modified. The tyrosine, threonine and serines can be phosphorylated; additionally, the threonine and serine can be glycosylated, and the proline can undergo isomerization (Zhang *et al.*, 2012). During initiation S_5 is phosphorylated by the TFIIH associated kinase Kin28 (Cdk7 in humans). The phosphorylation of S_5 is supported by the mediator-complex-associated kinase Srb10 (Cdk8 in humans) (Liao *et al.*, 1995; Rodriguez *et al.*, 2000; Zhang *et al.*, 2012). S_5 phosphorylation may help in promotor clearance, since inhibition of the two kinases leads to a decrease of RNAPII at the open reading frame (ORF) (Tietjen *et al.*, 2010). The structure of the chromatin is also a physical barrier to transcription that can be weakened through modification on the flexible linker of histones. The phosphorylation of S_5 recruits the methyltransferase Set1 that trimethylates histone H3 at the position K4. This mark is often associated with active transcription (Ng *et al.*, 2003; Workman, 2006). The recruitment of the capping enzyme complex, which places the m^7G cap on the nascent transcript, also depends on S_5

phosphorylation (Cho *et al.*, 1997). S_5 phosphorylation also plays a role in export by recruiting Sus1, a component of the SAGA and THSC/TREX-2 complexes (Pascual-García *et al.*, 2008). Kin28 is also the kinase that primarily phosphorylates S_7 (Akhtar *et al.*, 2009; Glover-Cutter *et al.*, 2009; Kim *et al.*, 2009), although the function of this phosphorylation at the promotor has to be further investigated (Zhang *et al.*, 2012).

Promotor clearance occurs after several abortive initiation cycles once the transcript exceeds a threshold length of approximately 10 nucleotides (Zhang *et al.*, 2012). The transition from initiation to elongation is marked by a change of phosphorylation of the CTD. Bur1 (the yeast homolog of Cdk9), a cyclin-dependent kinase, is recruited to the transcribed gene by phosphorylated S_5 and phosphorylates S_2 of the CTD, but also the CTR of Spt5 (Zhou *et al.*, 2009). The initial S_2 phosphorylation prepares the CTD for the recruitment of Ctk1 (Cdk12 in humans), the major S_2 kinase (Jones *et al.*, 2004). Bur1 travels with RNAPII and also phosphorylates S_7 (Tietjen *et al.*, 2010). The S_2 phosphorylation level stays high during transcription due to the opposing effects of the kinase Ctk1 and the phosphatase Fcp1 (Cho *et al.*, 2001). Simultaneously, most of the S_5 phosphorylation is removed near the +1 nucleosome by the phosphatase Rtr1, although a basal level persists throughout transcription of the open reading frame (Krishnamurthy *et al.*, 2004; Mayer *et al.*, 2010; Mosley *et al.*, 2009). Due to the changed phosphorylation pattern, the transcription initiation factors are exchanged for elongation factors. The recruitment of elongation factors like Spt4/5, Spt6, Spt16 and Paf1 is competitive on every gene independent of length, transcript type, or expression level (Mayer *et al.*, 2010). While Spt4/5 is essential for transcription processivity (Grohmann and Werner, 2011; Hartzog *et al.*, 1998; Martinez-Rucobo *et al.*, 2011), Spt6 and Spt16 reorganize nucleosomes to facilitate access of RNAPII to the DNA (Adkins and Tyler, 2006; Jamai *et al.*, 2009; Orphanides *et al.*, 1999; Youdell *et al.*, 2008). Paf1 is important for gene activation and 3´processing (Jaehning, 2010). The S_2-S_5 phosphorylation is involved in mRNP formation. Prp40, a subunit of the U1 snRNP of the spliceosome, preferably interacts with the CTD in a S_2-S_5 phosphorylation state (Morris and Greenleaf, 2000). Also, the SR-like protein Npl3 interacts directly with phosphorylated S_2. Npl3 functions in transcription elongation, 3´ end processing, splicing and mRNA export (Bucheli and Buratowski, 2005; Bucheli *et al.*, 2007; Dermody *et al.*, 2008; Lei *et al.*, 2001). The THO subcomplex of TREX that couples **tr**anscription to **ex**port binds directly to the phosphorylated CTD (Meinel *et al.*, 2013).

During elongation, the level of phosphorylated S_2 and Y_1 is increasing. At the poly(A) site, the phosphorylation level of Y_1 decreases, followed by the S_2 levels at the termination site (Mayer *et al.*, 2010; Mayer *et al.*, 2012; Tietjen *et al.*, 2010). The

decreasing Y_1 phosphorylation initiates the next event in the transcription cycle. Several 3´end processing factors and termination factors prefer this state of the CTD, including Pcf11, Rtt103, Rna14 (CFIA), Rna15 (CFIA), Ydh1 (cleavage and polyadenylation factor CPF) and Yhh1 (CPF) (Barillà *et al.*, 2001; Dichtl *et al.*, 2002; Kyburz *et al.*, 2003; Zhang *et al.*, 2012). Pcf11 is an essential component of the cleavage factor IA (CFIA) complex that binds to phosphorylated S_2 if Y_1 phosphorylation levels are low (Lunde *et al.*, 2010; Noble *et al.*, 2005; Zhang *et al.*, 2005). Rtt103 binds cooperatively with Pcf11 to the CTD and indirectly recruits the exonuclease Rat1 (Lunde *et al.*, 2010). Rna15 can bind to the RNA and promotes endonucleolytic cleavage followed by polyadenylation by Pap1 (polyadenylation polymerase). The transcript is protected by polyadenylation-binding proteins (PABs) from exonucleolytic degradation (Moore, 2005). The CTD is dephosphorylated by Ssu72 and Fcp1, two essential phosphatases (Ghosh *et al.*, 2008; Nedea *et al.*, 2003). This facilitates the release of RNAPII from the DNA, which than can be recycled for a new transcription cycle (Cho *et al.*, 1999; Steinmetz and Brow, 2003).

3.1.2.2 mRNA itself as recruitment platform

The (pre-)mRNA itself serves as a recruitment platform for RBPs. RBPs can bind structural elements of the RNA. Some, but not all, RBPs contain distinct conserved RNA-binding domains, such as RNA recognition motifs (RRM; (Cléry *et al.*, 2008; Maris *et al.*, 2005), arginine/glycine-rich domains (RGG/RG; (Ozdilek *et al.*, 2017), K homology domains (KH; (Valverde *et al.*, 2008) or zinc finger domains (ZnF; (Hall, 2005). For example, the spliceosome identifies its targets by RNA motifs, but it is not the proteins of the snRNPs that recognize the sequence, but the RNA components by base-pairing (Will and Lührmann, 2011). Some proteins do not recognize a specific RNA motif, but have a preference for certain sequences (Baejen *et al.*, 2014). Nab2 not only binds to poly(A) tails but also to degenerated A-rich motifs (Riordan *et al.*, 2011; Tuck and Tollervey, 2013). In contrast, Npl3 binds GU-rich sequences with a low affinity (Deka *et al.*, 2008). Moreover, some RBPs can mediate the recruitment of other RBPs to the mRNA. For example: Yra1, Npl3 and Nab2 act as adaptor proteins for the export receptor Mex67-Mtr2, which mediates the export of mRNAs.

3.1.2.3 The CTR of Spt5 is a possible recruitment platform

The general elongation factor Spt5 forms a duplex with Spt4 (Malone *et al.*, 1993; Swanson *et al.*, 1991). Spt4 is a small zinc finger protein that is conserved across eukaryotes and archaea but is not found in bacteria. In yeast, *spt4* null mutants are viable. Spt4 interacts via the NGN-domain with Spt5 (Chiang *et al.*, 1996; Malone *et al.*, 1993; Ponting, 2002). Spt5 is highly conserved multi-domain protein. It consists of an

N-terminal acidic domain, a NusG N-terminal (NGN) domain, multiple Kyprides, Ouzounis, Woese (KOW) domains and a C-terminal repeat region (CTR) (Ponting, 2002). The sequence of the repeats varies across different species. Like the CTD of RNAPII, the CTR contains residues that can be phosphorylated. In *S. cerevisiae,* the CTR contains 15 hexapeptides with a consensus sequence S,T/A,W,G,G,A/Q (Swanson *et al.*, 1991), while the human CTR has 7 pentapeptides with the sequence G,S,R/Q,T,P (Yamada *et al.*, 2006). Spt5 is the only transcription regulator that is conserved in all three domains of life (Grohmann and Werner, 2011). Spt5 associates with RNAPII in a transcription-dependent manner just downstream of the transcription start site and persists until the site of termination (Glover-Cutter *et al.*, 2008; Mayer *et al.*, 2010; Tardiff *et al.*, 2007). Bur1 phosphorylates the conserved serine of the CTR. In contrast to ∆*bur1* and ∆*spt5* mutants, the deletion of the CTR of Spt5 is not lethal in budding yeast (Liu *et al.*, 2009; Zhou *et al.*, 2009). The CTR serves as a recruitment platform for RBPs. The recruitment of the PAF complex depends on the phosphorylation of the CTR (Chen *et al.*, 2009). Over 90 proteins involved in transcription elongation and termination, as well as in mRNP formation and export can be co-purified with Spt5 (Lindstrom *et al.*, 2003). Spt5 interacts with the capping enzymes (Lidschreiber *et al.*, 2013; Pei and Shuman, 2002; Wen and Shatkin, 1999) and with the pre-mRNA cleavage factor I (CFI; (Mayer *et al.*, 2012)).

3.1.2.4 5´capping

The first step of mRNA processing is the capping of the 5´end. Capping occurs co-transcriptionally as soon as the first 20-25 nucleotides of the nascent mRNA emerge from RNAPII. All mRNAs contain a N7-methylated guanosine (m^7G) cap linked to the first nucleotide. The cap functions as protection from 5´ to 3´ degradation by exonucleases such as Rat1 and Xrn1 (Bousquet-Antonelli *et al.*, 2000; He and Jacobson, 2001). Furthermore, the cap co-transcriptionally recruits proteins that function in splicing of the pre-mRNA, polyadenylation, and mRNA export. In the nucleus, the cap is bound by the cap-binding complex (CBC), which consists of the small subunit Cbp20 and the large subunit Cbp80. In the cytoplasm, the cap is important for the initiation of protein synthesis and is bound by the general translation initiation factor eIF4E. The cap is generated through three enzymatic steps that are conserved in eukaryotes. First, the RNA triphosphatase (Cet1) removes the γ-phosphate from the 5´ triphosphate to generate a 5´ diphosphate (Rodriguez *et al.*, 1999; Tsukamoto *et al.*, 1997). In the next step, the RNA guanylyltransferase (Ceg1) transfers a guanine monophosphate (GMP) group from guanosine triphosphate (GTP) to the 5´ diphosphate (Shibagaki *et al.*, 1992). In the last step, the guanine-N7 methyltransferase (Abd1) adds a methyl group to the

N7 amine of the guanine cap (Mao *et al.*, 1995). Whereas in lower eukaryotes the enzymatic activities of the capping machinery are carried out by three individual enzymes, the RNA triphosphatase and the RNA guanylyltransferase are combined in a bifunctional protein in metazoans (Shuman, 2001). The capping enzymes interact with RNAPII. Ceg1 interacts with the phosphorylated S_5 of the CTD, while cryo-EM studies showed that Cet1 interacts with RNAPII outside of the CTD (Cho *et al.*, 1997; Ghosh *et al.*, 2011; Martinez-Rucobo *et al.*, 2015; McCracken *et al.*, 1997).

3.1.2.5 Splicing

Most eukaryotic pre-mRNAs contain noncoding sequences (introns) that must be removed before the coding sequences (exons) can be ligated together to produce a functional mRNA. This process is called splicing. In humans, most of the 20,000 protein-coding genes even contain multiple introns, which are often alternatively spliced. Alternative splicing enables these organisms to form different variants of mRNAs from a single pre-mRNA and thereby expand their proteome considerably (Chen and Manley, 2009; Keren *et al.*, 2010; Nilsen and Graveley, 2010; Sakharkar *et al.*, 2004). Only approximately 5 % of all protein-coding genes of *S. cerevisiae* contain introns. Nevertheless, the intron-containing transcripts make up to 30 % of all transcribed mRNAs (Hooks *et al.*, 2014). Three conserved sequences define Introns: The 5´splice site (5´SS), the internal branch point (BP), and the 3´splice site (3´SS). Two phosphoryl transfer reactions are necessary to remove an intron. The first catalytic step is a nucleophilic attack of the 2’ OH group of the BP of the adenosine on the 5’ SS. This produces a 5´ exon and the lariat intron-3´exon intermediate. In the second phosphoryl transfer reaction, the 3´-terminal OH group of the free 5´exon attacks the phosphate at the 3´SS. This leads to the ligation of the 5´ and 3´ ends of the exons (mRNA) and a free intron lariat (Will and Lührmann, 2011). The splicing is catalyzed by the spliceosome (Brody and Abelson, 1985). The spliceosome comprises five small nuclear RNAs (U1, U2, U4, U5 & U6) and approximately 70 proteins in *S. cerevisiae* (more than 100 in humans) organized into small nuclear ribonucleoprotein particles (snRNPs) (Kastner *et al.*, 2019). During splicing, non-snRNP proteins join the spliceosome. At least 10 distinct spliceosome states can be defined during splicing, which differ in their RNA or protein composition or state of the pre-mRNA substrate (Will and Lührmann, 2011). Eight conserved RNA helicases promote the transitions between different spliceosome states, among them the DEAD-box helicase Sub2 (Libri *et al.*, 2001; Semlow *et al.*, 2016).

3.1.2.6 3´end formation

3´ end formation or polyadenylation is the last step in pre-mRNA processing. The cleavage and polyadenylation factor (CPF) consists of more than 20 proteins and mediates the cleavage in the 3´UTR and the subsequent generation of a poly(A) tail. The CPF has three modules that mediate its functions: The nuclease module cleaves the transcript, the polymerase module contains the poly(A) polymerase Pap1 and adds the pol(A) tail, and the phosphatase/ ATP module regulates the processing (Casañal *et al.*, 2017). 3´end formation starts with the recognition of a specific sequence in the 3´UTR (untranslated region) of the pre-mRNA and the cleavage of the transcript. Some proteins of CPF bind to the phosphorylated CTD (Takagaki and Manley, 2000). After the cleavage of the transcript, the poly(A) polymerase adds ~60 adenosines in *S. cerevisiae* (~250 adenosines in mammals) that embody the poly(A) tail (Stewart, 2019). Polyadenylation is terminated by the release of Pap1 from the CPF (Wahle, 1995). Already during synthesis, the poly(A) tail is bound by poly(A)-binding proteins (PABs) like Pab1 and Nab2. These proteins stabilize the RNA. Nab2 regulates the length of the poly(A) tail and is a link to mRNA export because it interacts with Mex67 and Yra1. Mutants of Nab2 show a nuclear accumulation of bulk mRNA (Hector *et al.*, 2002; Iglesias and Stutz, 2008; Marfatia *et al.*, 2003; Soucek *et al.*, 2012; Vinciguerra *et al.*, 2005).

3.1.3 THO/TREX

Already during transcription, the evolutionarily conserved TREX complex, which couples transcription to export, is recruited to the transcribed gene (Chávez *et al.*, 2000; Meinel *et al.*, 2013; Strässer *et al.*, 2002). In yeast, the TREX complex consists of the pentameric THO-subcomplex (Tho2, Hpr1, Mft1, Thp2 and Tex1), the SR-like proteins Gbp2 and Hrb1, the DEAD-box RNA helicase Sub2, and the mRNA export adaptor Yra1 (Chávez *et al.*, 2000; Strässer *et al.*, 2002).

The THO complex interacts with the S_2 – S_5 phosphorylated CTD of RNAPII and with the nascent mRNA. The recruitment occurs co-transcriptionally and in a length-dependent manner with an increasing level towards the 3´end. Downstream of the polyadenylation site, the TREX complex does not associate with the chromatin, which implies that it functions in elongation and/or in 3´processing and that it leaves the chromatin with the mRNA (Abruzzi *et al.*, 2004; Ahn *et al.*, 2004; Gómez-González *et al.*, 2011; Kim *et al.*, 2004; Meinel *et al.*, 2013; Strässer *et al.*, 2002). In mutants of the THO/TREX complex, hyper-recombination occurs as a result of increased levels of R-loops (Jimeno *et al.*, 2002). R-loops are stable hybrids between the DNA template strand and the nascent

RNA. They can be an obstacle for transcription elongation and decrease genome stability through replication impairment and single strand breaks in the DNA strand that is not hybridized with RNA (Domínguez-Sánchez *et al.*, 2011; Gómez-González *et al.*, 2011; Huertas and Aguilera, 2003). Furthermore, it could be observed that 3´processing fails in TREX mutants, which results in defective mRNPs (Rougemaille *et al.*, 2008; Saguez *et al.*, 2008). In *S. cerevisiae,* the Prp19 complex, which functions in splicing, is needed for the recruitment of TREX to both intron-containing and intron-less genes (Chanarat *et al.*, 2011). In humans, the recruitment of TREX depends on the exon junction complex during splicing (Gromadzka *et al.*, 2016; Masuda *et al.*, 2005). The SR-like proteins Hrb1 and Gbp2 are involved in the control of correct splicing (Hackmann *et al.*, 2014). The recruitment of Yra1 to the mRNP is very variable, demonstrating at the same time that the TREX complex interacts with many factors involved in mRNP formation. First of all, Yra1 is recruited via the DEAD-box helicase Sub2 (Strässer and Hurt, 2001). Pcf11, a component of the CPF that binds directly to the CTD, also participates in the recruitment of Yra1 (Johnson *et al.*, 2009). Also, the ubiquitylation of the Histone H2B and the H3K4 methyltransferase play a role in the recruitment of Yra1 (Vitaliano-Prunier *et al.*, 2012) as well as the mRNA itself (Meinel *et al.*, 2013). When Yra1 has been recruited to the mRNP, it directly interacts with the mRNA export factors Mex67-Mtr2 (Strässer and Hurt, 2000). Yra1 is possibly not the only TREX component that can recruit Mex67-Mtr2 to the mRNP. For a subset of transcripts, it could be shown that the ubiquitylated version of Hpr1 can interact with ubiquitylated Mex67 and thereby recruit it to the mRNA (Gwizdek *et al.*, 2006; Hobeika *et al.*, 2009; Hobeika *et al.*, 2007). TREX is also recruited to the 5´end of the mRNA, where it interacts directly with the large subunit of the cap-binding complex Cbp80 (Cheng *et al.*, 2006; Nojima *et al.*, 2007). Recently, it could be shown that ALYREF is recruited to the 5´ and 3´ end of the mRNA and also functions in the export of non-polyadenylated RNAs (Shi *et al.*, 2017).

3.1.4 mRNA export

The transport of molecules between nucleus and cytoplasm is mediated by the nuclear pore complex (NPC). The NPC is a multiprotein complex of ~52 MDa that consists of about 30 different nucleoporines (nups) (Kim *et al.*, 2018). The heterodimer Mex67-Mtr2 is the general mRNP export factor in yeast whereas NXF1-NXT1 (also called TAP-p15) is the metazoan homolog. Mex67 and Mtr2 are highly conserved and bind RNA with a rather low affinity (Katahira *et al.*, 1999). Therefore, it is not surprising that Mex67-Mtr2 are mainly recruited through adaptor proteins like Yra1, Hpr1, Nab2 and Npl3 (Iglesias and Stutz, 2008; Kelly and Corbett, 2009; Köhler and Hurt, 2007). Mex67 binds directly to FG nups and to the Nup84 complex that forms the outer ring of the NPC. Disruption

of this interaction leads to an export defect, revealing an alternative docking site for mRNPs at the NPC (Strässer *et al.*, 2000; Yao *et al.*, 2007).

Nab2, a polyadenosine RNA binding Zn finger protein, functions in poly(A) tail length control by playing a part in the dissociation of Pap1 from the CPF and interacting with the 3´-5´riboexonuclease exosome to protect the poly(A) tail from digestion (Eckmann *et al.*, 2011; Soucek *et al.*, 2012; Wahle, 1995; Wahle and Rüegsegger, 1999). Nab2 is needed for the export of mRNPs and interacts with Yra1 and Mex67. Nab2 interacts with Mlp1 and thereby makes the first contact between the NPC and the mRNP (Fasken *et al.*, 2008). At the NPC, Yra1 becomes di-ubiquitylated by Tom1 and leaves the complex. After Yra1 has left the mRNP, the mRNA can pass through the NPC to the cytoplasm together with Nab2 (Iglesias *et al.*, 2010). At the cytoplasmic side of the NPC, the DEAD-box helicase Dbp5 remodels the mRNP ATP-dependently together with Gle1, dissociating Nab2 from the mRNP (Tran *et al.*, 2007). Kap104 mediates the re-import of Nab2 into the nucleus (Lee and Aitchison, 1999).

Npl3 is one of three SR-like proteins in *S. cerevisiae*. The other two are the two TREX components Gbp2 and Hrb1 (Gilbert *et al.*, 2001; Häcker and Krebber, 2004). As is characteristic of SR-like proteins, Npl3 contains two RNA recognition motifs (RRMs) and a RS/RGG domain in its C-terminus (Birney *et al.*, 1993; Deka *et al.*, 2008). All three SR-like proteins shuttle together with the mRNA into the cytoplasm (Flach *et al.*, 1994; Häcker and Krebber, 2004; Lee *et al.*, 1996). The phosphorylation of Npl3 by Sky1 in the cytoplasm leads to the release of the mRNA and Npl3 is imported back to the nucleus by Mtr10 (Gilbert *et al.*, 2001; Pemberton *et al.*, 1997; Senger *et al.*, 1998). In the nucleus, Npl3 is recruited co-transcriptionally by interaction with phosphorylated S_2 of the CTD and the mRNA (Dermody *et al.*, 2008; Meinel *et al.*, 2013). Furthermore, it could be shown that Npl3 is recruited to actively transcribed genes through the cap-binding complex (Sen *et al.*, 2019; Shen *et al.*, 2000). Besides mRNA export, Npl3 is involved in chromatin modification, transcription elongation and termination, splicing, R-loop prevention and translation (Baierlein *et al.*, 2013; Bucheli and Buratowski, 2005; Dermody *et al.*, 2008; Kress *et al.*, 2008; Moehle *et al.*, 2012; Pérez-Martínez *et al.*, 2020; Santos-Pereira *et al.*, 2013).

The conserved multifunctional THSC (TREX-2) complex consists of Thp1, Sac3, Sus1, Cdc31 and Sem1, and plays a role in mRNA export (Fischer *et al.*, 2004; Fischer *et al.*, 2002; Gallardo *et al.*, 2003; Rodríguez-Navarro *et al.*, 2004; Wilmes *et al.*, 2008). Thp1 and Sac3 attach the mRNP at the NPC by interacting with nups and Mex67-Mtr2. Furthermore, Thp1 and Sac3 interact with the export adaptor Yra1 (Fischer *et al.*, 2002).

Sus1 is also a part of the SAGA complex, which functions in transcription regulation (Köhler *et al.*, 2006). Moreover, the SAGA complex stabilizes the THSC complex (Köhler *et al.*, 2008). A further indication that the THSC complex not only functions in mRNA export but also in transcription is that the THSC mutants show similar phenotypes as the TREX complex, for example impairment of mRNA export, defects in transcription elongation and hyper-recombination (González-Aguilera *et al.*, 2008). Like the TREX complex, it seems that THSC links transcription to mRNA export.

3.2 PAF complex

The PAF complex was identified as a factor associated with RNAPII. In yeast, it consists of five subunits: Paf1, Ctr9, Leo1, Rtf1 and Cdc73 (Krogan *et al.*, 2002; Mueller and Jaehning, 2002; Shi *et al.*, 1996). In humans, the PAF complex has an additional subunit, hski8 (Zhu *et al.*, 2005). In *S. cerevisiae*, none of the subunits is essential but the deletion of *PAF1* and *CTR9* results in severe growth defect and the orthologs are essential in higher organisms (Bahrampour and Thor, 2016; Mosimann *et al.*, 2006). Rtf1 interacts with elongation factors including Spt4/5, Spt16/Pob3 and Dst1 (the yeast orthologs of DSIF, FACT, and TFIIS/SII (Chu *et al.*, 2007; Krogan *et al.*, 2003; Ng *et al.*, 2003; Wood *et al.*, 2003). The PAF complex is localized along the entire open reading frame of transcribed genes. The distribution resembles RNAPII and is different from the mediator and general initiation factors (Chen *et al.*, 2015; Wood *et al.*, 2003). Despite its association with RNAPII, the loss of the PAF complex leads to a change in abundance of only a small subset of transcripts in yeast (Mueller *et al.*, 2004; Penheiter *et al.*, 2005; Rondón *et al.*, 2004; Squazzo *et al.*, 2002). Combined, this has led to the assumption that the PAF complex is a transcription elongation factor. The PAF complex executes multiple roles in chromatin transcription. It functions in histone H3 methylation by Set1 and Dot1 (Krogan *et al.*, 2003). Rtf1 binds to Chd1, the chromatin remodeler (Simic *et al.*, 2003). Additionally, Rtf1 is required for H2B ubiquitination (Ng *et al.*, 2003; Wood *et al.*, 2003; Xiao *et al.*, 2005). The PAF complex is also involved in 3´processing (Penheiter *et al.*, 2005; Sheldon *et al.*, 2005). In humans, it contributes to cell differentiation and cancer (Chaudhary *et al.*, 2007).

The PAF complex affiliates with the RNAPII elongation complex downstream of the transcription start site and leaves at the polyadenylation site (Mayer *et al.*, 2010). The recruitment of the PAF complex depends on the cyclin-dependent kinase Bur1-Bur2. Bur1-Bur2 phosphorylates both the CTD of RNAPII and the CTR of Spt5 (Liu *et al.*, 2009; Qiu *et al.*, 2012). The PAF complex forms a tripartite complex in which Paf1 and Leo1 form a heterodimer that contacts RNAPII at Rpb2 (Xu *et al.*, 2017). Ctr9 forms a flexible

bridge between Paf1-Leo1 and Cdc73 and forms the scaffold of the PAF complex. Cdc73 binds Rpb3 and contacts phosphorylated CTD with its C-terminal domain (Chu *et al.*, 2013; Mbogning *et al.*, 2013; Xu *et al.*, 2017). Rtf1 is flexible and binds the phosphorylated CTR of Spt5 (Wier *et al.*, 2013; Xu *et al.*, 2017). However, the recruitment of the human PAF complex to the RNAPII probably is not primarily dependent on Rtf1, since Rtf1 is only weakly associated with the PAF complex in metazoans (Cao *et al.*, 2015).

3.3 Tho1

Tho1 was initially identified as a suppressor of the **t**ranscriptional defect of **H**pr1 by **o**verexpression (Piruat and Aguilera, 1998). The high-copy expression of Tho1 can suppress all phenotypes of the THO complex mutants, such as defects in gene expression, hyperrecombination and defects in mRNA export. Furthermore, overexpression can suppress some phenotypes of the *npl3* mutant, among them hyper-recombination and temperature sensitivity. Interestingly the rescue does not involve proteins like Sub2, Thp1, a component of the THSC complex, and Spt4 (Jimeno *et al.*, 2006; Santos-Pereira *et al.*, 2013). The Δ*tho1* mutant has no known phenotype, not even when combined with a Δ*hpr1* mutant (Piruat and Aguilera, 1998), but it can rescue the cryo-sensitivity of the *nab2 - 1* mutant (Jimeno *et al.*, 2006). Tho1 and its homologues CIP29 (human) and Mos11 (plant) are localized in the nucleus (Choong *et al.*, 2001; Dufu *et al.*, 2010; Germain *et al.*, 2010; Jimeno *et al.*, 2006). In *S. cerevisiae,* Tho1 is recruited to the transcribed gene dependent on the THO complex and the RNA. Although the SAP domain has only a weak RNA binding ability, Tho1 binds RNA via its C-terminus. The SAP domain binds double-stranded DNA (Jacobsen *et al.*, 2016; Jimeno *et al.*, 2006). For CIP29, recruitment to the transcribed gene was shown to be cap-dependent and to occur more efficiently to spliced mRNAs (Dufu *et al.*, 2010). Mos11 binds to ssRNA and dsRNA in a concentration-dependent manner (Sørensen *et al.*, 2017). Although Tho1 does not co-purify with THO/TREX in yeast, it could be shown that CIP29 co-purifies RNA-independently with TREX in the presence of ATP. UAP56 probably mediates the interaction between THO and CIP29 / Aly/REF (the human ortholog of Yra1). While the interaction between THO and UAP56 is ATP-independent, the interaction between UAP56 and CIP29 / Aly/REF depends on ATP. CIP29 also binds to Aly/REF (Dufu *et al.*, 2010; Kang *et al.*, 2020). CIP29 co-purifies with the ATP-dependent RNA helicase UAP56 and DDX39. In both cases it could be shown that CIP29 enhances the helicase activity but cannot unwind DNA on its own. In the case of UAP56 it also stimulates the ATPase activity (Chang *et al.*, 2013; Sugiura *et al.*, 2007). In plants, it could be shown that the double mutant of *mos11* and *tex1* has a severe phenotype whereas the single

mutants have a rather mild phenotype. Furthermore, it seems like these proteins have distinct functions even though the double mutant enhances the respective phenotype. For example, mRNA export is impaired in the *mos11* mutant, while *tex1* has no mRNA export effect and the double mutant has increased nuclear retention of mRNA. And while alternative splicing and protein synthesis are disturbed in *tex1* and the double mutant, it is not changed in the *mos11* mutant (Germain *et al.*, 2010; Sørensen *et al.*, 2017).

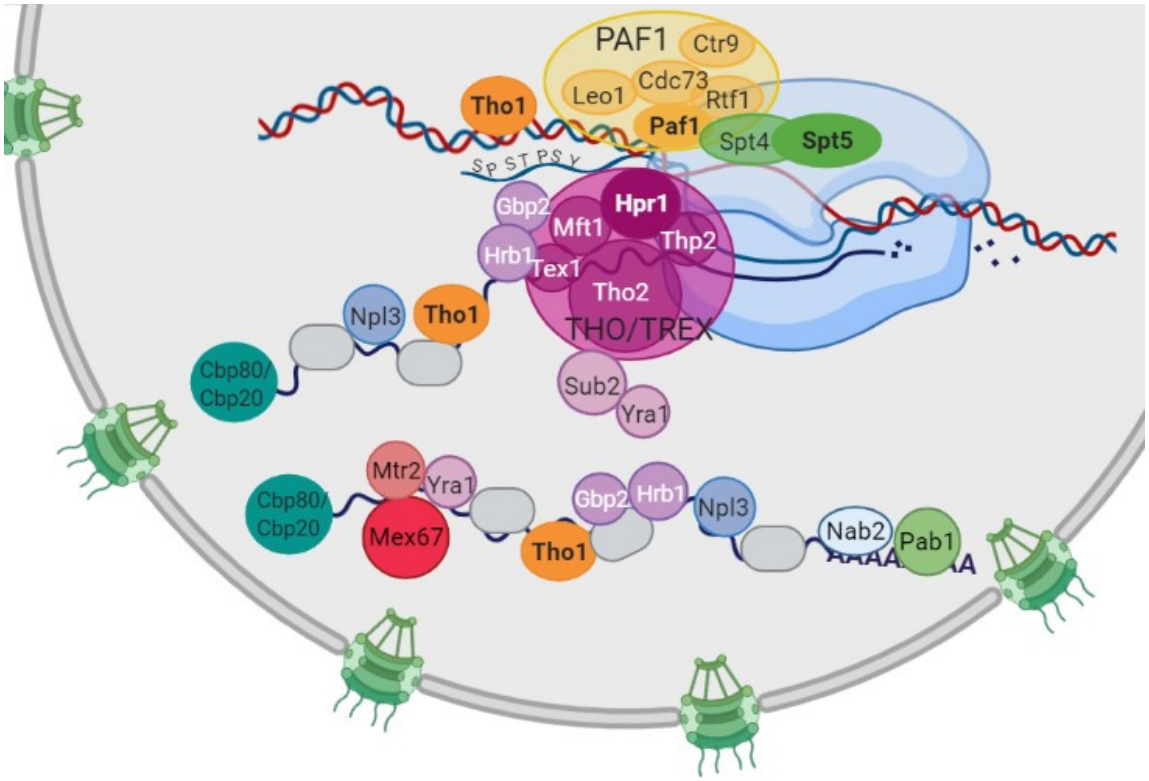

Figure 3: Recruitment of Tho1, TREX and the PAF complex. After the recruitment of the transcription-factors like Spt4/5 and the PAF complex, RNPII transcribes DNA into nascent RNA. The nascent RNA is immediately bound by the TREX complex and various other RBPs. The composition of the mRNP changes along the way to an export-competent mRNP. In the end the mRNP is transported through the nuclear pore complex into the cytoplasm. Created with BioRender.com.

3.4 Aim and scope

Tho1 was identified due to its ability to suppress the phenotype of THO mutants if overexpressed. The deletion of *THO1* does not show a phenotype in humans or yeast, and only a mild mRNA export defect in plants (Jimeno *et al.*, 2006; Piruat and Aguilera, 1998; Sørensen *et al.*, 2017). As mentioned above (3.3), everything indicates that Tho1 functions in a manner similar to the THO/TREX complex or together with THO/TREX; in some processes, Tho1 seems to depend on THO. Dominik Meinel a former PhD student of our group performed chromatin immunoprecipitation (ChIP) assays of CTR mutants of Spt5. He could show that the recruitment of Tho1 to transcribed genes is increased

and rather similar to the recruitment of Paf1 in a CTR phospho mimic mutant. The recruitment of Hpr1 is in this mutant compared to the wild-type decreased (Meinel, 2013). Paf1 is an elongation factor whose recruitment to the transcribed gene depends on the correct phosphorylation of Spt5 and RNAPII (Liu *et al.*, 2009; Qiu *et al.*, 2012). This was a first hint that Tho1 might function independently of the THO/TREX complex. During my studies, another evidence arose: the double mutant of *tex1* and *mos11* has a severe phenotype while the single mutants show only mild phenotypes. Even though the mutants enhance each other they have distinct functions (Sørensen *et al.*, 2017).

The aim of this project was to identify the function of Tho1 in the mRNP formation. One main focus was the role of Tho1 in the recruitment of RBPs to the transcribed genes, especially of the TREX component Hpr1 and the elongation factor Paf1. To get a first hint whether a genetic interaction between Tho1, Hpr1 and Paf1 exists, a growth assay of the Δ*tho1*, Δ*hpr1* and Δ*paf1* mutants was performed. Moreover, we checked whether Tho1 co-purifies with the TREX complex or Paf1. To assess whether Tho1, Hpr1 and Paf1 influence each other in the recruitment to the transcribed gene, ChIP experiments in mutants and strains overexpressing Tho1 were performed. The influence between these proteins was confirmed by tandem affinity purification (TAP) and analyzed by Western blot. Furthermore, the role of Tho1 in the formation of mRNPs and the mRNA export was assessed in the *THO1* deletion and overexpression strains via a TAP of the cap-binding complex and fluorescence *in situ* hybridization (FISH) experiments.

4 Material

4.1 Chemicals and consumables

Table 1: List of chemicals

Chemicals and Consumables	Supplier
2-Propanol	Carl Roth
Acetic acid	VWR Chemicals
Acrylamide (29:1) 40 %	AppliChem GmbH
Adenine hemisulfate salt	Sigma-Aldrich
Agar Bacteriology grade	Applichem GmbH
Agarose	Applichem GmbH
Ammonium persulfate (APS)	VWR Chemicals
Ampicillin	Applichem GmbH
ANTI-FLAG® M2 Affinity Gel	Sigma-Aldrich
Bacto™ Peptone	BD Biosciences
Bacto™ Yeast extract	BD Biosciences
Benzamidine HCl	MP Biomedicals
Bovine serum albumin (BSA)	Carl Roth
Bromophenol blue	Applichem
Calcium chloride ($CaCl_2$)	Fluka
Calmodulin Affinity resin	Agilent Technologies
Chloroform	Merck
Coomassie Brilliant Blue G-250	Applichem
Coomassie Brilliant Blue R-250	Applichem
Dextran sulfate	Sigma-Aldrich
D-Glucose Monohydrate	Sigma-Aldrich
Dimethyl sulfoxide (DMSO)	Grüssing GmbH
Dipotassium phosphate (K_2HPO_4)	Grüssing GmbH
Disodium phosphate (Na_2HPO_4)	Carl Roth
Dithiothreitol (DTT)	Sigma-Aldrich
dNTPs (dATP, dTTP, dCTP, dGTP)	Thermo Fisher Scientific
D-Sorbitol	Carl Roth
Dynabeads™ M-280 Tosylactivated	Invitrogen
Dynabeads™ Protein G	Invitrogen
E. coli tRNA	Roche diagnostics
ECL Solution	Applichem
Ethanol	Fisher Chemical
Ethylenediaminetetraacetic acid (EDTA)	Sigma-Aldrich
Ethyleneglycol-bis(aminoethylether)tetraacetic acid (EGTA)	Merck
Ficoll® 400	Carl Roth
FLAG® Peptide	Sigma-Aldrich
Formaldehyde	ORG Laborchemie
Formamide	Merck
Gel loading dye, purple (6x)	NEB
Gel loading dye, purple (6x) w/o SDS	NEB
Genetecin (G418)	ThermoFischer (Gibco)
Glutathione Sepharose 4B	GE Healthcare
Glycerol	Carl Roth
Glycine	Labochem international
HDGreen™ DNA stain	Intas
HEPES	Carl Roth

Herring Sperm DNA	ThermoFischer (Invitrogen)
Hydrochloric acid (HCl)	Carl Roth
IGEPAL CA-630	Sigma-Aldrich
IgG Sepharose 6 Fast Flow	GE Healthcare
Imidazole	Merck
Isopropyl β-D-1-thiogalactopyranoside (IPTG)	Carl Roth
Kanamycin	Merck
L-Arginine-HCl	Biomol GmbH
L-Aspartic acid	Sigma-Aldrich
Leupeptin (Hemisulfate)	Carl Roth
L-Histidine	Sigma-Aldrich
L-Isoleucine	Sigma-Aldrich
Lithium acetate (LiOAc)	Carl Roth
Lithium chloride (LiCl)	Merck
L-Leucine	Sigma-Aldrich
L-Lysine Monohydrochloride	Sigma-Aldrich
L-Methionine	Sigma-Aldrich
L-Phenylalanine	Sigma-Aldrich
L-Threonine	Sigma-Aldrich
L-Tryptophan	Sigma-Aldrich
L-Tyrosine	Sigma-Aldrich
L-Valine	Biomol GmbH
Magnesium chloride ($MgCl_2$)	Merck
Magnesium sulfate ($MgSO_4$)	Carl Roth
Methanol	Merck-Millipore
Monopotassium phosphate (KH_2PO_4)	Carl Roth
Monosodium phosphate (NaH_2PO_4)	Merck
Nicotinamide adenine dinucleotide (NAD)	Sigma Aldrich
Octylphenoxypolyethoxyethanol (IGEPAL CA-630)	Sigma-Aldrich
Pepstatin A	Applichem GmbH
Phenylmethane sulfonyl fluoride (PMSF)	Carl Roth
Phosphoric acid	Carl Roth
Polyethylene glycol (PEG) 3800/4000	Carl Roth
Polyethylene glycol (PEG) 8000	Fluka
Polylysine	Sigma-Aldrich
Polysorbate 20 (Tween 20)	Merck
Polyvinylpyrrolidone (PVP)	Sigma-Aldrich
Ponceau S	Serva
Potassium chloride (KCl)	ORG Laborchemie
Potassium hydroxide (KOH)	Merck
Powdered milk, fat free, blotting grade	Carl Roth
Protino® Ni-NTA Agarose	Macherey-Nagel
Rothi®-Mount FluorCare DAPI	Carl Roth
Roti®-Aqua-Phenol	Carl Roth
Salmon sperm DNA (SSD)	Applichem GmbH
Sodium acetate (NaOAc)	Merck
Sodium chloride (NaCl)	Merck
Sodium citrate	Carl Roth
Sodium deoxycholate	Sigma-Aldrich
Sodium dodecyl sulfate (SDS)	Serva
Sodium hydroxide (NaOH)	Merck
Sulfosalicylic acid	Merck
Tetramethylethylendiamin (TEMED)	Carl Roth
Thiolutin	Sigma-Aldrich
Trichloroacetic acid (TCA)	Merck

Tris(hydroxymethyl)aminomethane (Tris)	Applichem GmbH
Triton X-100	Applichem GmbH
Tryptone BioChemica	Applichem GmbH
Uracil	Sigma-Aldrich
Yeast nitrogen base, w/o amino acids	Formedium

4.2 Equipment and devices

Used equipment and devices are listed in Table 2.

Table 2: Equipment and devices

Name	Supplier
70 Ti	Beckman Coulter
AM100, micro scale	Mettler-Toledo
Apollo®, liquid nitrogen container	Cryotherm
Avanti JXN-26 Centrifuge	Beckman Coulter
Axio observer, fluorescence microscope	Zeiss
Bioruptor UCD-200, Sonication System	Diagenode
ChemoCam Imager ECL HR 16-3200	Intas
Duomax 1030, tumbling shaker	Heidolph Instruments
EPS 301, electrophoresis power supply	GE Healthcare
FastPrep-24™ 5G	MP Biomedicals
Freezer/Mill® 6870D	Spex®SamplePrep
Gel iX20, Transilluminator/gel docu	Intas
Hera safe, laminar flow cabinet	Thermo Fisher Scientific
HeraFreeze HFU T Series	Thermo Scientific
HT Multitron Pro shaking incubator	Infors
HXP 120 V, light source	Kübler Codix
IKA® KS 4000 ic control, shaking incubator	IKA Labortechnik
IKAMAG® RCT, magnetic stirrer	IKA Labortechnik
Incubator with HT Labotron, shaker	Aqua Lytic / Infors
Incubators	Memmert
Innova®44 shaking incubator	Eppendorf / New Brunswick
JLA-8.1, JA-25.50, JA-10	Beckman Coulter
Lab phenomenal pH 1000L, pH meter	VWR
LED bluelight transilluminator	Nippon genetics
Megafuge 40R	Thermo Scientific, Heraeus
Milli-Q® integral water purification system	Merck
Mini-Protean® Tetra Electrophoresis Cell	Bio-Rad Laboratories
ND-1000, Spectrophotometer	NanoDrop
Optima XPN-80 Ultracentrifuge	Beckman Coulter
PeqStar XS Thermocycler	Peqlab
Pipetboy acu	IBS Integra Biosciences
PM2000, scale	Mettler-Toledo
Quant Studio 3, Real Time PCR System	Applied Biosystems, Thermo Fisher Scientific
RCT basic, magnetic stirrer	IKA Labortechnik
Research Pipettes 2, 10, 20, 100, 200, 1000	Gibbson
Rotator	neoLab

SBH130D, block heater	Stuart®
Sonifier 250	Branson Ultrasonics™
Sunrise Microplate Absorbance Reader	Tecan Group
Superdex 75 10/300 GL	GE Healthcare
SW22, shaking waterbath	Julabo
T3 Thermocycler	Biometra
Tabletop Centrifuge 5424, 5424R	Eppendorf
Tabletop Centrifuge 5430, 5430R	Eppendorf
Thermomixer 5436	Eppendorf
Trans-Blot® Turbo Transfer System	Bio-Rad Laboratories
Typhoon FLA 9500	GE Healthcare
Unichromat 1500	Uniequip
Vakulan CVC 3000	Vacuubrand
VF2, vortex mixer	IKA Labortechnik
VX-150, autoclave	Systec
WT 12, tumbling shaker	Biometra

4.3 Buffers, Media and Solutions

4.3.1 Water

The water used for any solutions and media was filtered/purified by the Milli-Q-synthesis System (Millipore) and autoclaved at 120°C for 20 min. Heat-sensitive solutions and buffers were sterile-filtered through a 0.22 µm filter.

4.3.2 Media

Lysogeny broth (LB) for 1 L
10 g peptone
5 g yeast extract
5 g NaCl
adjust to pH 7.2 (NaOH)
(15 g agar for plates)

SOC for 100 mL
2 g tryptone
0.5 g yeast extract
10 mM NaCl
0.5 mM KCl
10 mM $MgCl_2$
10 mM $MgSO_4$
adjust to pH 7.0 (NaOH)

Synthetic dropout medium (SDC) for 1 L
6.75 g yeast nitrogen base (w/o aa)
0.6 g complete synthetic amino acid mix (CSM)
20 g glucose
10 mL of each 100x aa stock except the required drop out*
adjust to pH 5.5 (NaOH)
(15 g agar for plates // 1 g 5-FOA if required)

Yeast complete medium (YPD) for 1 L
10 g yeast extract
20 g peptone
20 g glucose
adjust to pH 5.5 (HCl)
(15 g agar for plates)

4.3.3 Buffers and solutions

Cloning

50x TAE buffer
2 M TRIS
1 M NaOAc
50 mM EDTA (pH 8.0)
adjust to pH 8.0 (acetic acid)

6 x Agarose loading dye
0.03 % Bromphenol blue
0.03 % Xylen cyanol
60 % Glycerin
60 mM EDTA
10 mM TRIS

5x Isothermal reaction buffer
25 % PEG-8000
500 mM TRIS (pH 7.5)
50 mM $MgCl_2$
50 mM DTT
1 mM of each dNTP
5 mM NAD^+

Gibson assembly master mix
1 × Isothermal reaction buffer
4 U/µL T5 exonuclease
4 U/µL Taq DNA ligase
25 U/mL Phusion DNA polymerase

SDS-PAGE

4x Separating buffer
1.5 M TRIS (pH 8.8)
8 mM EDTA
0.6 % SDS

4x Stacking buffer
0.5 M TRIS (pH 6.8)
8 mM EDTA
0.6 % SDS

Separating gel (10 %)
3 mL acrylamide (40 %; 29:1)
3 mL 4x separating buffer
6 mL H_2O
100 µL 10 % APS
20 µL TEMED

Stacking gel (4 %)
400 µL acrylamid (40 %; 29:1)
1 mL 4x stacking buffer
2.6 mL H_2O
30 µL 10 % APS
10 µL TEMED

6x SDS loading dye
7 mL stacking buffer
40 % glycerol
10 % SDS
0.5 M DTT
0.03 % bromphenol blue
1 % β-mercaptoethanol

Hot-Coomassie
0.5 % Coomassie R250
25 % isopropanol
10 % acetic acid

Detain solution
10 % acetic acid

10x Running buffer
250 mM TRIS
1.9 M Glycin
1 % SDS

Western blotting

10x TBS-T (TRIS buffered saline + tween)
500 mM TRIS (pH 7.5)
1.5 M NaCl
1 % Tween 20

Semi dry Western blot buffer

25 mM TRIS
192 mM Glycin
20 % Methanol

Yeast transformation

Solution I
1x TE
100 mM LiOAc

Solution II
1x TE
100 mM LiOAc
40 % PEG 3,800 (or PEG 4,000)

10x TE
100 mM TRIS (pH 7.5)
10 mM EDTA (pH 8.0)

ChIP

Low-salt buffer
50 mM HEPES (pH 7.5)
150 mM NaCl
1 mM EDTA
1 % Triton-X 100
0.1 % SDS
0.1 % sodium deoxycholate

High-salt buffer
50 mM HEPES (pH 7.5)
500 mM NaCl
1 mM EDTA
1 % Triton-X 100
0.1 % SDS
0.1 % sodium deoxycholate

TLEND
10 mM TRIS (pH 8.0)
0.25 M LiCl
1 mM EDTA
0.5 % NP-40
0.5 % sodium deoxycholate

Elution buffer
50 mM TRIS (pH 7.5)
10 mM EDTA
1 % SDS

10x TE
100 mM TRIS (pH 7.5)
10 mM EDTA

Fluorescence *in* situ hybridization (FISH)

Prehybridisation buffer
50 % formamide
10 % dextran sulphate
125 µg/mL tRNA (*E. coli*)
500 µg/mL herring sperm DNA
4 x SSC
1 x Denhardt's solution

20 x SSC (pH 7.0)
3 M NaCl
300 mM sodium citrate

50x Denhardt's solution
1 % Polyvinylpyrrolidone (PVP)
1 % Bovine serum albumin (BSA)
1 % Ficoll-400

Wash buffer
1.2 M sorbitol
100 mM KPO_4 (pH 6.4)

TAP purification

Wash buffer

50 mM TRIS (pH 7.5)
1.5 mM $MgCl_2$
200 mM KCl
0.15 % NP 40
1 mM DTT
(1x protease inhibitor)

100x protease inhibitor (in 50 mL EtOH)
6.85 mg Pepstatin A
1.42 mg Leupeptin hemisulfat
850 mg PMSF
1.65 g Benzamide HCl

4.4 Organisms

4.4.1 Yeast strains

A *THO1* deletion strain was freshly generated at the latest four weeks after transformation, because it loses its phenotype over time. The Δ*tho1* strain was generated by transforming a SacI + XhoI digested of pBS-Δ*tho1* plasmid to replace the endogenous *THO1* locus by a marker cassette.

Table 3: Yeast strains

Yeast strain	Genotype	Reference
RS453	MATa; ade2-1; his3-11,15; ura3-52; leu2-3,112; trp1-1 can1-100; GAL+;	(Strässer and Hurt, 2000)
BY4743	Mat a; his3Δ0; leu2Δ0; LYS2Δ0; ura3Δ0;	Euroscarf
W303	Mata; ura3-1; trp1-1; his3-11,15; leu2-3,112; ade2-1; can1-100; GAL+	(Thomas and Rothstein, 1989)
Δ*hpr1*	Mata; ura3-1; ade2-1; his3-11,5; trp1-1; leu2-3,112; can1-100; hpr1::HIS3	
HPR1-TAP	HPR1-CBP-TEV-protA::TRP1; MATa; ade2-1; his3-11,15; ura3-52; leu2-3,112; trp1-1 can1-100; GAL+;	
SUB2-TAP	SUB2-CBP-TEV-protA::TRP1; MATa; ade2-1; his3-11,15; ura3-52; leu2-3,112; trp1-1 can1-100; GAL+;	(Strässer and Hurt, 2000)
THO1-TAP (RS453)	THO1-CBP-TEV-protA::TRP1; MATa; ade2-1; his3-11,15; ura3-52; leu2-3,112; trp1-1 can1-100; GAL+;	
MEX67-TAP	MEX67-CBP-TEV-protA::TRP1; MATa; ade2-1; his3-11,15; ura3-52; leu2-3,112; trp1-1 can1-100; GAL+;	
SPT5-TAP	SPT5-CBP-TEV-protA::TRP1; Mat a; ade2-1; his3-11,15; ura3-52; leu2-3,112; trp1-1; can1-100; GAL+	
Δ*mex67* + *pUN100-MEX67*	mex67::HIS3; MATa; ura3; ade2; his3; leu2; trp1	(Hurt *et al.*, 1999)
Δ*mex67* + *pUN100-mex67-5*	mex67::HIS3; MATa; ura3; ade2; his3; leu2; trp1	(Hurt *et al.*, 1999)
Δ*paf1*	MATa; ade2-1; his3-11,15; ura3-52; leu2-3,112; trp1-1 can1-100; GAL+; YBR279W::kanMX4	this study
Tho1-TAP Δ*paf1*	THO1-CBP-TEV-protA::TRP1-KL; MATa; ura3, ade2, his3, leu2, trp1; YBR279W::kanMX4	this study
PAF1-TAP (RS453)	PAF1-CBP-TEV-protA::TRP1; MATa; ade2-1; his3-11,15; ura3-52; leu2-3,112; trp1-1 can1-100; GAL+	Wierschem 2021
Δ*tho1 (RS453)*	MATa; ade2-1; his3-11,15; ura3-52; leu2-3,112; trp1-1; can1-100; GAL+; YER063W::URA	this study
Δ*tho1 (BY4743)*	BY4743; Mat a; his3D; leu2D0; LYS2; ura3D0; YER063W::ura3	this study
Δ*tho1 (W303)*	Mat a; ura3-1; trp1-1; his3-11,15; leu2-3,112; ade2-1; can1-100; GAL+; YER063W::ura3	this study
Δ*tho1 (RS453)*	MATa; ade2-1; his3-11,15; ura3-52; leu2-3,112; trp1-1; can1-100; GAL+; YER063W::TRP	this study
Δ*tho1 (W303)*	Mat a; ura3-1; trp1-1; his3-11,15; leu2-3,112; ade2-1; can1-100; GAL+; YER063W::TRP	this study
Δ*hpr1*Δ*tho1 (W303)*	Mat a; ura3-1; trp1-1; his3-11,15; leu2-3,112; ade2-1; can1-100; GAL+; hpr1::HIS3; YER063W::TRP	this study

Δpaf1Δtho1	MATa; ade2-1; his3-11,15; ura3-52; leu2-3,112; trp1-1 can1-100; GAL+; YBR279W::kanMX4; YER063W::TRP	this study
PAF1-TAP Δtho1	PAF1-CBP-TEV-protA::TRP1; MATa; ade2-1; his3-11,15; ura3-52; leu2-3,112; trp1-1 can1-100; GAL+; YER063W::URA	this study
HPR1-TAP Δtho1	HPR1-CBP-TEV-protA::TRP1-KL; MAT alpha; ura3-52; ade2-1; his3-11,15; leu2-3,112; trp1-1; YER063W::URA	this study
CBP80-FTpA	CBP80-FLAG-TEV-protA::HIS3MX4; MATa; ade2-1, his3-11,15, ura3-52, leu2-3,112, trp1-1, can1-100, GAL+	Philipp Keil
SPT5-TAP Δtho1	SPT5-CBP-TEV-protA::TRP1-KL;MAT alpha;ura3;ade2;his3,leu2,trp1;YER063W::kanMX4	this study
THO1-TAP (W303)	THO1-CBP-TEV-protA::TRP1; Mata; ura3-1; trp1-1; his3-11,15; leu2-3,112; ade2-1; can1-100; GAL+	this study
THO1-TAP Δhpr1	THO1-CBP-TEV-protA::TRP1; Mata; ura3-1; ade2-1; his3-11,5; trp1-1; leu2-3,112; can1-100; hpr1::HIS3	this study
PAF1-TAP (W303)	Paf1-CBP-TEV-protA::TRP1; MATa; ura3-1; trp1-1; his3-11,15; leu2-3,112; ade2-1; can1-100; GAL+	this study
PAF1-TAP Δhpr1	Paf1-CBP-TEV-protA::TRP1; Mata; ura3-1, ade2-1, his3-11,5, trp1-1, leu2-3,112, can1-100; hpr1::HIS3	this study
Δtex1	MAT a; ade2-1; his3-11,15; ura3-52; leu2-3,112;trp1-1 can1-100; GAL+; YNL253W::kanMX4	this study
Δtex1Δtho1	MAT a; ade2-1; his3-11,15; ura3-52; leu2-3,112;trp1-1 can1-100; GAL+; YNL253W::kanMX4; YER063W::URA	this study
HPR1-TAP Δpaf1	Hpr1-CBP-TEV-protA::TRP;MAT a; ade2-1; his3-11,15; ura3-52; leu2-3,112;trp1-1 can1-100; GAL+; YBR279W::kanMX4	this study
CBP80-FTpA HPR1-HA	CBP80-FLAG-TEV-protA::HIS3MX4; Hpr1-HA::kanMX4; MATa; ade2-1, his3-11,15, ura3-52, leu2-3,112, trp1-1, can1-100, GAL+	this study
CBP80-FTpA HPR1-HA Δtho1	CBP80-FLAG-TEV-protA::HIS3MX4; Hpr1-HA::kanMX4; MATa; ade2-1, his3-11,15, ura3-52, leu2-3,112, trp1-1, can1-100, GAL+ YER063W::URA	this study
THO1-TAP Hpr1-HA	THO1-CBP-TEV-protA::TRP1; Hpr1-HA::HIS3 MATa; ade2-1; his3-11,15; ura3-52; leu2-3,112; trp1-1 can1-100; GAL+;	this study
THO1-TAP Hpr1-HA Δpaf1	THO1-CBP-TEV-protA::TRP1; Hpr1-HA::HIS3; MATa; ade2-1; his3-11,15; ura3-52; leu2-3,112; trp1-1 can1-100; GAL+; YBR279W::kanMX4	this study
THO1-TAP PAF1-HA	THO1-CBP-TEV-protA::TRP1; PAF1-HA::HIS3; Mata; ura3-1; ade2-1; his3-11,5; trp1-1; leu2-3,112; can1-100;	this study
THO1-TAP Δhpr1	THO1-CBP-TEV-protA::TRP1; Mata; ura3-1; ade2-1; his3-11,5; trp1-1; leu2-3,112; can1-100; hpr1::HIS3	this study
HPR1-TAP PAF1-HA	HPR1-CBP-TEV-protA::TRP1; PAF1-HA::KanMX; MATa; ade2-1; his3-11,15; ura3-52; leu2-3,112; trp1-1 can1-100; GAL+;	this study
HPR1-TAP PAF1-HA Δtho1	HPR1-CBP-TEV-protA::TRP1; PAF1-HA::KanMX; MATa; ade2-1; his3-11,15; ura3-52; leu2-3,112; trp1-1 can1-100; GAL+; YER063W::URA	this study

4.4.2 *E. coli* strains

For cloning DH5α cells were used. BL21 Star (DE3) were used for heterologous protein expression.

Table 4: *E. coli* strains

E. coli strain	Genotype	Reference
DH5α	F– endA1 glnV44 thi-1 recA1 relA1 gyrA96 deoR nupG purB20 φ80dlacZΔM15 Δ(lacZYA-argF)U169, hsdR17(rK– mK+), λ–	(Taylor *et al.*, 1993)
BL21 Star (DE3)	F– ompT gal dcm lon hsdSB(rB–mB–) λ(DE3 [lacI lacUV5-T7p07 ind1 sam7 nin5]) [malB+]K-12(λS) rne131	(Wood, 1966)

4.5 Plasmids

Table 5: Plasmids

Plasmid	Description	Reference
pBS1479	For genomic C-terminal TAP-tagging (CBP-TEV-2x protein A), *TRP1-KL*	(Puig *et al.*, 2001)
pYM14	PCR template for C-terminal 6x HA tag with kanMX marker	Euroscarf
PYM15	PCR template for C-terminal 6x HA tag with *HIS3* marker	Euroscarf
pRS314	pBlueScript-based centromere vector with *TRP1* marker	Sikorski and Hieter, 1989)
pRS316	pBlueScript-based centromere vector with *URA3* marker	Sikorski and Hieter, 1989)
pRS426	pBlueScript-based centromere vector with *URA3* marker for high copy propagation in yeast	Sikorski and Hieter, 1989)
pRS426-*THO1*	pBlueScript based yeast centromere vector with *URA3* marker and ORF + 500 bp of 5' and 300 bp of 3' UTR of *THO1* for high copy propagation in yeast	Meinel 2013
pBS-Δ*tho1*	*URA3* marker was cloned in between + 300 bp of 5´ and 300 bp of 3´UTR of *THO1* and cloned into pBlueScript	This study
pBS-Δ*tho1*	kanMX marker was cloned in between + 300 bp of 5´ and 300 bp of 3´UTR of *THO1* and cloned into pBlueScript	This study
pBS-Δ*tho1*	*TRP1* marker was cloned in between + 300 bp of 5´ and 300 bp of 3´UTR of *THO1* and cloned into pBlueScript	This study

4.6 Primers

Table 6: Oligonucleotides used for Gibson assembly

Number	Name	Sequence
BB35	pRS316 seq fw	TGT AGC GGT CAC GCT GCG CGT AAC
BB36	pRS316 seq rev	CCG CGC GTT GGC CGA TTC ATT AAT
BB130	Deletion Tho1_Vektor rev	GTCTGCTTTCGGGGGATCCACTAGTTCT
BB131	Deletion Tho1_Vektor fwd	ATTTTGAAATGGGCTGCAGGAATTCGATATCA
BB132	Deletion Tho1_1 Fragment fwd	TGGATCCCCCGAAAGCAGACGATTGGAATTGGTAT
BB133	Deletion Tho1_1 Fragment rev	gatgaattgaaTGTAAGTGCTTGTGCTGGC
BB134	Deletion Tho1_2 Fragment fwd	AAGCACTTACAttcaattcatcatttttttttattctttttttgatttcg
BB135	Deletion Tho1_2 Fragment rev	GCTTGAGCCTttagttttgctggccgcat
BB136	Deletion Tho1_3 Fragment fwd	gcaaaactaaAGGCTCAAGCCGTTTTGGTG

BB137	Deletion Tho1_3 Fragment rev	CCTGCAGCCCATTTCAAAATAAATAGGCCCGCTTG
BK209	pBSdtho1_TRP_Vector rev	TAGTAATGTCGTTTGTAAGTGCTTGTGCTGGC
BK210	pBSdtho1_TRP_Vector fw	GCTAAGAAATAGAGGCTCAAGCCGTTTTG
BK211	pBSdtho1_TRP_Fragment fw	CGGCTTGAGCCTCTATTTCTTAGCATTTTTGACGAAATTTG
BK212	pBSdtho1_KanMX_Vector rev	CAAGCACTTACAAACGACATTACTATATATATAATATAGGAA GCATT
BK213	pBSdtho1_KanMX_Vector fw	ggcctccatgtcTGTAAGTGCTTGTGCTGGC
BK214	pBSdtho1_KanMX_Fragment rev	gtcgctatactgAGGCTCAAGCCGTTTTG
BK215	pBSdtho1_KanMX_Fragment fw	CGGCTTGAGCCTcagtatagcgaccagcatt
BK216	pBSdtho1_KanMX_Fragment fw	CAAGCACTTACAgacatggaggcccagaatac

Table 7: Oligonucleotides used for genomic integration of affinity tags and deletion mutants

Number	Name	Sequence
CW	Tho1-TAP fw	AGAGTAAGTAAAAACAGGAGAGGCAACCGCTCTGGTTACAGAAGATCC ATGGAAAAGAGAAG
CW	Tho1-TAP rev	CCGAAACTAGAATGAAAAACTCCACCAAAACGGCTTGAGCCTTTATACG ACTCACTATAGGG
BB5	-300 bp paf1 fw	ATA CAT ATA CAT ACA CGC AAT GAG AA
BB6	+300 bp paf1 rev	GAA ACA TTA GGG TCG TTA AGC CCA CG
BB11	Hpr1-TAP fw	GCAGCTACT TCGAACATT TCTAATGGT TCATCTACCCAAGAT ATGAAATCCATGGAAAAGAGAAG
BB12	Hpr1-TAP rev	TGCATGAAT TTCTTATCAGTTTAAAATTTCTATTAAGAGGATAATTTATACACTCACTA TAGGG
BB61	HIS3 fwd	AGA TCT TTC GAA CAG GCC GT
BB62	HIS3 rev	ACG GCC TGT TCG AAA GAT CT
BB79	-500 bp Hpr1 fwd:	CGCCTACAAACCAGATTACCGG
BB80	+500 bp Hpr1 rev	TGGAAAGAGAGGAAAAGCGTGG
BB91	+500 bp TEX1 fw	CTGGAGTTGTCTTCAGTATC
BB92	-500 bp TEX1 rev	GACAATTGAGCAGGACCTTA
BB93	TEX1 koloniepcr fw	AAGCTTCCCATTTTAGCGAC
BB98	Tho1 fw kolonie	GATTGTGGGGCACAGATGAT
BB138	URA3 rev	tccttggtggtacgaacatc
BK169	TRP1 fw	GTGTTGATGTAAGCGGAGGT
BK170	TRP1 rev	CAATGGACCAGAACTACCTG
BK171	LEU2 fw	CGGCTGTGATTTCTTGACCA
BK172	LEU2 rev	TTCCAACAGTACCACCGAAG
BK221	Tho1-HA fw	CAACCGCTCCAGAGTAAGTAAAAACAGGAGAGGCAACCGCTCTGGTTACA GAAGA CGTACGCTGCAGGTCGAC
BK222	Tho1-HA rev	AAGTGGGAAAGAACCGAAACTAGAATGAAAAACTCCACCAAAACGGCTTGA GCCTTTA ATCGATGAATTCGAGCTCG
BK223	Paf1-HA fw	TGCTGTTCATACTGAACAAAAACCAGAGGAAGAAAAGGAAACTTTACAAGA AGAA CGTACGCTGCAGGTCGAC

BK224	Paf1-HA rev	CAAATGTAAAAAGAACTACAGGTTTAAAATCAATCTCCCTTCACTTCTCAATA TTCTA ATCGATGAATTCGAGCTCG

Table 8: Oligos for Assays

Name	Sequence	Assay
Oligo(dT_{50})-Cy3	TTTTTTTTTTTTTTTTTTTTTTTTTTTTTTTTTTTTTTTTTT TTTTTTTTTT-(Cy3)	FISH

Table 9: qPCR oliqonucleotides

Name	Sequence
Yer1 (NTR)fwd	TGCGTACAAAAAGTGTCAAGAGAT T
Yer1 (NTR) rev	ATG CGC AAG AAG GTG CCT AT
ADH1-5' fwd	GTTGTCGGCATGGGTGAAA
ADH1-5' rev	GGCGTAGTCACCGATCTTCC
ADH1-M fwd	AGCCGCTCACATTCCTCAAG
ADH1-M rev	ACGGTGATACCAGCACACAAGA
ADH1-3' fwd	TTGGACTTCTTCGCCAGAGG
ADH1-3' rev	GCCGACAACCTTGATTGGAG
PGK1-5' fwd	TTGCCAACCATCAAGTACGTTT
PGK1-5' rev	CCCAAGTGAGAAGCCAAGACA
PGK1-M fwd	GGTAAGGCTTTGGAGAACCCAAC
PGK1-M rev	CGACCTTGTCCAACAAGTTGTC
PGK1-3' fwd	TGACAAGATCTCCCATGTCTCTACTG
PGK1-3' rev	TGGCAATTCCTTACCTTCCAA
PMA1-5' fwd	GTTTTTCGTCGGTCCAATTCA
PMA1-5' rev	AACCGGCAGCCAAAATAGC
PMA1-3' fwd	CAGAGCTGCTGGTCCATTCTG
PMA1-3' rev	GAAGACGGCACCAGCCAAT
CCW12 5´ fwd 2	ACTGTCGCTTCTATCGCCGC
CCW12 5´ rev 2	TTGGCTGACAGTAGCAGTGG
CCW12 M fwd	CTGTCTCCCCAGCTTTGGTT
CCW12 M rev	GGCACCAGGTGGTGTATTGA
CCW12 3´ fwd	TGAAGCTCCAAAGAACACCACC
CCW12 3´rev	AGCAGCAGCACCAGTGTAAG
ILV5 5´fwd	AAGAGAACCTTTGCTTTGGC
ILV5 5´rev	TTGGCTTAACGAAACGGGCA
ILV5 M fwd	TGCCGCTCAATCAGAAACCT
ILV5 M rev	GGGAGAAACCGTGGGAGAAG
ILV5 3´fwd	TGGTACCCAATCTTCAAGAATGC
ILV5 3´rev	ACCGTTCTTGGTAGATTCGTACA
YEF3 5' fwd	GCTGACCCAACTGAAGTTCC
YEF3 5' rev	GGGACCATGATGGACAAAGT
YEF3 M fwd	GGTATCTGTGGTCCAAACG
YEF3 M rev	GGGTTGGGAAACCATCAA
YEF3 3' fwd	TCTGGTCACAACTGGGTTAGTG
YEF3 3' rev	GCAATCTTGTTACCCATAGCATCGA

4.7 Enzymes

Table 10: Enzymes

Enzyme	Supplier
Phusion® High-Fidelity DNA Polymerase	NEB
RNase A	Thermo Fisher Scientific
DNase I	Thermo Fisher Scientific
Proteinase K	Sigma Aldrich
Tobacco etch virus (TEV)-protease	self-made
Zymolyase 100T	Carl Roth
Zymolyase 20T	Carl Roth
Taq DNA Polymerase	self-made
T5 Exconuclease	NEB
Taq DNA Ligase	NEB
Restriction Enzymes	NEB

4.8 Antibodies

Table 11: Antibodies

Name	Source	Dilution	Supplier
anti-Mex67	rabbit	1:5000	(Strässer *et al.*, 2000)
anti-HA-HRP	rabbit	1:1000	R&D Systems
anti-Nab2	mouse	1:5000	Swanson lab (3F2)
anti-Npl3	rabbit	1:5000	Tracy Kress lab
anti-Sto1	rabbit	1:20000	Dirk Görlich lab
anti-Sub2	rabbit	1:10000	(Strässer *et al.*, 2000)
anti-Tho1	rabbit	1:5000	Pineda lab
Anti-Pab1	mouse	1:2000	Encor Biotechnologies
anti-Pgk1	mouse, monoclonal	1:5000	Abcam
Peroxidase anti-Peroxidase (PAP)	rabbit, monoclonal	1:5000	Sigma-Aldrich
RNAPII (8WG16)	mouse	1:250	Covance
ChromPure rabbit IgG for ChIP	Rabbit		Jackson IR Laboratories
anti-rabbit-HRP	goat, monoclonal	1:3000	Biorad; #170-6515
anti-mouse-HRP	goat, monoclonal	1:3000	Biorad; #170-6516
anti-rabbit-Alexa488	Goat	1:200	Invirtogen

5 Methods

5.1 Cloning

Unless further explained in the sections below, standard molecular cloning techniques like growth of bacteria, DNA isolation and DNA analysis on agarose gels in 1x TAE were performed according to (Sambrook and Russell, 2001) or as described in manufactures' manuals. For small-scale plasmid preparation from *E. coli* the NucleoSpin® Plasmid (NoLid)-kit or for mid-scale the NucleoSnap Plasmid Midi-kit (Macherey-Nagel) was used. Purifying and gel extraction of DNA samples were carried out by NucleoSpin® Gel and PCR Clean-up-kit (Macherey-Nagel). All plasmids that have been cloned for this study have been confirmed by sequencing (Microsynth). For visualizing DNA or RNA on agarose gels Intas HDGreenTM was used.

5.1.1 PCR

Phusion High-Fidelity DNA polymerase (cloning and genomic integration) or the self-made Taq DNA polymerase (colony PCR) was used to perform PCRs. The annealing temperature was set according to the used primers and the elongation time was dependent on the length of the expected PCR product. In the tables below, a typical PCR reaction for the Phusion High-Fidelity DNA polymerase (Table 12) as well as the PCR cycling conditions is shown (Table 13).

For PCR products that were supposed to be transformed into yeast, a 300 µL PCR reaction was performed. The amplified PCR product was precipitated and washed by an EtOH precipitation (Ethanol precipitation5.1.4). The pellet was dissolved in 15 µL water.

Table 12: Reaction setup for a standard PCR using Phusion *High-Fidelity* DNA polymerase.

Component	Amount [µL]	Final concentration/amount	Stock concentration
dNTPs	4	200 µM	2.5 mM
Buffer	10	1x	5x
Primer fwd.	0.25	500 nM	100 µM
Primer rev.	0.25	500 nM	100 µM
Template (plasmid)	0.5	≤ 10 ng	Varies
Water	34.5		
Phusion DNA Polymerase	0.5	1 U	2 U/µL
	50 µL		

Table 13: Example for thermocycling condition of a standard PCR reaction using Phusion *High-Fidelity* DNA polymerase

Temperature	Time	
98°C	30 sec	
98°C	10 sec	x32
54°C	30 sec	
72°C	30 sec/kb	
72°C	5-10 min	
4°C	∞	

5.1.1.1 E. coli colony PCR

To screen for successful plasmid cloning, up to 8 freshly grown *E. coli* single colonies were picked with a yellow tip and suspended in 20 µL water. 5 µL cell suspension was used for a PCR reaction (Table 14 & Table 15) and analysed on a 1 % agarose gel in TAE. For two positive clones the rest of the 20 µL cell suspension was used to inoculate a 3 mL LB culture with appropriate antibiotic.

Table 14: Reaction set up for *E. coli* colony PCR.

Component	Amount [µL]	Final concentration/amount	Stock concentration
dNTPs	1.6	200 µM	2.5 mM
Buffer	2	1x	10x
Primer fwd.	0.1	500 nM	100 µM
Primer rev.	0.1	500 nM	100 µM
Template (cell suspension)	5		
Water	10.8		
Taq DNA Polymerase	0.4		
	20 µL		

Table 15: Example for thermocycling condition of a standard PCR reaction using homemade Taq DNA polymerase

Temperature	Time	
95°C	5 min	
95°C	30 sec	x32
48°C	45 sec	
68°C	1 min/kb	
68°C	5-10 min	
4°C	∞	

5.1.1.2 Yeast colony PCR

To screen for positive genomic integration of protein tags or genomic deletions, a small amount of freshly grown cells was picked and suspended in 15 µL zymolyase 20T (2.5 mg/mL) solution to digest the cell wall. The mixture was incubated for 20 min at RT, moved to 37°C for 5 min and afterwards boiled for 5 min at 95°C. The cell suspension was diluted with 60 µL water. Afterwards, 5 µL of the diluted cell suspension were added to a typical PCR reaction (Table 15) and analysed on a 1 % agarose gel in TAE.

5.1.2 Gibson assembly

Gibson assembly was used for cloning of plasmids; adapted to (Gibson *et al.*, 2009). The vector and the inserts were linearized by PCR. The primers for this reaction were designed by using the computer software SnapGene. The emerging PCR products have an overlapping region of about 20-25 bp. The PCR products were digested for one hour with DpnI and gel purified. For a typical Gibson assembly, 50 ng vector was used. A 1:1 ratio between insert and vector was set in the reaction and mixed with 15 µL Gibson assembly master mix and filled up to 20 µL with water. The mixture was incubated for 30 min at 50°C, then 2 µL of the mixture were transformed into *E. coli*.

5.1.3 Digest

A double digest was performed to linearize a plasmid that contains the 5´ and 3´ UTR of *THO1* of *S. cerevisiae* as well as an URA3/TRP1/KanMX cassette to generate a Δ*tho1* strain. The reaction set-up is shown in Table 16. The digest was incubated at 37°C overnight and precipitated with EtOH (5.1.4).

Table 16: Double digest of a plasmid

Component	Amount [µL]
DNA (10 µg)	20
10 x NEBuffer (CutSmart® buffer)	10
Restriction enzyme (XhoI)	1
Restriction enzyme (SacI)	1
Water	68
	100 µL

5.1.4 Ethanol precipitation

DNA was precipitated by adding 2.5 - 3 volumes of 100 % EtOH and 1/10 volume 3 M NaOAc (pH 5.2). After shortly vortexing it was incubated for at least 20 min at -20°C followed by a centrifugation step at 4°C at 12000 g for 20 min. The pellet was washed once with 70 % EtOH and dried at RT. The pellet was resolved in 15 µL pure water.

5.2 Yeast and *E. coli* cultivation

5.2.1 *E. coli* transformation

According to manufacturer's manual for the Mix & Go *E. coli* Transformation Kit (Zymo Research Corp.), competent cells were made and stored at -80°C until needed. Per transformation a 50 µL aliquot was thawed on ice and 2 µL Gibson assembly mix or 0.5 µL of plasmid-miniprep was added. It was mixed by flicking several times against the tube and incubated for 10 min on ice. The cells were heat shocked for 45 sec at 42°C and immediately put on ice for 1 min. For recovery, 400 µL SOC were added and the mix was incubated for 1 hour at 37°C on a shaker at 200 rpm. Afterwards the cells were pelleted at 10.000 g for 10 sec and resuspended in 150 µL water. The cells were spread on selective LB-plate and incubated overnight at 37°C.

5.2.2 Yeast cultivation

S. cerevisiae cells were streaked out every four weeks on plates containing full media (YPD) or synthetic complete (SDC) media (lacking at least one amino acid for selection). The cells were cultivated for two days at 30°C after this time the plates were kept at 4°C. For liquid cultures, a single colony was picked for inoculation. The cells were shaking at 30 °C with 1200 rpm, usually overnight. The optical density (OD) was determined in a spectrometer at 600 nm.

5.2.3 Transformation in *S. cerevisiae*

For five to six yeast transformations of a plasmid or linearized DNA, the overnight pre-culture was diluted to an OD_{600} = 0.2 in 50 mL. The cells were grown at 30°C and

1200 rpm shaking to log phase (OD_{600} 0.6 - 0.8) and harvested by centrifugation for 3 min at 2800 g. Cells were washed with 10 mL water. The pellet was resuspended in 500 µL solution I and transferred in a 2 mL tube. Cells were pelleted at 1200 g for 3 min and resuspended in 250 µL solution I. For each transformation, 50 µL cells were incubated with either 500 ng plasmid DNA or 10 µg linearized DNA, 5 µL carrier DNA (2 mg/ µL) and 300 µL solution II for 30 min on a turning wheel at RT. Cells were heat shocked for 10 min at 42°C and then transferred to ice for 3 min. For dilution of solution II, 1 mL water was added to the transformation mix and cells were pelleted at 1200 g for 3 min. For genomic integrations, cells were recovered for at least 2 h shaking at 1200 rpm at 30 °C in YPD. After recovery the cells were pelleted and resuspended in 100 µL water and spread out on selective media plates. Cells transformed with a plasmid were directly spread out on selective media without recovery. Plates were incubated 2 - 4 days at 30°C.

5.3 Dot Spots

A dot spot assay was performed to identify a potential growth defect in mutant strains. Yeast cells were picked with a white loop and suspended in 1 mL water. The OD_{600} was measured and the cell suspension adjusted to 0.15 to ensure that all strains had the same amount of cells. A 10-fold serial dilution with 4 steps was done for each strain. 5 µL of each dilution and strain were spotted on respective media plates. The plate was air-dried and incubated at 16°C, 25°C, 30°C and 37°C for up to 10 days.

5.4 Survival assay

For the survival assay the overnight pre-culture was diluted to an OD_{600} = 0.2 in 50 mL. After the cells had attained an OD_{600} = 0.6, three different 10 mL aliquots were collected. One aliquot was harvested and used as 30°C control. One aliquot was shifted to 42°C for 30 min to determine the survival rate after heat stress. The third aliquot was shifted to 52°C to determine the survival rate (Zander *et al.*, 2016). Following the heat shock the cells were also harvested, all aliquots were resuspended in 1 mL water and adjusted to OD_{600} = 0.6. The cells were diluted 1:100 and 200 µL cells of the 52°C sample were spread on YPD plates. The cells of the 30°C and 42°C samples were again diluted 1:100 and 200 µL spread on YPD plates. The plates were incubated for two days at 30°C followed by scanning and counting with ImageJ.

5.5 Tandem Affinity Purification (TAP)

The TAP was performed to purify the fused protein and its interacting proteins from yeast. Tandem affinity purification (TAP) was performed according to (Puig *et al.*, 2001; Rigaut

et al., 1999). The used TAP tags consist of two minimal protein A domains followed by a TEV cleavage site and either a calmodulin-binding peptide (CBP) or a FLAG-tag.

For one purification, the cell pellet of 2 L yeast culture with an OD_{600} = 3.5 was used. Cells were harvested with 7000 g for 5 min at RT and resuspended in 2.5 mL TAP LB buffer. The suspension was dropped into a container filled with liquid nitrogen to get flash frozen pearls. The pearls were lysed by using a freezer mill 6870D (SPEX SamplePrep). The lysed cells were kept at -80°C until use.

Before thawing the lysate, 10 mL TAP-buffer + 1x protease inhibitor and 1 mM DTT were added. The thawed lysate was centrifuged at 3500 g for 12 min at 4°C to preclear; this step was followed by an ultracentrifugation step for 1 h at 4°C at 165,000 g. During this step, 500 µL IgG Sepharose 6 fast flow affinity resin per purification were washed three times with 10 mL TAP-buffer by centrifugation at 700 g for 3 min and distributed to a 50 mL tube. After the ultracentrifugation step, the fatty phase was removed by vacuum pump and the clear supernatant was transferred to the IgG Sepharose. In case of an RNase A digest, 100 µg/mL RNase A was added to the clear supernatant after ultracentrifugation and incubated at RT for 15 min on a rotating wheel before the IgG Sepharose was added. The supernatant was incubated with IgG Sepharose for 2 hours at 4°C on a rotating wheel. Afterwards the IgG Sepharose was centrifuged at 700 g for 3 min and the supernatant was thoroughly removed by vacuum pump. The IgG Sepharose was transferred to a Mobicol (MoBiTec) and washed with 10 mL TAP-buffer by gravity flow. To release the bound protein complex, the Mobicol was closed and 140 µL TAP-buffer + 7.5 µL TEV-protease were added and incubated at 16°C for 1 hour on a rotating wheel. The TEV-eluate was spun into a fresh 2 mL tube. The TEV-eluate was generally used for western blotting to verify interacting partners.

5.6 SDS-polyacrylamide gel electrophoresis

Sodium dodecylsulfate polyacrylamide gel electrophoresis (SDS-PAGE) was done according to (Laemmli, 1970). The gels were cast in Mini-Protean II system (Biorad) according to (Sambrook and Russell, 2001). After electrophoresis the separated proteins were either transferred to a membrane for western blotting or directly stained with a modified Fairbanks Coomassie-staining method (Fairbanks *et al.*, 1971; Wong *et al.*, 2000). For staining, the gel was covered with Coomassie-solution, heated up in the microwave and incubated on a rocker at RT for 15 min. Afterwards the Coomassie was removed and destain-solution was added to clear the background. The gel and destain-solution were heated up in the microwave and incubated on a rocker at RT until the

destain-solution was cooled. This step was repeated two to three times until the background was completely destained.

5.7 Western blot

To transfer proteins from a SDS-PAGE gel onto a nitro-cellulose membrane (Porablot NCL, Macherey-Nagel), a semi dry blotting device (Trans-Blot Turbo Transfer System; Biorad) was used. To assemble the blotting device, an extra thick western blotting filter paper (Thermo scientific) followed by a nitro-cellulose membrane and the SDS-PAGE gel and another filter paper were stacked. All components were presoaked in 1x Semi-dry buffer Towbin. Proteins were transferred at 25 V for 30 min. Membrane was blocked with 5 % milk powder in TBST followed by incubation with primary antibody (Table 11) at 4°C overnight. The membrane was washed 3x for 10 min with 1x TBST. Thereafter the membrane was incubated for 2 h at RT with the corresponding secondary antibody and washed 3x for 10 min with 1x TBST. The proteins were detected with CheLuminate-HRP ECLsolution (Applichem) and the chemiluminescence signals were imaged using a ChemoCam Imager (Intas) and quantified by using FIJI.

5.8 Chromatin Immunoprecipitation (ChIP)

To investigate the relative occupancy of proteins on target genes, **ch**romatin **i**mmuno**p**recipitation (ChIP) was performed. An adapted ChIP protocol according to (Aparicio *et al.*, 2005) was used.

An overnight pre-culture was diluted to OD_{600} = 0.2 in 100 mL appropriate medium. When reaching an OD_{600} = 0.8, cells were crosslinked with 1 % formaldehyde on a rocker at RT for 20 min. The reaction was stopped by adding 12.5 mL glycine (3 M) for 10 min. The cells were harvested at 2800 g for 3 min and washed 3 times in 1x PBS. The cell pellet was flash frozen in liquid nitrogen and stored at -80°C until use.

The pellet was thawed on ice and resuspended in 800 µL low salt buffer and transferred to a screw cap tube that was prefilled with ~300 µL glass beads. The cells were lysed with a FastPrep 24G device two times for 45 sec (6.5 m/s setting) with 2 min on ice in between. To get rid of the glass beads, a hole was punched in the cap and bottom of the tube with a hot needle and centrifuged for 30 sec at 500 rpm. To shear the chromatin to ~250 bp fragments, the lysate was sonicated in a Bioruptor three times for 15 min with two min breaks on ice. The lysate was cleared by centrifugation at 18000 g, once for 5 min and once for 10 min. The supernatant was transferred to a fresh tube between centrifugation steps. The DNA concentration was measured at the NanoDrop and

adjusted to the lowest measured sample. After the adjustment, 10 µL input sample were transferred to a low binding tube and kept at 4°C. For TAP-tagged proteins, 15 µL magnetic Dynabeads coupled with IgG were added to the remaining sample and incubated for 2.5 hours on a rotating wheel at RT. For RNAPII-ChIPs 4 µL of α-RPB1 antibody (CTD repeat YSPTSPS; 8WG16; 1 mg/mL) were added and incubated for 1.5 hours on a rotating wheel at RT before 15 µL of Dynabeads coupled with protein G were added for another hour. The beads were collected on a magnetic particle collector (MPC) and washed with 800 µL buffer (2x low-salt buffer, 2x high-salt buffer, 2x TLEND, 1x TE) for 2 min on a rotating wheel. To elute the proteins and the bound DNA fragments, 130 µL ChIP elution buffer were added to the beads and incubated on a thermo-shaker at 65°C at 1000 rpm for 20 min. After short incubation on the MPC, the supernatant was transferred to a fresh low binding tube and 80 µL of 1x TE and 10 µL proteinase K (10 mg/L) were added. The input sample was mixed with 80 µL ChIP-elution buffer, 80 µL 1x TE and 10 µL proteinase K. Reverse crosslinking was done by incubating the samples for 2 hours at 37°C followed by 12-14 hours at 65°C. The DNA was purified using the *PCR NucleoSpin® Gel and PCR Clean-up-kit* (Macherey-Nagel) according to the manufacturer's manual, except that elution was done in 140 µL elution buffer.

5.9 qPCR

The purified DNA from the ChIP experiment was analyzed by quantitative real-time PCR. For quantification, the QuantStudio 3 cycler (Applied Biosystems) was used. To determine the primer efficiencies, a standard curve was used. Every sample was measured as a technical triplicate and standard curve and controls were measured as duplicates. Melting curve analysis was performed to verify the specificity of the primers. A typical qPCR reaction mix is displayed in Table 18 and the cycling conditions in Table 17. The purified DNA was diluted 1:20. Ct values (cycle threshold) were calculated by the Design and Analysis Software v1.5.1 QuantStudio 3 and 5 systems (Applied Biosystems). For calculation of the relative enrichment, a non-transcribed region (NTR) on Chromosome V (174131-174200) was used. Occupancies were calculated as enrichment of the tested gene relative to the NTR with the following formula (comparative Ct method): (E^(CTIPCTINP))NTR/(E^(CTIP-CTINP)YFG) as described by (Livak and Schmittgen, 2001).

Table 17: Cycling conditions qPCR

Temperature	Time	
95°C	10 min	
95°C	15 sec	x 40
60°C	60 sec	
Melting curve		
95°C	15 sec	
60°C	60 sec	0.05°C/s
95°C	15sec	

Table 18: reaction mix qPCR

Component	Amount [µL]	Final concentration
2xPowerUp™ SYBR® Green Mastermix	5	
Primer fw	0.1	100 pmol/µL
Primer rev	0.1	100 pmol/µL
Water	2.3	
Template	2.5	
	10 µL	

5.10 Fluorescence *in situ* hybridization (FISH)

In situ hybridization against poly(A)+ RNA was done according to (Amberg *et al.*, 1992). Cells were grown at 30°C in YPD to mid-log phase before shifting to 18°C or 37°C for one hour. Before the cells were shifted, a 10 mL aliquot was removed and immediately cross linked as non-treated control. Cells were fixed with 4 % formaldehyde for 90 min on a rotating wheel. If cells were shifted, the first 15 min of the fixation step were done at the according temperature. Cells were washed once with 5 mL and once with 1 mL 0.1 M KPO4. A third washing step with washing buffer followed. Cells were spheroplasted with 100T zymolase for 30 min at 30°C and washed. Cells were resuspended in approximately the 10 x volume and one drop was pipetted on a slide well pre-coated with poly-lysine. The cell suspension was removed after 5 min to get rid of non-adherent cells. The slide was dried on the bench for one hour, followed by an incubation with 100 µL 2x SSC for 10 min. The cells were prehybridized for 1 hour at 37°C in prehybridization buffer in a humid chamber. To hybridize with oligo d(T50)-Cy3, 0.75 µL of 1 pmol/µL probe was added and incubated at 37°C O/N in a humid chamber. Cells were washed with 0.5 x SSC for 30 min, mounted with ROTI®Mount FluorCare DAPI and covered with a coverslip. The cells were inspected with an Axio observer fluorescence microscope (Zeiss) connected to a CCD camera.

5.11 Determination of mRNA stability and possible splicing defects

To determine the half-life of selected transcripts, the cells were treated with thiolutin a polymerase II inhibitor. The cells were grown at 30°C until they reached an OD_{600} of 0.5.

A 10 mL aliquot of cells was removed and immediately harvested (timepoint 0). The rest of the cells were treated with a final concentration of 8 µg/mL thiolutin. After 15, 30 and 90 min a 10 mL aliquot was harvested and flash frozen in liquid nitrogen. The RNA was extracted according to 5.12 and used for reverse transcription using super script III according to manufacturer's protocol. The cDNA was analyzed by qPCR.

To assess whether a splicing defect exists, the cDNA of the timepoint 0 was analyzed by qPCR using one primer pair flanking an intron and one primer pair with a primer within the intron and a primer 3' of the Intron. Afterwards the ratio of the ct values of these two primer pairs was calculated to see if the amount of retained introns is changing in the ∆*tho1* mutant.

5.12 RNA extraction

For RNA extraction, the cell pellet was resuspended in 1 mL Trizol via up and down pipetting. After an incubation of 5 min at RT, 200 µL chloroform were added and incubated for another 3 min. The sample was centrifuged at 18,000 g for 20 min at 4°C to separate nucleic acids and proteins. The upper aqueous phase containing the nucleic acids was transferred to a fresh tube. 0.5 mL isopropanol and 2 µL glycogen were added and incubated on ice for 10 min for precipitation. Afterwards it was pelleted at 13,500 g for 10 min. The pellet was washed with 75 % EtOH, dried and dissolved in DEPC-treated RNase-free water. The remaining DNA was digested by DNase I for 30 min at 37°C. During this step, RNase inhibitor was present.

6 Results

Already during transcription, the emerging (pre-)mRNA is bound by RNA-binding proteins (RBPs). Tho1, a conserved nuclear RNA binding-protein binds to the chromatin and the mRNA in a length-dependent manner (Jimeno *et al.*, 2006; Meinel, 2013). The aim of this project was to elucidate the role of Tho1 in the formation of export competent mRNPs.

6.1 Assessment of growth defects

To examine whether deletion or overexpression of Tho1 have an effect on the fitness of cells, dot spot assays were performed. Cells were spotted on YPD or respective selective media and grown at different temperatures for 2 to 7 days.

6.1.1 *THO1* deletion strain grows like wild type in three different strain backgrounds

THO1 was deleted via homologous recombination of a *URA3* cassette into the *THO1* gene locus in the three strain backgrounds RS453, W303 and BY4743. Growth was then tested at 16°C, 25°C, 30°C and 37°C degrees. Cells with BY4743 background grow faster compared to the other tested genotypes at all temperatures. RS453 has the slowest growth, which is especially prominent at 16°C. The Δ*tho1* mutant grows like the corresponding wild-type cells in all three genotypes at all temperatures (Figure 4).

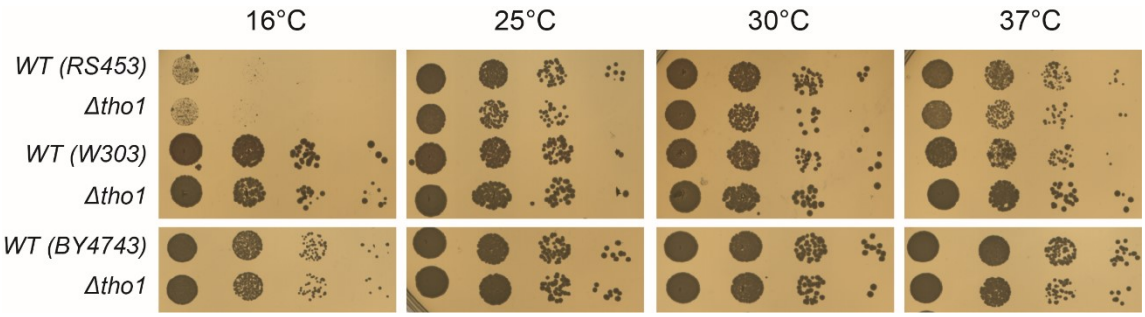

Figure 4: Dot spots of *THO1* deletion strains. Δ*tho1* cells grow like the corresponding wild type. The three distinct wild types show different growth rates, especially prominent at 16°C. The cells were spotted on YPD in a 10 times serial dilution. The cells were incubated for 2-3 days at 25°C, 30°C and 37°C and up to 7 days at 16°C.

6.1.2 Deletion of *THO1* rescues the growth phenotypes of Δ*paf1* and Δ*hpr1*

It is assumed that Tho1 for the most part behaves like Hpr1. In a previous study, it could be shown that the recruitment of Tho1 to the transcribed gene is at least partly dependent

on the correct phosphorylation of Spt5. The recruitment of Tho1 resembles the recruitment of Paf1 and is converse to Hpr1 (Meinel, 2013). For this reason, we became interested in the relationship between these three proteins. Δ*hpr1*Δ*tho1* and Δ*paf1*Δ*tho1* double deletion mutants were produced by homologous recombination of a *TRP1* cassette into the *THO1* locus. A *KanMX* cassette was integrated into the *PAF1* locus and a *HIS3* cassette into the *HPR1* locus. Because a Δ*hpr1*Δ*paf1* double mutant is inviable (Betz *et al.*, 2002; Chang *et al.*, 1999), this strain was not included in this assay. A dot spot assay at different temperatures (16°C, 25°C, 30°C and 37°C) was performed. While Δ*tho1* shows no growth defect, Δ*hpr1* shows a growth defect at all temperatures, which is more prominent at 16°C and 37°C than at 25°C or 30°C. The single mutant Δ*paf1* shows a strong growth defect at all temperatures and is lethal at 37°C. The additional deletion of *THO1* rescued the phenotype of both single mutants at 16°C. The effect might be present as well for 25°C, 30°C, and for Δ*hpr1* also at 37°C, but not as strong as at 16°C. Like the Δ*paf1* single mutant, the double deletion mutant of Δ*paf1*Δ*tho1* is dead at 37°C (Figure 5).

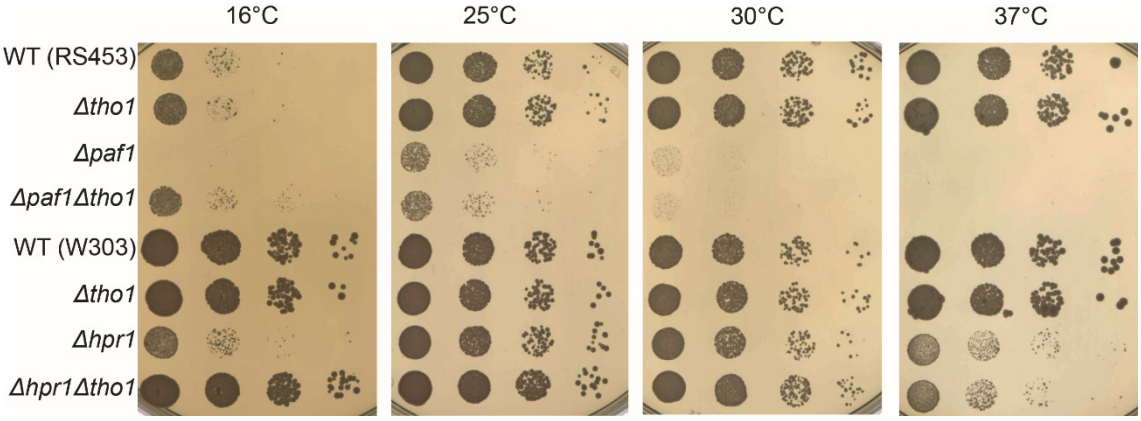

Figure 5: Deletion of *THO1* rescues the growth defect of Δ*paf1* and Δ*hpr1*. The Δ*paf1* single mutant displays a strong growth defect at all temperatures. Additional deletion of *THO1* rescues the growth defect of Δ*paf1* at the lower temperatures 16°C and 25°C. No rescue effect of Δ*tho1* is observable at 30°C and 37°C in the Δ*paf1*Δ*tho1* double mutant. Δ*tho1* rescues the mild growth defect of Δ*hpr*1 at all temperatures. *PAF1* was deleted by insertion of a *KanMX* cassette into the gene. *HPR1* deletion was introduced via homologous recombination of *HIS3* cassette into the gene. The additional deletion of *THO1* was inserted via homologous recombination of *TRP1* cassette into the *THO1* gene. Cells were spotted on YPD and grown for 2-4 days at 25°C, 30°C and 37°C and up to 7 days at 16°C.

To verify that the rescue by Δ*tho1* in the double mutant does not depend on the inserted *TRP1* cassette (González *et al.*, 2008) rather than the deletion of *THO1* itself, the wild-type cells and the Δ*paf1* and Δ*hpr1* single mutants were transformed with an empty plasmid (pRS314) that contains a *TRP1* cassette. The dot spot assay was repeated on SDC-TRP plates at 16°C and 30°C. The temperatures were chosen because the

observed effect was strongest at 16°C; 30°C served as control. After transforming the strains with the *TRP1* cassette-containing plasmid, the single mutants still showed the same growth defect as before (cf. Figure 5 and Figure 6). The additional deletion of *THO1* reduces the growth defect of Δ*hpr1* and Δ*paf1* (Figure 6). The effect seems to be weaker than before but is still present (cf. Figure 5 and Figure 6).

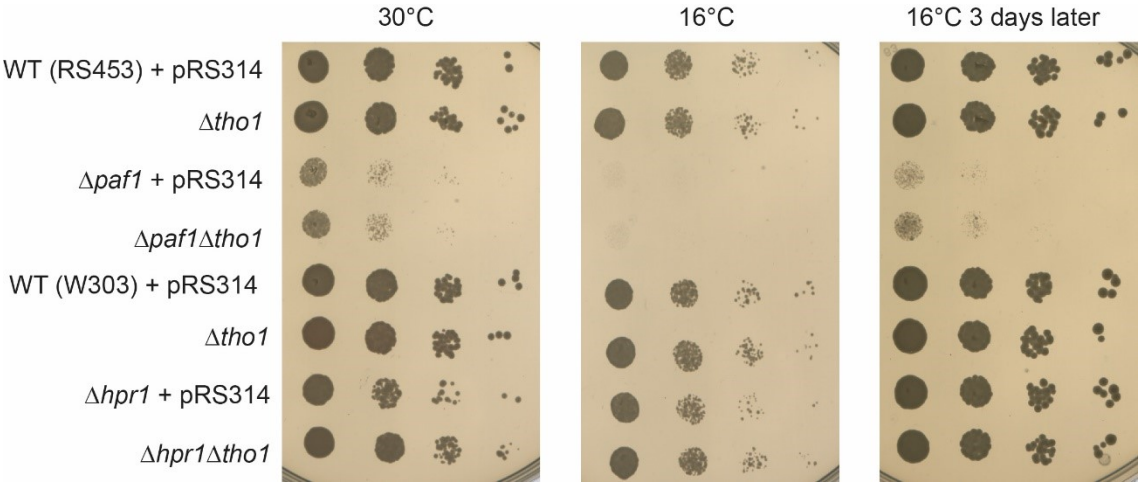

Figure 6: The rescue effect of Δ*tho1* is not dependent on the inserted *TRP1* cassette. The rescue effect of Δ*tho1* is still observable at 16°C and also 30°C even though it is not as strong as without the *TRP1*-cassette. *PAF1* was deleted via insertion of a *KanMX* cassette into the gene. *HPR1* deletion was introduced via homologous recombination of the *HIS3* cassette into the gene. The additional deletion of *THO1* was inserted via homologous recombination of the *TRP1* cassette into the *THO1* gene. The wild-type cells, Δ*paf1* and Δ*hpr1* cells were transformed with an additional pRS314 plasmid. Cells were spotted on SDC-TRP and grown for 2-4 days at 30°C and up to 9 days at 16°C.

6.1.3 Additional expression of *THO1* does not change the growth of cells

The growth of cells expressing the multicopy plasmid *pRS426-THO1* is not affected in the genotypes RS453 and BY4743. The cells were spotted on SDC-URA plates and the growth was tested at 16°C, 25°C, 30°C and 37°C (Figure 7).

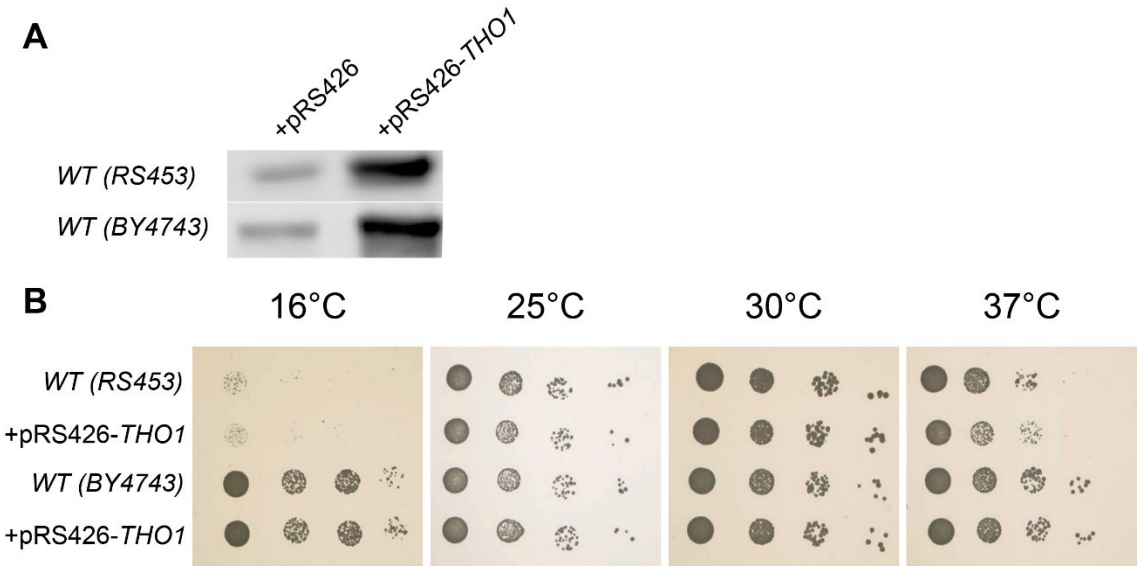

Figure 7: Dot spots of cells expressing pRS426-*THO1*. A) Western blot against Tho1 shows that the transformation of pRS426-*THO1* results in an overexpression of Tho1. B) The growth of cells overexpressing *THO1* is unaffected. Cells were spotted on SDC-URA in a 10 times serial dilution. The cells grew for 2-3 days at 25°C, 30°C and 37°C and up to 7 days at 16°C.

6.2 Survival of Δ*tho1* cells is not significantly changed at high temperatures

Since Δ*tho1* does not show a growth defect, the survival of cells after heat shock was assessed. The cells were grown to mid log phase and shifted to 42°C or 52°C for 30 min. After the treatment, all cells were adjusted to OD_{600} = 0.6 and a 1:100 or 1:1000 dilution was plated on YPD. After 2 days at 30°C, the cells were counted. No effect between the wild type and Δ*tho1* cells was observed at 30°C and 42°C. Also, the cell number between these two temperatures was not much altered (Figure 8A & B). The survival rate after the 52°C treatment was low in the wild-type and mutant cells. The Δ*tho1* cells indicate a decrease that is not significant.

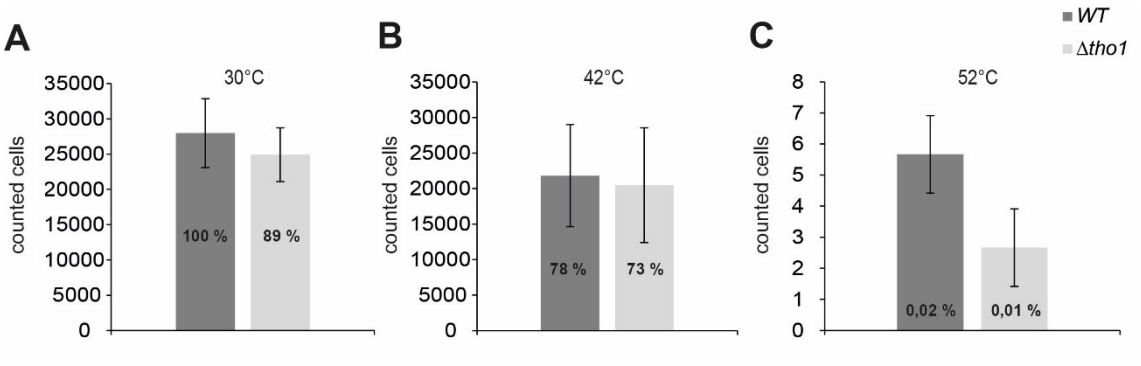

Figure 8: Survival of Δ*tho1* cells at high temperatures. No change in the cell number at 30°C and 42°C between WT and Δ*tho1* cells (**A**&**B**). After treatment with 52°C, the survival rate was very low. Δ*tho1* cells display an even lower survival rate than WT (**C**). The cells were grown to mid log phase. The 30°C sample was harvested while the other two sample were shifted to the respective temperature for 30 min. After harvesting, the cells were adjusted to OD_{600} = 0.6. A 1:1000 dilution for 30°C and 42°C sample and a 1:100 dilution for the 52°C sample were plated on YPD plates and grown for 2 days at 30°C, followed by counting the cells with ImageJ. The mean ± standard deviation was calculated for three biological replicates. The student t-test resulted in no significant change. The survival rate was calculated in comparison to wild-type cells at 30°C.

6.3 Tho1 functions in the recruitment of Hpr1 and Paf1 to the transcribed gene

The recruitment of Tho1 to transcribed genes depends partly on the correct phosphorylation of Spt5. In the phospho-mimic mutant *spt5-S1D*, the recruitment of Tho1 increases at the transcribed gene and resembles the occupancy of Paf1. The occupancy of Hpr1 decreases in this mutant (Meinel, 2013). At this point, we became interested in the interplay between these three proteins. Therefore, chromatin immunoprecipitation (ChIP) experiments were performed to elucidate the role of Tho1 in the recruitment of these proteins to four exemplary tested genes at three regions (*PMA*, *ILV5*, *CCW12* and *YEF3* (Figure 9A, Figure 10A, Figure 11A, Figure 12A)). The selected genes are intron-less, vary in length and are highly transcribed by RNAPII ((Geisberg *et al.*, 2014) tested in a preliminary experiment). First, the occupancy of RNAPII was determined in the different mutants. Since the recruitment of proteins to transcribed genes depends on transcription, it is essential to assess whether the effect of a mutation is due to a change in transcription or directly affects recruitment. No change could be observed for the occupancy of RNAPII in Δ*tho1* cells compared to wild-type cells (Figure 9B). In Δ*hpr1* and Δ*paf1* cells, RNAPII occupancy is decreased at the transcribed genes (Figure 10B & Figure 11B). Therefore, the occupancy of analyzed proteins at transcribed genes was normalized to the level of RNAPII in Δ*hpr1* and Δ*paf1* cells.

After deletion of *THO1,* an increased amount of Hpr1 can be detected at transcribed genes (Figure 9C). At the same time, the occupancy of Paf1 is decreased (Figure 9D). Hpr1 and Paf1 reconfirm their opposite recruitment pattern (cf. Figure 9C & D). The occupancy of Spt5 is not altered in Δ*tho1* cells compared to wild-type cells (Figure 9E).

Deletion of *HPR1* leads to a strong decrease of Tho1 recruitment to transcribed genes, with Tho1 levels nearly dropping to background level (Figure 10C). Even after normalization to RNAPII, Tho1 levels are significant decreased at transcribed genes in Δ*hpr1* (Figure 10E). In Δ*hpr1* cells, the occupancy of Paf1 is increased compared to the wildtype after normalization to RNAPII (Figure 10F). In Δ*hpr1* cells, Tho1 and Paf1 occupancies at transcribed genes are inversely correlated (cf. Figure 10E & F).

After normalization to RNAPII, Tho1 occupancy increased in Δ*paf1* cells at transcribed genes (Figure 11E). The occupancy of Hpr1 at transcribed genes was mostly not changed in Δ*paf1* cells (Figure 11D). After normalization to RNAPII, the occupancy of Hpr1 was increased at three (*PMA*, *ILV5* and *CCW12*) out of four genes. For *YEF3* no significant increase could be observed, probably due to the low decrease in the RNAPII ChIP (Figure 11A & F). The occupancy of Hpr1 and Tho1 was increased.

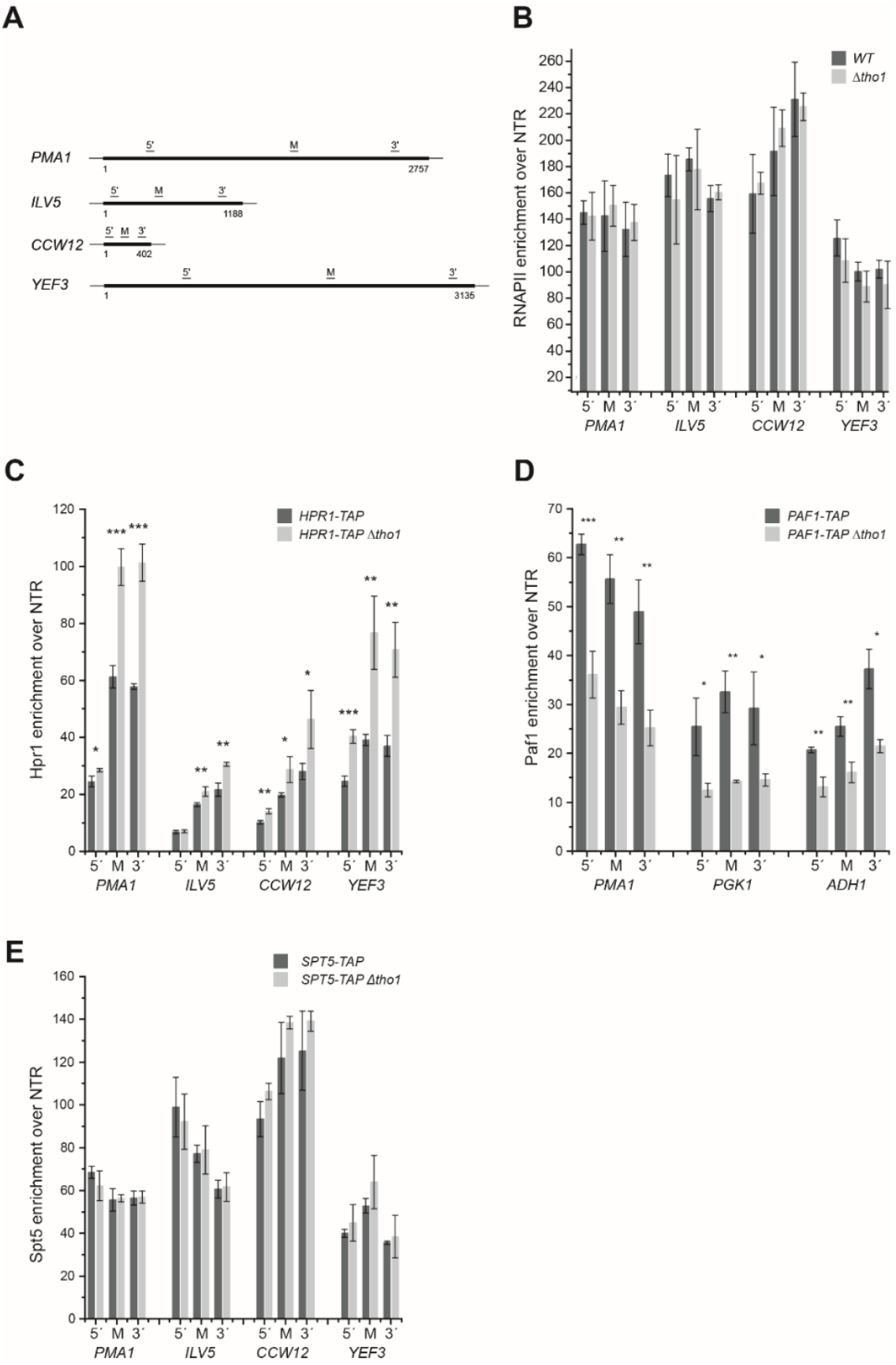

Figure 9: Δ*tho1* leads to increased occupancy of Hpr1 and to a decreased occupancy of Paf1 at transcribed genes. The recruitment of the proteins of interest to transcribed genes was assessed by

chromatin immunoprecipitation (ChIP). The enrichment of the respective protein was calculated over a non-transcribed region (NTR). For the pull-down of RNAPII, the 8WG16 antibody with Protein G Dynabeads was used. For the other Proteins the TAP-tag version of the protein with IgG coupled Dynabeads was used. (**A**) Scheme representing the four tested genes (*PMA*, *CCW12*, *ILV5* and *YEF3)*. The solid line represents the open reading frame (ORF). The primers used for qPCR are represented by bars above the genes. 5´ = 5´ region, M = middle region and 3´ = 3´region of the ORF. (**B**) Deletion of *THO1* does not change the occupancy of RNAPII at transcribed genes. (**C**) Deletion of *THO1* increases the occupancy of Hpr1 at the transcribed genes. (**D**) A decrease in the occupancy of Paf1 at transcribed genes was detected in Δ*tho1* cells. (ChIP was performed by Christoph Wierschem) (**E**) No change in the occupancy of Spt5 could be detected in Δ*tho1 cells.* The mean ± standard deviation was calculated for three biological replicates. * P value 0.05, ** P value 0.01, *** P value 0.001 students t-test.

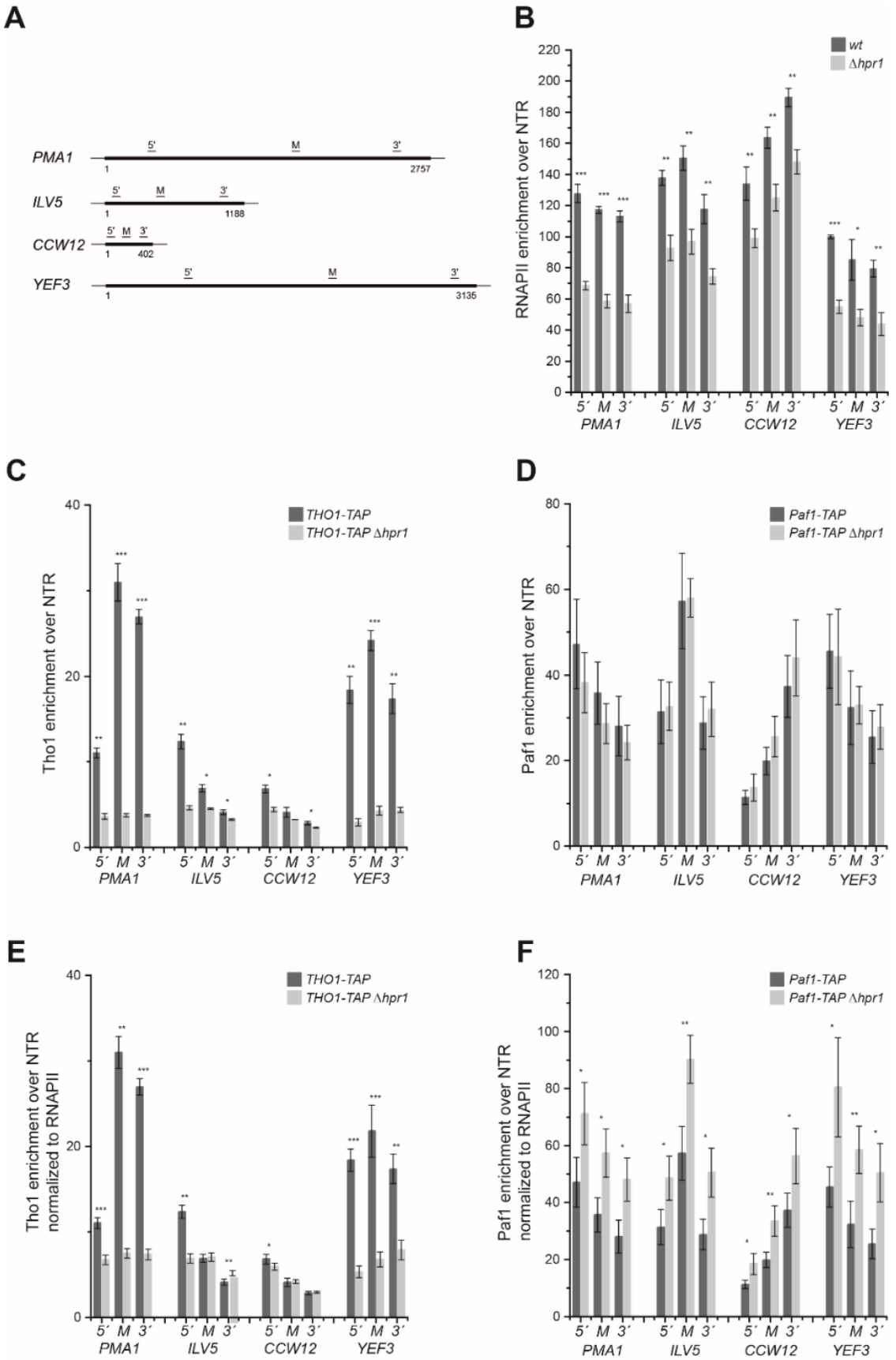

Figure 10: Deletion of *HPR1* abolished the recruitment of Tho1 but increased the occupancy of Paf1.
The recruitment of the proteins of interest to transcribed genes was assessed by chromatin

immunoprecipitation (ChIP). The enrichment of the respective protein was calculated over a non-transcribed region (NTR). For the pull-down of RNAPII, the 8WG16 antibody with Protein G Dynabeads was used. For the other proteins, the TAP-tag version of the protein with IgG-coupled Dynabeads was used. (**A**) Scheme representing the four genes (*PMA*, *CCW12*, *ILV5* and *YEF3)* tested. The solid line represents the open reading frame (ORF). The primers used for qPCR are represented by bars above the genes. 5´= 5´ region, M= middle region and 3´= 3´region of the ORF. (**B**) Deletion of *HPR1* leads to a decreased occupancy of RNAPII at transcribed genes. (**C**) Deletion of *HPR1* decreased the occupancy of Tho1 to nearly background level. (**D**) No change in the occupancy of Paf1 at transcribed genes if *HPR1* is deleted. (**E**&**F**) Normalization to the RNAPII of Tho1 and Paf1 ChIPs. Even after normalization to RNAPII, Tho1 displays a reduced occupancy. Paf1 shows an increased occupancy afterwards. The mean ± standard deviation was calculated for three biological replicates. * P value 0.05, ** P value 0.01, *** P value 0.001 students t-test.

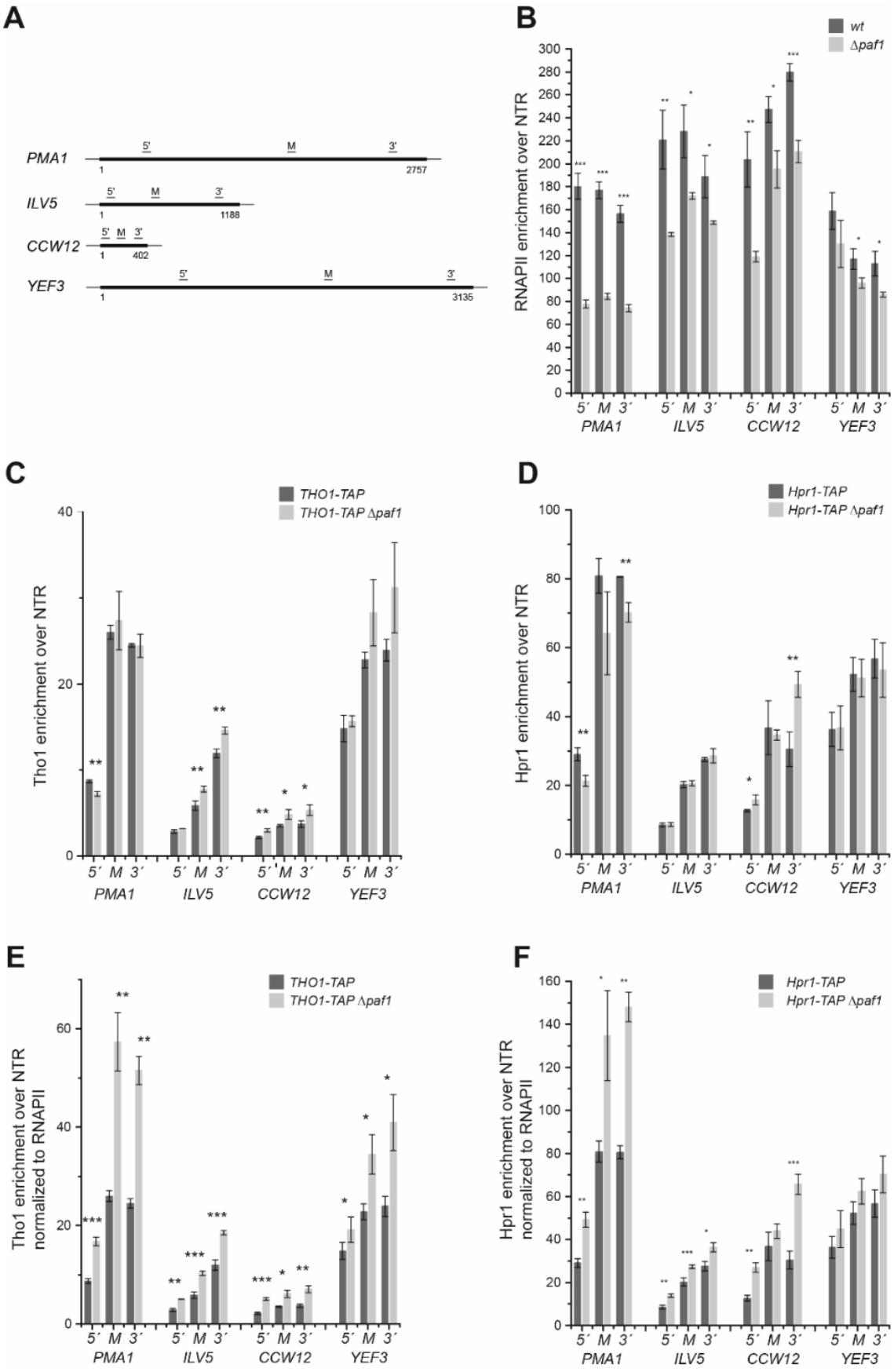

Figure 11: Δ*paf1* leads to increased Tho1 and Hpr1 occupancy at transcribed genes. The recruitment of the proteins of interest to transcribed genes was assessed by chromatin immunoprecipitation (ChIP). The

enrichment of the respective protein was calculated over a non-transcribed region (NTR). For the pull-down of RNAPII, the 8WG16 antibody with Protein G Dynabeads was used. For the other proteins, the TAP-tag version of the protein with IgG-coupled Dynabeads was used. (**A**) Scheme representing the four tested genes (*PMA*, *CCW12*, *ILV5* and *YEF3)*. The solid line represents the open reading frame (ORF). The primers used for qPCR are represented by bars above the genes. 5´ = 5´ region, M = middle region and 3´ = 3´region of the ORF. (**B & C**) Deletion of *PAF1* leads to varying occupancies of Tho1 and Hpr1 at transcribed genes. After normalization to RNAPII, Tho1 and Hpr1 show an increased occupancy at transcribed genes (**D & E**) The mean ± standard deviation was calculated for three biological replicates. * P value 0.05, ** P value 0.01, *** P value 0.001 students t-test.

The overexpression of Tho1 induced by the multicopy plasmid pRS426-*THO1* does not affect the occupancies of RNAPII and Paf1 at transcribed genes (Figure 12B & C).

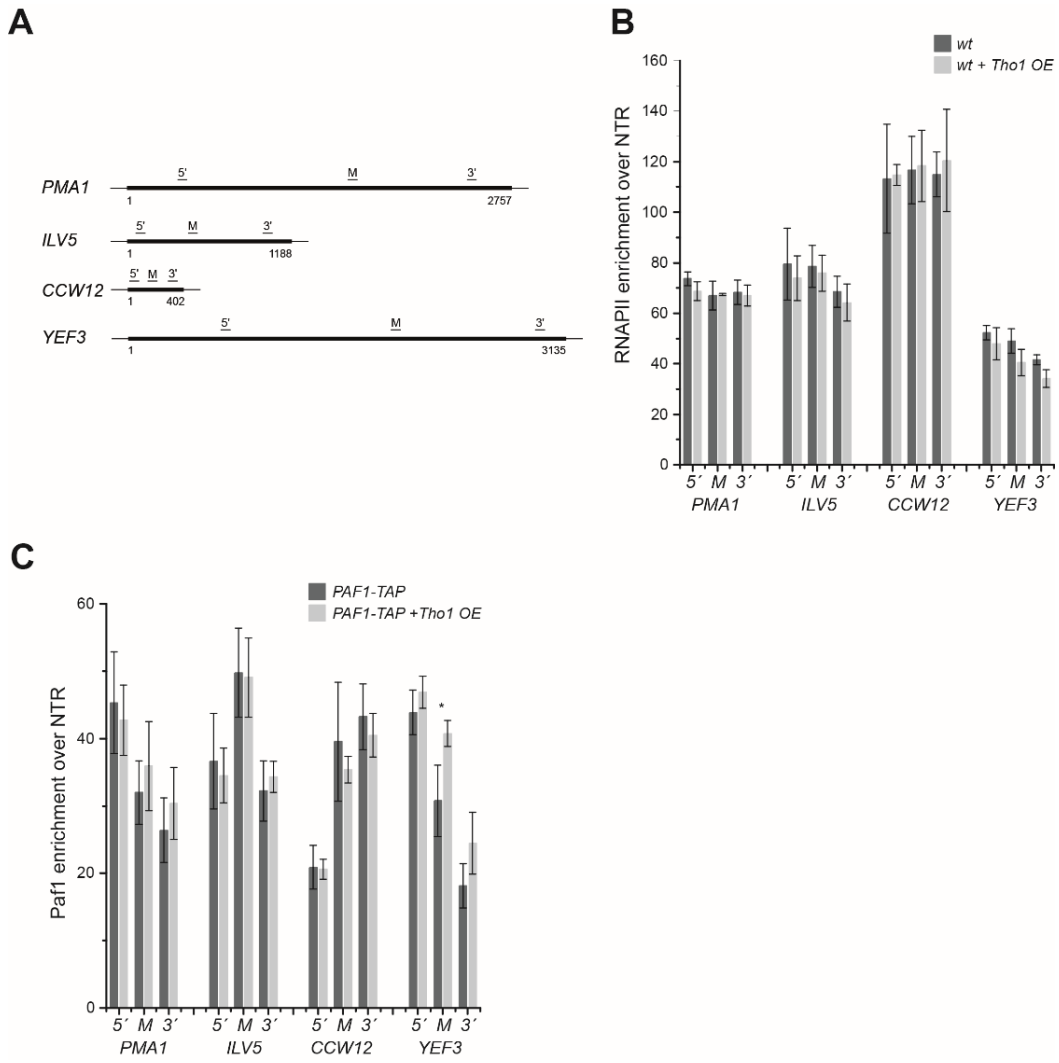

Figure 12: Additional expression of Tho1 by multicopy plasmid does not have any effect on RNAPII and Paf1 occupancies at transcribed genes. The recruitment of the proteins of interest to transcribed genes was assessed by chromatin immunoprecipitation (ChIP). The enrichment of the respective protein was calculated over a non-transcribed region (NTR). For the pull-down of RNAPII, the 8WG16 antibody with

Protein G Dynabeads was used. For the other proteins, the TAP-tag version of the protein with IgG coupled Dynabeads was used. (**A**) Scheme representing the four tested genes (*PMA*, *CCW12*, *ILV5* and *YEF3)*. The solid line represents the open reading frame (ORF). The primers used for qPCR are represented by bars above the genes. 5´ = 5´ region, M = middle region and 3´ = 3´region of the ORF. (**B&C**) The occupancies of RNAPII and Paf1 exhibit no change at transcribed genes when Tho1 is overexpressed (OE). The mean ± standard deviation was calculated for three biological replicates. The student t-test resulted in no significant change.

Table 19: Summary of ChIP results

strain	decrease	increase	no change
Δ*tho1*	Paf1 (Wierschem)	Hpr1	RNAPII
Δ*hpr1*	Tho1 RNAPII	Paf1	
Δ*paf1*	RNAPII	Tho1 Hpr1	
Tho1 OE	Hpr1 (Meinel)		RNAPII Paf1

The ChIP results clearly show that a lack of any of the three proteins Tho1, Hpr1 or Paf1 results in a changed occupancy of the two remaining proteins at the transcribed gene.

6.4 Tho1 co-purifies with transcription elongation factors, components of the TREX complex and Mex67 in an RNA-independent manner

Tandem affinity purification (TAP) with and without RNase A treatment was performed to address the question whether Tho1 co-purifies with components of the TREX complex (Hpr1, Sub2), the transcription elongation factors Spt5 and Paf1, and the mRNA export factor Mex67. The TEV-eluates were blotted against Mex67, Sub2, Yra1 and Tho1. As control, a sample without TAP-tag (WT) was purified. In the control purification, no proteins could be detected. Tho1 could be detected in all purifications. Sub2 pulled down the most Tho1 protein, besides the Tho1 purification itself. Comparison between the samples with and without RNase A shows that after adding RNase A, less Tho1 is pulled down in the Sub2 purification (Figure 13). Mex67 could be detected in all samples without RNase A treatment. In the RNase-treated samples, Mex67 could only be detected in the Mex67 and Sub2 purifications and very faintly in the Tho1 sample. The faint band in the WT sample is probably spilled sample from the Mex67 purification (Figure 13). Sub2 was co-purified with Hpr1 without RNase. In the blot with RNase, the typically lower unspecific Sub2 band was detected in all purifications. The specific Sub2 band was detected in Mex67 and as a weak band in the Tho1 and Paf1 samples (Figure 13). Yra1 is detected

in all purifications with and without RNase. The strongest signal can be detected in the purifications of Sub2, Mex67, Hpr1 and Tho1. Yra1 co-purification is reduced in Sub2, Hpr1, Paf1 and Spt5 if the sample is treated with RNase A (Figure 13).

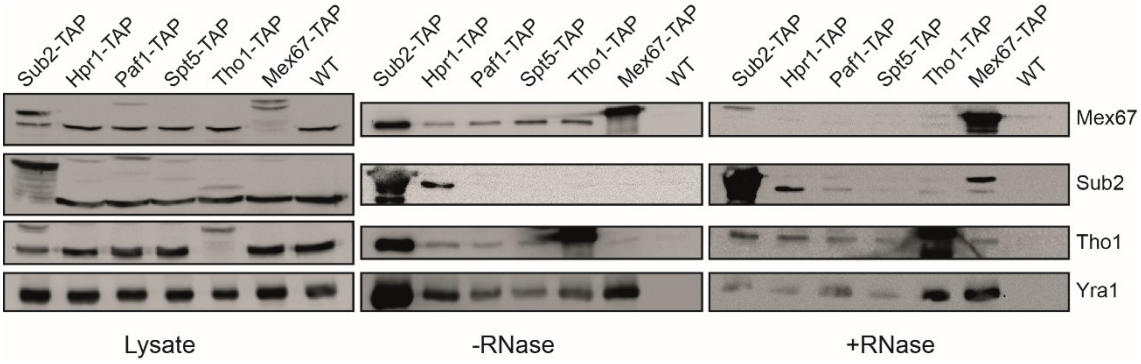

Figure 13: Tho1 co-purifies with transcription elongation factors, the TREX complex and Mex67. Tho1 and Yra1 could be detected in all purifications. Mex67 can be detected in the purifications without RNase A. Sub2 can be detected in Hpr1 without RNase and in Mex67 with RNase. Yra1 can be co-purified with all proteins in varying amounts. The first purification step of a TAP until TEV-cleavage was performed. The supernatant after the ultra-centrifugation step (lysate) was divided into two samples - one of them was treated for 30 min with 100 µg/mL RNase A at RT before IgG Sepharose was added.

6.5 Deletion of *HPR1* increases the co-purification of Paf1 with Tho1

To specify whether the deletion of one of the three proteins (Tho1, Hpr1 and Paf1) has an influence on the co-purification of the other two proteins, a TAP-purification until TEV-elution with subsequent quantification by Western blot of HA-tagged target protein was performed. One of the three proteins was tagged with a TAP-tag for the purification, the second was tagged with an HA-tag for the detection in Western blot and the third protein was deleted. An antibody against calmodulin-binding peptide of the TAP-tag was used for normalization of the purification. Independently of the pull down, Tho1, Hpr1 and Paf1 could always be detected as a co-purifier (Figure 13 & Figure 14 A). It could also be shown that Hpr1 and Paf1 co-purify (Figure 14 A). Δ*paf1* has no influence on the co-purification between Tho1 and Hpr1 (Figure 14 A & B). The deletion of *HPR1* increases the co-purification between Tho1 and Paf1 (Figure 14 A & C). Even though the deletion of *THO1* leads to a strongly increased co-purification between Paf1 and Hpr1 in two out three replicates, this is not significant due to the third replicate (Figure 14 A & D). The deletion of *HPR1* and *THO1* has an impact in the co-purification between Paf1 and the respectively other protein.

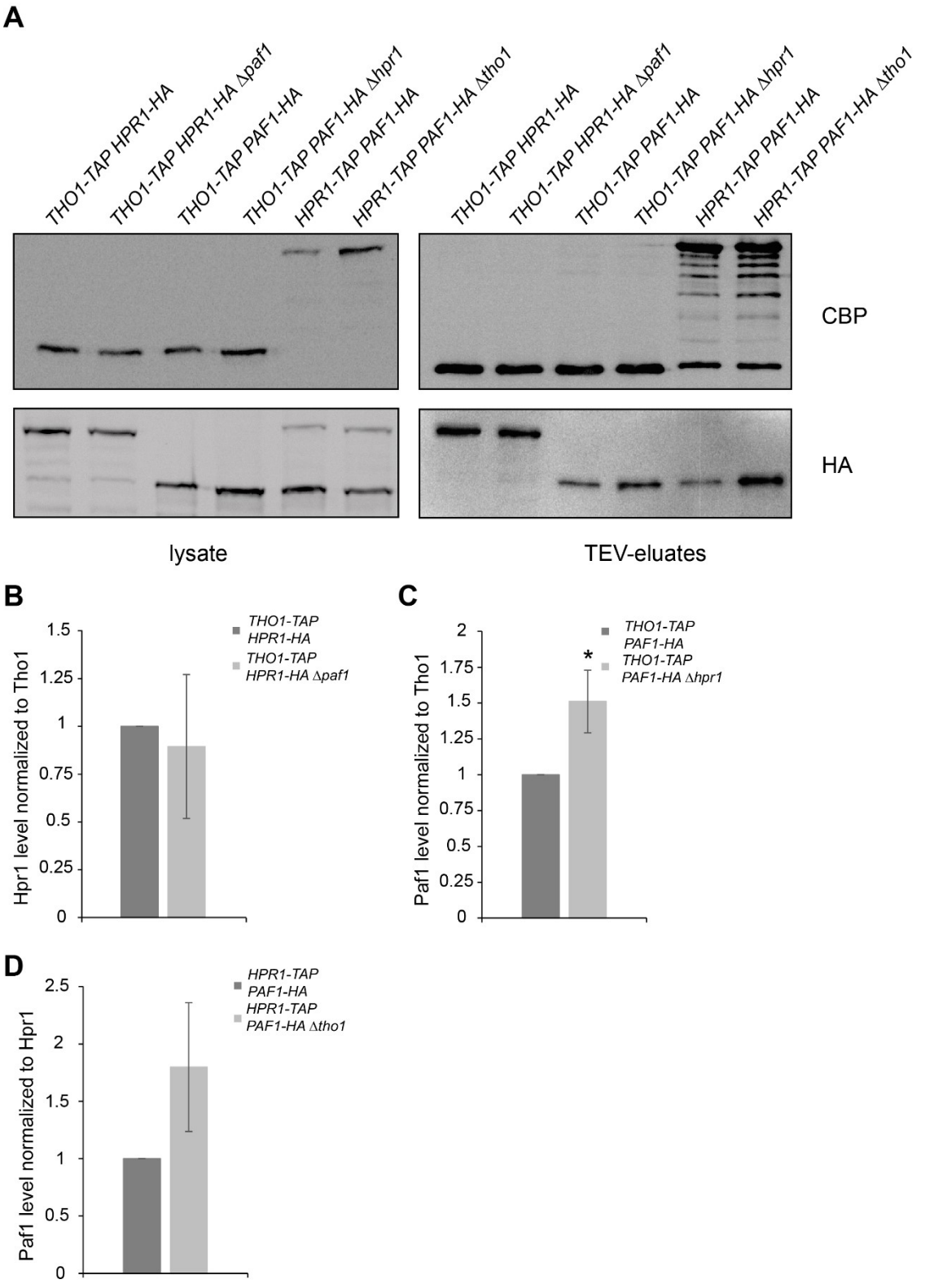

Figure 14: Co-purification between Paf1 and Hpr1 or Tho1 is changed if one of these proteins is lacking. Tho1-TAP and Hpr1-TAP were purified until TEV-elution followed by Western blot against the CBP and HA for detection of the purified and co-purified proteins. (**A**). Quantification of a Tho1-purification in Δ*paf1* (**B**), of a Tho1-purification in Δ*hpr1* (**C**) and of an Hpr1-purification in Δ*tho1* (**D**). Three biological replicates were quantified. The values of wild-type cells were set to 1 and normalized to the pulled protein. * P value 0.05, students t-test.

6.6 Altered levels of Tho1 impact the composition of nuclear mRNPs

To analyze the composition of nuclear mRNPs in *THO1* deletion strains or cells overexpressing Tho1, Cbp80 was purified by a genomically integrated TAP-tag. The purification was performed until the TEV-elution step. Afterwards, a quantitative Western blot of co-purified proteins was carried out. For the Western blot, Tho1, the TREX components Hpr1, Sub2 and Yra1, the poly (A) binding proteins Nab2 and Pab1, the SR-like protein Npl3 as well as the export factor Mex67 were chosen. The relative protein levels were normalized to Cbp80. No protein can be detected in the blot against Tho1 in the lysate sample of Δ*tho1* cells. In the Tho1 blot of the TEV-elution sample of Δ*tho1* cells, a faint band can be detected. We assume that this is an unspecific protein that is enriched during the purification. In the TEV-eluates of the Δ*tho1* cells, the TREX components Hpr1 and Sub2 are decreased. Noticeable that Yra1, the third tested TREX component, is not affected in the purification. Considering that remarkable amounts of Yra1 protein could be co-purified with Tho1 even after an RNase A treatment, this is even more surprising (Figure 13). Additionally, Hpr1 is decreased in mRNPs but increased at transcribed genes in a Δ*tho1* strain (cf. Figure 9 & Figure 15). The Western blot of the lysate of Tho1 shows a strong overexpression in the cells expressing pRS426-*THO1*. The TEV-eluate samples reveal that purified mRNPs contain more Tho1 than mRNPs in the corresponding wild-type cells (Figure 15). When Tho1 is overexpressed, the amount of Mex67 is decreased in the TEV-eluate (Figure 15). Since Mex67 is the export factor for mRNA and its protein level is reduced in mRNP a FISH was performed to assess mRNA export (Figure 18). No change could be observed for the proteins Nab2, Pab1, Npl3 and Yra1 in the mRNP if the cells have an altered level of Tho1.

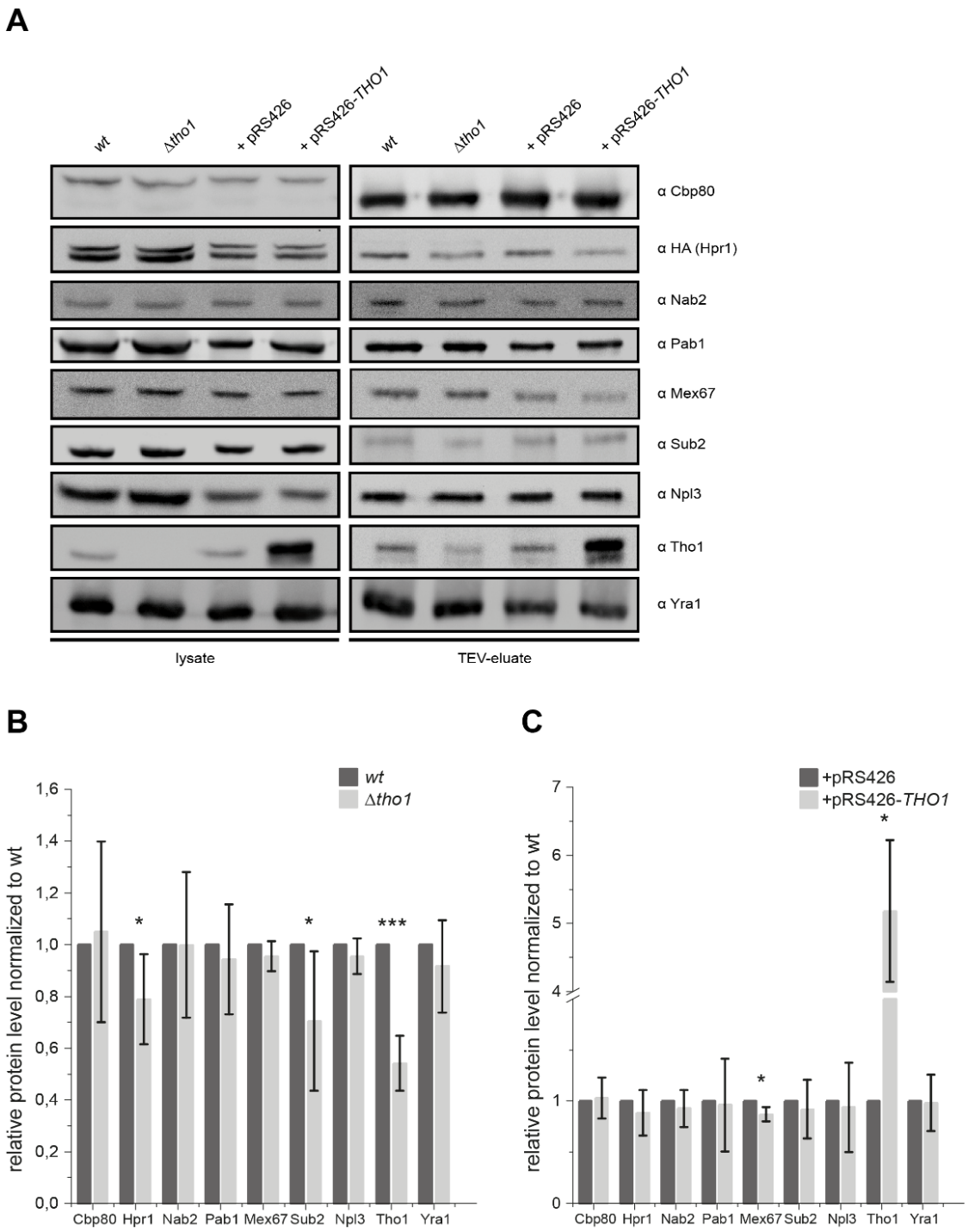

Figure 15: Δ*tho1* shows a decreased level of the TREX components Hpr1 and Sub2 and Tho1 OE shows a decrease of Mex67 in nuclear mRNPs. Nuclear mRNPs were purified via CBP80-TAP until the TEV-eluate. The purified sample was subjected for western blot against RBPs (**A**). The blots of three biological replicates were quantified in Δ*tho1* cells (**B**) and cells additionally expressing Tho1 via a pRS426 plasmid (**C**). The values of wild-type cells were set to 1 and normalized to the pulled protein. The mean ± standard deviation was calculated for three biological replicates. * P value < 0,5. * P value 0.05, ** P value 0.01, *** P value 0.001 students t-test.

6.7 Splicing and mRNA stability are not changed in the Δ*tho1* strain

To determine the half-lives of selected transcripts, wild-type and Δ*tho1* cells were treated with thiolutin to block transcription. The cells were harvested before thiolutin addition and 15, 30, 60 and 90 min after the treatment. Total RNA was extracted, reverse transcribed and analyzed by qPCR. Three intron-less transcripts (*PMA1*, *CCW12* and *YEF3*) and three intron-containing transcripts (*DBP2*, *ASC1* and *RPL28*) were chosen based on their abundance and their differing half-lives. The determined half-lives of the intron-less transcripts *PMA1*, *CCW12* and *YEF3* are 17.6 ± 0.8 min, 38.2 ±1.9 min and 20.8 ± 4.2 min and of the intron-containing transcripts *DBP2*, *ASC1* and *RPL28* are 8.1 ± 1.7 min, 18.9 ± 2.5 and 35.3 ± 3.7, respectively. The measured half-lives are similar to published data (Geisberg *et al.*, 2014). The deletion of *THO1* does not lead to detectable changes in the stabilities of the tested mRNAs (Figure 16).

To determine whether the splicing is affected in Δ*tho1* cells, RNA was extracted, reverse transcribed and analyzed by qPCR. For the analysis, the three intron-containing transcripts *DBP2*, *ASC1* and *RPL28* were chosen and the ratio of two amplicons of intron-flanking primers and the 3´prime region was calculated and normalized to 1. If the intron is regularly spliced, there should be no or only minor differences between the PCR product of the intron-flanking primer pair and the 3´region. If a splicing defect is present, less product should be amplified because the product including the intron would be too large to be amplified during the qPCR cycles. To exclude that the larger intron-containing product can be amplified with the intron-flanking primer pair as well, the PCR was visualized on an agarose gel. No significant differences between Δ*tho1* and wild type are detectable (Figure 17 B). (Figure 17 C). Alongside the fact that only the small, intron-less product can be observed, no difference between wild type and mutant is visible in the PCR products. Furthermore, there is no difference between the primer pairs flanking the intron and the 3´region. Only a faint band is visible for the primer pair inside the intron, confirming that splicing takes place (Figure 17 C).

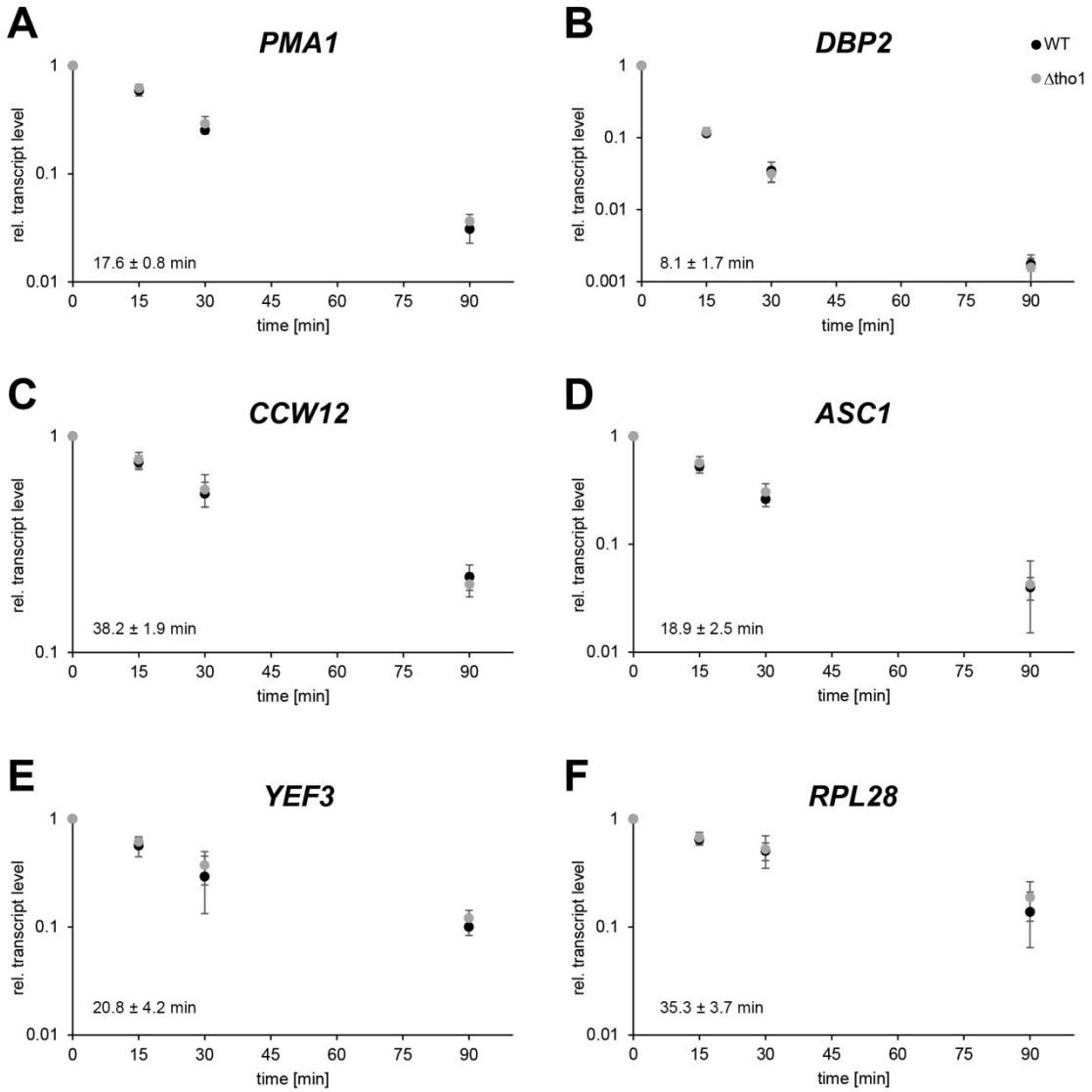

Figure 16: The stability of mRNAs is not changed in the Δ*tho1* mutant. For the determination of the half-lives of selected transcripts, cells were treated with thiolutin to block transcription. The cells were harvested before the treatment and 15, 30, 60, 90 min after the treatment. Total RNA was extracted, reverse transcribed and analyzed by qPCR. Three intron-less transcripts (*PMA1* (**A**), *CCW12* (**C**) and *YEF3* (**E**)) and three intron-containing transcripts (*DBP2* (**B**), *ASC1* (**D**) and *RPL28* (**F**)) were chosen based on their abundance and transcript half-lives. The measured half-life of each transcript is stated in the lower, left position in each panel. The timepoint 90 min after thiolutin treatment was not used for the calculation of the half-lives because the Ct values of the qPCR were already or almost at background level.

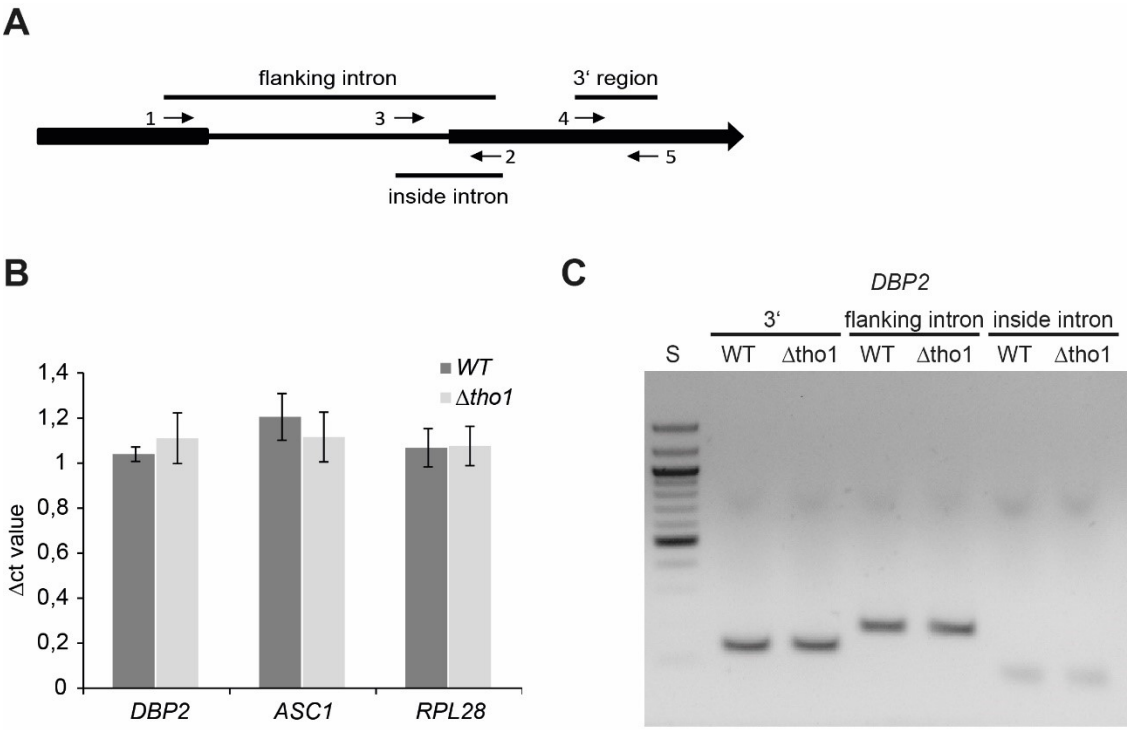

Figure 17: Splicing is not altered in Δ*tho1* cells. Splicing was assessed by calculating the ratio between intron-flanking and 3´region of three intron-containing genes (DBP2, ASC1 and RPL28). Before that, the mRNA was extracted, reverse transcribed and analyzed by qPCR. (**A**) Scheme represents the primer position. (**B**) Comparison of ΔCT values normalized to 1 of the Δ*tho1* mutant compared to the wild type. (**C**) PCR products visualized on an agarose gel.

6.8 Altered expression level of Tho1 doesn’t lead to an mRNA export defect

In a Cbp80 purification to analyze the mRNP composition, it could be observed that the level of Mex67 is reduced in a Tho1 overexpression strain (Figure 15). Considering that Mex67 is – together with Mtr2 - the mRNA export factor in *S. cerevisiae,* we examined whether the overexpression of Tho1 has an influence on the export of bulk mRNA by *in situ* fluorescence hybridization. Therefore, an oligo(dT_{50}) coupled to Cy3 against poly(A) tails was used for visualization of the bulk mRNA. The DNA was stained with DAPI. Neither at 30°C nor at 37°C could any defect in mRNA export could be observed in the Tho1 overexpression strain (Figure 18).

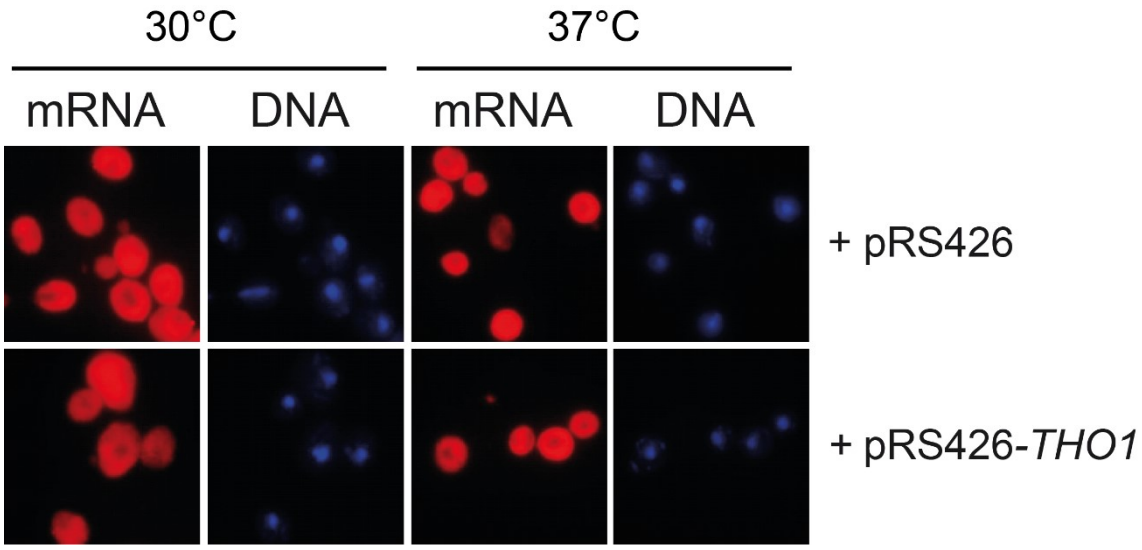

Figure 18: Overexpression of Tho1 has no influence on mRNA export in fluorescence *in situ* hybridization experiments. Bulk mRNA was visualized by oligo(dT_{50}) coupled to Cy3-fluorescent dye. DNA was stained with DAPI. Cells were grown at 30°C and an aliquot was shifted to 37°C for one hour.

A Δ*tex1*Δ*mos11* strain, the orthologs of Tex1 and Tho1 in *A. thaliana*, shows a strong mRNA export defect, while the single mutant Δ*tex1* has no influence on mRNA export and Δ*mos11* only a mild effect. Therefore, FISH experiments were performed at 18°C, 30°C and 37°C to determine whether the deletion of *THO1* and *TEX1* or the double mutant display an mRNA export defect. The *mex67-5* mutant was included as a positive control. At all tested temperatures, the single and double Δ*tho1* and Δ*tex1* mutants behave like wild type and no export defect can be observed. *mex67-5* shows an mRNA export defect at 37°C (Figure 19). Taken together, neither an overexpression of *THO1* nor the single and double deletion of *THO1* and *TEX1* result in an accumulation of bulk mRNA in the nucleus, indicating that Tho1 has no function in mRNA export.

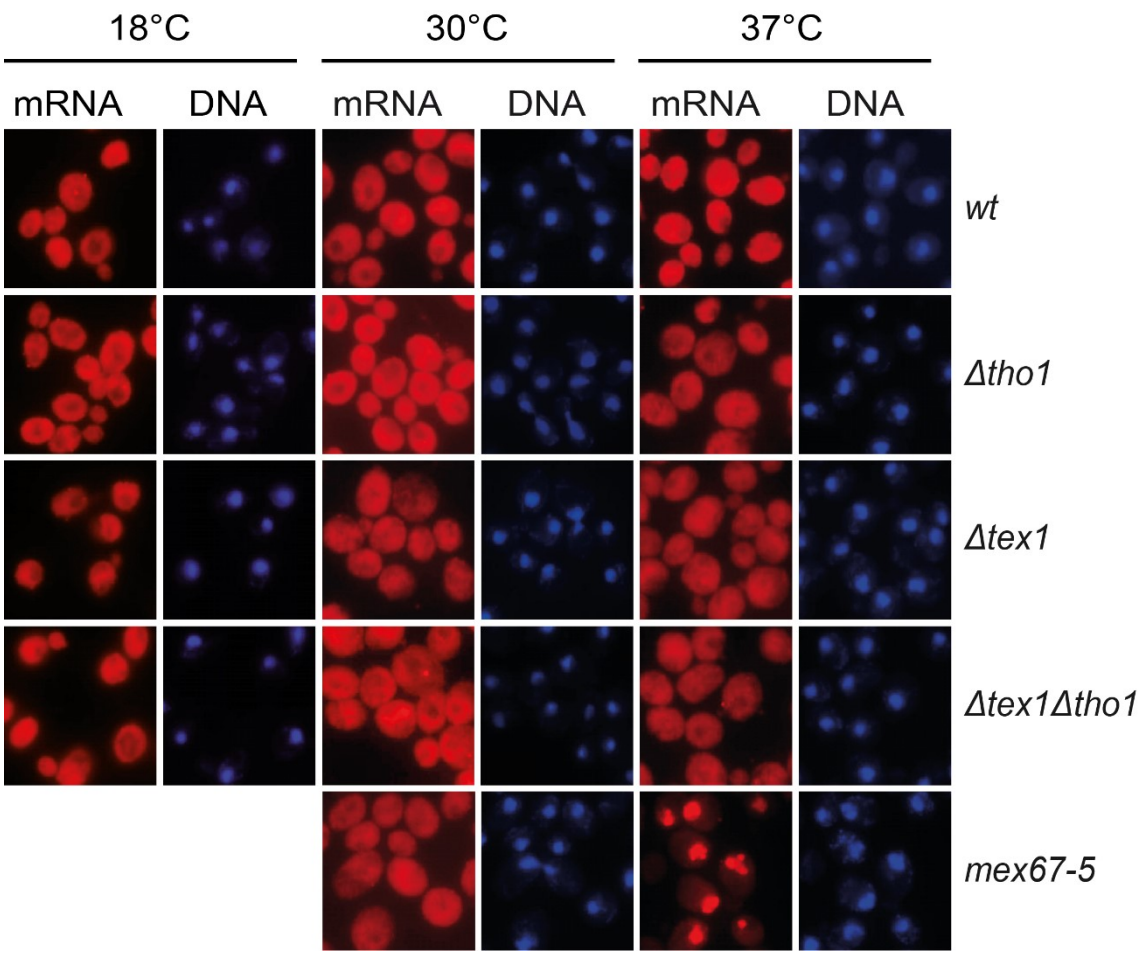

Figure 19: No mRNA export defect could be observed in the Δ*tho1* and Δ*tex1* mutants. Neither Δ*tho1*, Δ*tex1*, nor the double mutant of these two show an mRNA export defect at 18°C, 30°C and 37°C in fluorescence *in situ* hybridization experiments. *mex67-5* mutant was used as a control and displays an mRNA export defect at 37°C. Bulk mRNA was visualized by oligo(dT_{50}) coupled to Cy3-fluorescent dye. DNA was stained with DAPI. Cells were grown at 30°C and afterward an aliquot was shifted to 18°C or 37°C for one hour.

7 Discussion

The aim of this study was to identify the role of Tho1 in the recruitment of RBPs to transcribed genes, especially of the TREX component Hpr1 and the elongation factor Paf1. Furthermore, the interaction between Tho1 and Hpr1 and Tho1 and Paf1 was assessed. Also, the role of Tho1 in the formation of mRNPs and mRNA export was analyzed.

7.1 Deletion of *THO1* does not induce a growth phenotype but rescues the phenotypes of Δ*hpr1* and Δ*paf1*

As yeast emerged as a model organism, laboratory strains were generated to possess important characteristics like the ability to mate, sporulate and be transformed with high efficiency. W303 and BY4743 are both widely used laboratory strains and are descendants of the laboratory strain S288C (Brachmann *et al.*, 1998; Matheson *et al.*, 2017; Ralser *et al.*, 2012). Analyses of the proteome of various laboratory strains showed that proteins can be expressed differently (Rogowska-Wrzesinska *et al.*, 2001). Furthermore, the strain background has an impact on the characteristic of the mutation. For example, the DEAD-box helicase Sub2 is lethal in FY1679 background but shows only slow growth in CEN.PK2 (López *et al.*, 1998). In light of this, we checked whether the genotypic strain background has an influence on the phenotype of the Δ*tho1* mutant. Furthermore, we checked if different temperatures have an influence on the growth of the Δ*tho1* mutant. The deletion of *THO1* does not induce a growth defect at any applied temperature or in any of the three tested genotypes: RS453, W303, and BY4743 (Figure 4). The absence of a growth phenotype for the Δ*tho1* strain in a W303 background at 30°C had been shown before (Piruat and Aguilera, 1998). Changes in the expression level of Tho1 do not seem to have an impact on the growth of *S. cerevisiae.* The expression of a high copy plasmid with *THO1* does not lead to a detectable growth defect at any given temperature in two different strains (Figure 7). We assume that Tho1 has no essential role in yeast or that its function is redundant with other proteins.

Both Δ*paf1* and Δ*hpr1* are especially sensitive to higher (37°C) and lower (16°C) temperatures (Betz *et al.*, 2002). A less severe phenotype is observable if *THO1* is deleted in addition to any of the other two mutants (Figure 5 & Figure 6), revealing a genetic interaction between Tho1 and Hpr1 and Paf1. Furthermore, it can be assumed that at least the respective pair functions in one pathway or that they even operate in concert (Mani *et al.*, 2008). Potentially, even all three proteins function together in one pathway. This point is underscored through the fact that overexpression of Tho1 rescues

the phenotypes of the THO complex (Hpr1; (Jimeno *et al.*, 2006)), and the double deletion of Δ*hpr1* and Δ*paf1* is synthetically lethal (Chang *et al.*, 1999). The insertion of a *TRP* cassette can lead to better growth in yeast cells (González *et al.*, 2008). The Δ*tho1* strain was generated by introducing a *TRP* cassette into the *THO1* gene locus. To exclude that the rescue effect was due to the inserted *TRP* cassette, the experiment was repeated in strains carrying an additional empty plasmid with a *TRP* marker (Figure 6). The rescue effect of Δ*tho1* is weaker when all strains carry an additional *TRP*-cassette but is still present (cf. Figure 5 & Figure 6). There are two possible explanations for the weaker effect: i) the *TRP* cassette affects growth of the cells (González *et al.*, 2008). This assumption is contradicted by the experiment itself. The single Δ*tho1* cells in both backgrounds do not grow better than the corresponding wild type (Figure 5); ii) the deletion of *THO1* loses its phenotype over time. This phenome could be observed before in *HPR1-TAP* Δ*tho1* ChIP experiments (data not shown).

We were surprised that no (growth) phenotype could be observed for a Δ*tho1* strain; Tho1 is a conserved and highly abundant protein, and the abundance of Tho1 is even 10x higher than the abundance of Hpr1 (Kulak *et al.*, 2014). To assess whether Tho1 plays a role under heat shock conditions, the survival of cells after 30 min at 42°C and 52°C was checked (Zander *et al.*, 2016). No change could be observed at 42°C but a 2-fold change between the wild-type and Δ*tho1* cells at 52°C. However, the change was not significant (Figure 8).

7.2 Tho1 functions in the recruitment of Hpr1 and Paf1 to transcribed genes

The recruitment of RBPs to transcribed genes is often regulated through more than one mechanism. Tho1 is recruited to actively transcribed genes during transcription elongation and dissociates near the polyadenylation and cleavage site. Furthermore, recruitment depends on the length of the gene and mirrors the recruitment of the THO/TREX complex (Meinel, 2013). The recruitment depends on both the mRNA itself and the THO complex (Figure 10 C & E; (Jimeno *et al.*, 2006; Meinel, 2013)). Additionally, the correct phosphorylation of the CTR recruits Tho1 to the transcription start site. Interestingly, it seems like this phosphorylation decreases the recruitment of Hpr1 to the transcribed genes indicating a difference in the recruitment mechanisms of Hpr1 and Tho1 (Meinel 2013). Furthermore, we could show that the elongation factor Paf1 probably regulates the recruitment of Tho1 negatively, since the deletion of *PAF1* leads to an increased occupancy of Tho1 at transcribed genes (Figure 11 E).

Hpr1 (THO) is recruited to transcribed genes through the phosphorylated CTD and the mRNA (Meinel *et al.*, 2013). Additionally, it could be shown that Tho1 regulates the recruitment of Hpr1. An increased amount of Hpr1 is recruited to transcribed genes in Δ*tho1* cells (Figure 9 C). This increased level of Hpr1 at transcribed genes fits the data from the CTR mutants. If less or no Tho1 is present at the transcribed gene, the amount of Hpr1 increases (Meinel 2013). Furthermore, the additional expression of the high copy plasmid *pRS426-THO1* leads to a decreased amount of Hpr1 on transcribed genes (Meinel 2013). This leads to the assumption that the THO complex does not depend on Tho1 for recruitment since the deletion leads to an increase and the overexpression to a decrease of Hpr1 at transcribed genes. Its rather that Tho1 is necessary for the regulation of this process. Alongside Tho1, Paf1 seems to play a role in the regulation of the recruitment of the THO complex to the transcribed gene. In Δ*paf1* cells, the amount of Hpr1 at transcribed genes increases (Figure 11 F).

The recruitment of Paf1 to transcribed genes depends on the phosphorylation of the CTD and the CTR. Both are phosphorylated through the cyclin-dependent kinase Bur1-Bur2 (Qiu *et al.*, 2009; Zhou *et al.*, 2009). Interestingly, the recruitment of Paf1 is decreased in Δ*tho1* cells, indicating that Tho1 seems to be necessary for the complete recruitment of Paf1 (Figure 9). Additional expression of a multicopy plasmid of Tho1 does not change the recruitment of Paf1 to transcribed genes (Figure 12). Since the recruitment of Paf1 depends on Spt5 and RNAPII, we checked whether Tho1 has an influence on the recruitment of these two essential proteins. In case of RNAPII, neither the overexpression nor the deletion of *THO1* has an influence on its recruitment (Figure 9B & Figure 12 B). Likewise, the deletion of *THO1* does not affect recruitment of Spt5. This leads to the conclusion that the effect of the deletion of *THO1* on the recruitment of Paf1 is not mediated through Spt5 or RNAPII. Even though the double mutant Δ*paf1*Δ*hpr1* is synthetically lethal (Chang *et al.*, 1999), it seems that Hpr1 plays only a minor role in the recruitment of Paf1 to transcribed genes. Deletion of *HPR1* results in an increased occupancy of Paf1, leading to the assumption that Hpr1 has more of a regulatory role (Figure 10).

Based on the ChIP data from Meinel 2013 and this study, the following model for the recruitment of the THO complex, the PAF complex and Tho1 to transcribed genes is proposed: The S_2-S_5 phosphorylation of Spt5 is needed for the recruitment of the PAF complex and Tho1 (Chen *et al.*, 2009; Meinel, 2013). In addition to Spt5, the THO complex is necessary for the recruitment of Tho1 (Figure 10; Jimeno *et al*. 2006; Meinel 2013). However, Tho1 is needed for the recruitment of Paf1 (Figure 9). Strikingly, the occupancy of Hpr1 at transcribed genes is increased if the occupancy of Paf1 decreases

(Figure 6 & Figure 8; Table 19; Meinel 2013). Additionally, the same can be observed for Hpr1. If the occupancy of Hpr1 is decreased at the transcribed gene, the occupancy of Paf1 increases (Figure 7; Table 19). It seems that, if the recruitment of either the THO/TREX complex or the PAF complex fails, more of the corresponding complex is recruited, so that the obstacles for transcription are not too high for elongating RNAPII. It cannot be full compensation, because the occupancy of RNAPII is reduced at transcribed genes in both the Δ*hpr1* and the Δ*paf1* mutant (Figure 10 & Figure 11). Furthermore, the fact that the double mutant Δ*hpr1*Δ*paf1* is synthetically lethal emphasizes that at least one of the complexes is needed for transcription to occur (Chang *et al.*, 1999). Another explanation for the phenomena that the occupancy of one complex is increased when the other one is missing or decreased in its occupancy could be that the lacking of one complex results in more space for other components. Maybe, this space is simply occupied by the other complex. In addition to being involved in the recruitment of the PAF complex, Tho1 appears to be a negative regulator of the THO complex. A first hint was that Hpr1 occupancy is increased in the CTR mutants while Tho1 is decreased (Meinel 2013). The same pattern can be observed in the Δ*tho1* mutant (Figure 9). Additionally, the overexpression of Tho1 decreases the occupancy of Hpr1 on transcribed genes (Meinel 2013). This model would also imply that the recruitment of Tho1 and Hpr1 is not inversely regulated but rather that the increased occupancy of Hpr1 at a transcribed gene is a result of decreased Paf1 occupancy. The PAF complex seems to have a regulatory effect of Tho1 since its occupancy is increased in the Δ*paf1* mutant (Figure 11). If we keep in mind that Tho1 regulates the THO complex, we can maybe propose that Tho1 acts as a coordinator between the THO and the PAF complexes.

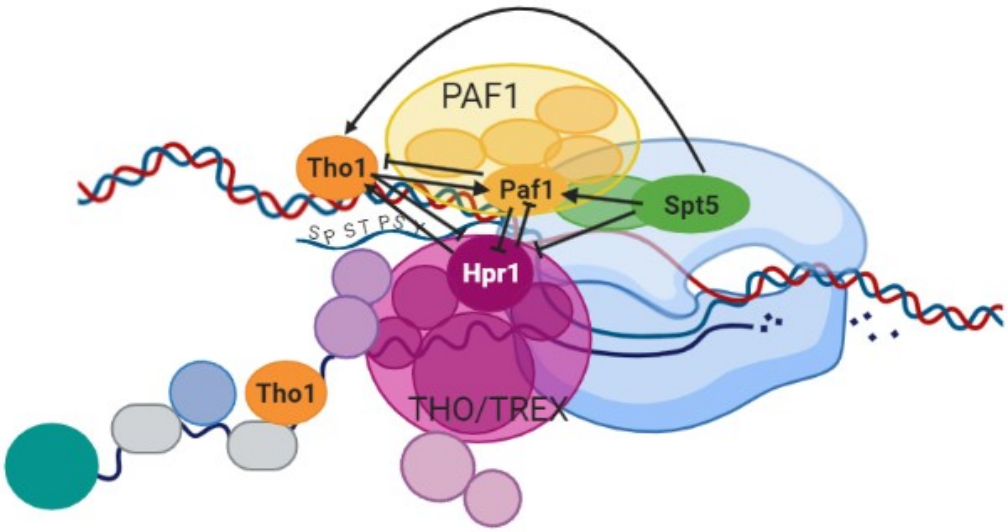

Figure 20: Dependence of the recruitment of Tho1, Hpr1 and Paf1 to the transcribed gene. During transcription, the PAF complex is recruited by the phosphorylated CTR of Spt5 as well as the CTD of the

RNAPII. The TREX complex is recruited by the CTD and the mRNA itself while the recruitment of Tho1 depends on the mRNA and THO. The recruitment of these three components depends not only on the previous described mechanisms but also depends on the presence or absence of each other. Tho1 seems to have a regulatory role in these processes. Created with BioRender.com.

7.3 Tho1 co-purifies with transcription elongation factors, the TREX complex and the export factor Mex67 in yeast

Tho1 co-purifies with Hpr1, Sub2 and Yra1 of the pentameric THO/TREX complex. Furthermore, the co-purification is RNA-independent (Figure 13 & Figure 14). A previous study showed that Tho1 can be co-purified with TREX in humans. Here, we show that Tho1 co-purifies with TREX in *S. cerevisiae* as well. The co-purification with the THO/TREX complex strengthens the assumption that Tho1 is loosely associated with the TREX complex (Dufu *et al.*, 2010). Noticeably more Yra1 than Sub2 is co-purified with Tho1, indicating that not only Sub2 but also Yra1 is important for the interaction between Tho1 and the TREX complex (Dufu *et al.*, 2010; Kang *et al.*, 2020). We could confirm that Tho1 co-purifies with the elongation factor Spt5 (Lindstrom *et al.*, 2003). Additionally, we found that Tho1 co-purifies with another elongation factor, Paf1, in an RNA-independent manner (Figure 13). Tho1 not only co-purifies with transcription elongation factors, but also functions in the recruitment of the THO and PAF complexes (6.3). Last but not least, Tho1 also co-purifies with the mRNA export factor Mex67 in yeast. The co-purification can be observed in both ways: Tho1 is a co-purifier in a Mex67 purification and Mex67 appears as a co-purifier in a Tho1 purification. The co-purification between these proteins is independent of mRNA (Figure 13). Furthermore, Tho1 interacts genetically with Nab2, a protein involved in 3´processing and poly(A) tail length control (Jimeno *et al.*, 2006). Like the TREX complex, Tho1 functions in all steps of mRNA biogenesis. Like Tho1, Yra1 co-purifies with all tested proteins. Some of the co-purifiers or interactors are (partially) RNA-dependent and show a stronger interaction without RNase A treatment (Fischl *et al.*, 2017; Krogan *et al.*, 2006; Lindstrom *et al.*, 2003; Strässer and Hurt, 2000; Strässer *et al.*, 2002).

7.4 The deletion of *HPR1* influences the co-purification of Tho1 and Paf1

Even so the recruitment to the transcribed gene of Hpr1, Paf1 and Tho1 is depending on each other (6.3), it seems like the co-purification between Tho1 and Hpr1 is independent of Paf1 (Figure 14 B). This might indicate that the connection between Tho1 and Hpr1 is closer than one of these two with Paf1. If *HPR1* is deleted, Tho1 co-purifies more Paf1

(Figure 14 C). That reflects the ChIP data: Missing or reduced levels of Hpr1 lead to an increased amount of Paf1 at transcribed genes (Figure 10). Since Tho1 is necessary for the recruitment of Paf1 to transcribed genes (Figure 9), it might be that Hpr1 prevents or regulates the binding between Paf1 and Tho1. Thus, more Paf1 can be co-purified if *HPR1* is deleted. The deletion of *THO1* might also lead to an increase of co-purified Paf1 with Hpr1. This increase is not significant (Figure 14 D). A possible explanation for the increase of co-purified Paf1 with Hpr1 could be that Tho1 inhibits the interaction between Hpr1 and Paf1 (Figure 14 D; (Chang *et al.*, 1999)). If Tho1 is missing, it strengthens the interaction between Hpr1 and Paf1, thus more Paf1 can be co-purified with Hpr1.

7.5 Altered levels of Tho1 lead to changes in nuclear mRNP formation but have no effect on mRNA stability or export

Since Tho1 affects the recruitment of Paf1 and Hpr1 to transcribed genes (6.3) and also co-purifies with several proteins important for mRNP formation (Figure 13) I purified nuclear mRNPs by TAP-tagged Cbp80 (the large subunit of the cap-binding complex) in Δ*tho1* cells and cells expressing pRS426-*THO1*. In Δ*tho1* cells, only the TREX components Hpr1 and Sub2 are depleted from nuclear mRNPs, all other tested components of mRNPs are not changed. Interestingly, the recruitment to nuclear mRNPs of Yra1, a third tested TREX component is not changed (Figure 15). This is especially surprising since Yra1 co-purifies strongly with Tho1 (Figure 13). A possible explanation could be that Yra1 is not only recruited to the mRNP via the TREX complex but has alternative ways for its recruitment to nuclear mRNPs. Also, Pcf11, part of the CPF, and the H3K4 methyltransferase play a role in the recruitment of Yra1 (Johnson *et al.*, 2009; Vitaliano-Prunier *et al.*, 2012). Finally, mRNA itself recruits Yra1, highlighting the importance of Yra1 for the formation of mRNPs (Johnson *et al.*, 2009; Meinel *et al.*, 2013; Strässer and Hurt, 2001; Vitaliano-Prunier *et al.*, 2012). The deletion of *THO1* probably does not affect all the recruitment pathways of Yra1 to mRNPs (Figure 15). Hpr1 is decreased in the purified mRNP in Δ*tho1* cells. This is opposite to the results of the ChIP experiments that showed that the recruitment of Hpr1 to transcribed genes is increased (Figure 10 C). Since 5´capping is the first mRNA processing step, it can be assumed that nuclear mRNPs purified by Cbp80-TAP are differently processed. Assuming that the mRNP composition changes during different processing steps, it could explain that the level of Hpr1 differ between mRNPs at transcribed genes and further processed mRNPs. It might also indicate that Tho1 is not necessary for the recruitment of the TREX complex to nuclear mRNPs but rather for the retention of the components at the mRNP.

In cells expressing additional Tho1, less Mex67 is present in mRNPs. The level of other tested mRNP components was not changed (Figure 15). Tho1 co-purifies with both, Yra1 and Mex67 (Figure 13). The mRNP purification indicates that the co-purification between Tho1 and Mex67 is not only mediated through Yra1 since the levels of Yra1 in the mRNP are not changed in response to overexpression of Tho1. Hence, Tho1 may not be necessary for the recruitment of Mex67 but rather has a negative regulatory role.

Since Tho1 co-purifies with Mex67 and the additional expression of Tho1 leads to a reduced recruitment of Mex67 to mRNPs, FISH experiments were performed to assess the role of Tho1 in mRNA export (Figure 18). Although nuclear mRNPs contain less Mex67 in cells overexpressing Tho1 (Figure 15A & C), no mRNA export defect was detected, indicating that sufficient amounts of Mex67 are recruited for the export of bulk mRNA to work. Furthermore, Δ*tho1* has no effect on mRNA export at 18°C, 30°C or 37°C (Figure 19). In humans and plants, deletion or knockdown of CIP29/MOS11, the Tho1 homologues, leads to mRNA export defects (Germain *et al.*, 2010; Kang *et al.*, 2020; Sørensen *et al.*, 2017). In plants, the additional deletion of *TEX1*, a component of the TREX complex that is not required for export, enhances the mRNA export defect of a Δ*mos11* mutant. Unlike in plants, combination of Δ*tex1* and Δ*tho1* does not result in an mRNA export defect in yeast at any of the tested temperatures (Figure 19; (Sørensen *et al.*, 2017)). It might be that Tho1 has a minor regulatory effect on Mex67 (Figure 13A & C, & Figure 15A & C), but the effect is too weak to disturb mRNA export. It might also be possible that the export of only a subset of mRNAs depends on Tho1. An RNA sequencing experiment would reveal whether the expression of some transcripts is changed in cells with altered levels of Tho1. Following the RNA-seq, a single-molecule FISH for specific mRNAs could be performed to assess whether these specific mRNAs are retained in the nucleus.

Changed levels of Tho1 alter the formation of nuclear mRNPs. In Δ*tho1* cells, Sub2 and Hpr1 is reduced and additional expression of Tho1 leads to reduced Mex67 in mRNPs (Figure 15). Although Mex67 is reduced in mRNPs, the mRNA export is not affected. Therefore, we checked the stability of the mRNA itself. No change between wild type and Δ*tho1* cells could be observed for six representative transcripts (*PMA1, CCW12, YEF3, DBP2, ASC1, RPL28*). Whether this is only the case for these transcripts, or is true globally is unclear. RNA sequencing could provide this information. The absence of an mRNA export defect cannot be explained by decrease mRNA stability, at least not for the tested mRNAs. The human orthologue of Tho1, CIP29, is found in nuclear speckles associated with splicing and export (Kang *et al.*, 2020; Schumann *et al.*, 2016). From my results I can conclude that Tho1 does not have an influence on the stability or the splicing

of mRNAs. The tested half-lives correspond to published half-lives for the transcripts (Geisberg *et al*. 2014). Whether this is a global phenomenon or specific for the tested transcripts has to be tested further.

7.6 Conclusions

In this study I could show that the deletion of *THO1* does not result in a growth phenotype as a single mutation. However, the additional deletion of *THO1* suppresses the phenotype of Δ*paf1* and Δ*hpr1* at lower temperatures, indicating a genetic interaction between Tho1 and Hpr1, and Tho1 and Paf1. Additionally, Tho1 co-purifies with the components of the TREX complex as well as with Paf1 and Mex67, indicating that Tho1 functions in multiple processes of mRNP formation. The following model for the role of Tho1 in the recruitment of the TREX complex and PAF complex could be possible: Tho1 seems to be necessary for the full recruitment of Paf1 to transcribed genes. Although the THO complex is necessary for the recruitment of Tho1, Tho1 seems to regulate the occupancy of Hpr1 at transcribed genes. If the occupancy of Paf1 or Hpr1 is decreased at transcribed genes, the occupancy of the other is increased. If the recruitment of either the THO/TREX complex or the PAF complex fails, more of the corresponding complex is recruited to prevent formation of obstacles of transcription that are too big for elongating RNAPII. Tho1 might be a mediator of these two complexes. Furthermore, the deletion of *HPR1* leads to an increased co-purification between Tho1 and Paf1, supporting the model from the ChIP data. Changed levels of Tho1 result in an altered composition of the mRNP. Nevertheless, no effect on mRNA stability, splicing or mRNA export could be observed for Δ*tho1*. However, only specific mRNAs were assayed for splicing defects and stability, so it is not clear whether this is only true for a subset of transcripts. RNA sequencing could give a global picture whether changes in the level of Tho1 lead to defects in splicing and or mRNA stability. Furthermore, changed transcripts could be analyzed in single molecule FISH to assess if specific mRNAs are retained in the nucleus or exported to the cytoplasm. Since Tho1 co-purifies with the TREX complex and also functions closely with TREX, it is possible that Tho1 is not only a loosely associated member of the TREX complex in humans and plants but also in yeast. Although Tho1 is not a member of the TREX complex it seems to function in multiple steps of mRNP formation. Since it has no severe phenotype, the function appears to be redundant to at least one protein or a complex.

8 References

Abruzzi, K. C., Lacadie, S., Rosbash, M. (2004) Biochemical analysis of TREX complex recruitment to intronless and intron-containing yeast genes. *The EMBO journal* 23, 2620-2631.

Adkins, M. W., Tyler, J. K. (2006) Transcriptional activators are dispensable for transcription in the absence of Spt6-mediated chromatin reassembly of promoter regions. *Mol Cell* 21, 405-416.

Ahn, S. H., Kim, M., Buratowski, S. (2004) Phosphorylation of serine 2 within the RNA polymerase II C-terminal domain couples transcription and 3' end processing. *Mol Cell* 13, 67-76.

Akhtar, M. S., Heidemann, M., Tietjen, J. R., Zhang, D. W., Chapman, R. D., Eick, D., Ansari, A. Z. (2009) TFIIH kinase places bivalent marks on the carboxy-terminal domain of RNA polymerase II. *Mol Cell* 34, 387-393.

Amberg, D. C., Goldstein, A. L., Cole, C. N. (1992) Isolation and characterization of RAT1: an essential gene of Saccharomyces cerevisiae required for the efficient nucleocytoplasmic trafficking of mRNA. *Genes & development* 6, 1173-1189.

Aparicio, O., Geisberg, J. V., Sekinger, E., Yang, A., Moqtaderi, Z., Struhl, K. (2005) Chromatin immunoprecipitation for determining the association of proteins with specific genomic sequences in vivo. *Current protocols in molecular biology* Chapter 21, Unit 21 23.

Baejen, C., Torkler, P., Gressel, S., Essig, K., Söding, J., Cramer, P. (2014) Transcriptome maps of mRNP biogenesis factors define pre-mRNA recognition. *Mol Cell* 55, 745-757.

Bahrampour, S., Thor, S. (2016) Ctr9, a Key Component of the Paf1 Complex, Affects Proliferation and Terminal Differentiation in the Developing Drosophila Nervous System. *G3 (Bethesda)* 6, 3229-3239.

Baierlein, C., Hackmann, A., Gross, T., Henker, L., Hinz, F., Krebber, H. (2013) Monosome formation during translation initiation requires the serine/arginine-rich protein Npl3. *Molecular and cellular biology* 33, 4811-4823.

Barillà, D., Lee, B. A., Proudfoot, N. J. (2001) Cleavage/polyadenylation factor IA associates with the carboxyl-terminal domain of RNA polymerase II in Saccharomyces cerevisiae. *Proc Natl Acad Sci U S A* 98, 445-450.

Batisse, J., Batisse, C., Budd, A., Böttcher, B., Hurt, E. (2009) Purification of nuclear poly(A)-binding protein Nab2 reveals association with the yeast transcriptome and a messenger ribonucleoprotein core structure. *The Journal of biological chemistry* 284, 34911-34917.

Betz, J. L., Chang, M., Washburn, T. M., Porter, S. E., Mueller, C. L., Jaehning, J. A. (2002) Phenotypic analysis of Paf1/RNA polymerase II complex mutations reveals connections to cell cycle regulation, protein synthesis, and lipid and nucleic acid metabolism. *Molecular genetics and genomics : MGG* 268, 272-285.

Birney, E., Kumar, S., Krainer, A. R. (1993) Analysis of the RNA-recognition motif and RS and RGG domains: conservation in metazoan pre-mRNA splicing factors. *Nucleic acids research* 21, 5803-5816.

Bousquet-Antonelli, C., Presutti, C., Tollervey, D. (2000) Identification of a regulated pathway for nuclear pre-mRNA turnover. *Cell* 102, 765-775.

Brachmann, C. B., Davies, A., Cost, G. J., Caputo, E., Li, J., Hieter, P., Boeke, J. D. (1998) Designer deletion strains derived from Saccharomyces cerevisiae S288C: a useful set of strains and plasmids for PCR-mediated gene disruption and other applications. *Yeast (Chichester, England)* 14, 115-132.

Brody, E., Abelson, J. (1985) The "spliceosome": yeast pre-messenger RNA associates with a 40S complex in a splicing-dependent reaction. *Science (New York, N.Y.)* 228, 963-967.

Bucheli, M. E., Buratowski, S. (2005) Npl3 is an antagonist of mRNA 3' end formation by RNA polymerase II. *The EMBO journal* 24, 2150-2160.

Bucheli, M. E., He, X., Kaplan, C. D., Moore, C. L., Buratowski, S. (2007) Polyadenylation site choice in yeast is affected by competition between Npl3 and polyadenylation factor CFI. *RNA (New York, N.Y.)* 13, 1756-1764.

Buratowski, S., Hahn, S., Guarente, L., Sharp, P. A. (1989) Five intermediate complexes in transcription initiation by RNA polymerase II. *Cell* 56, 549-561.

Cao, Q. F., Yamamoto, J., Isobe, T., Tateno, S., Murase, Y., Chen, Y., Handa, H., Yamaguchi, Y. (2015) Characterization of the Human Transcription Elongation Factor Rtf1: Evidence for Nonoverlapping Functions of Rtf1 and the Paf1 Complex. *Molecular and cellular biology* 35, 3459-3470.

Casañal, A. *et al.* (2017) Architecture of eukaryotic mRNA 3'-end processing machinery. *Science (New York, N.Y.)* 358, 1056-1059.

Chanarat, S., Seizl, M., Strässer, K. (2011) The Prp19 complex is a novel transcription elongation factor required for TREX occupancy at transcribed genes. *Genes & development* 25, 1147-1158.

Chang, C. T., Hautbergue, G. M., Walsh, M. J., Viphakone, N., van Dijk, T. B., Philipsen, S., Wilson, S. A. (2013) Chtop is a component of the dynamic TREX mRNA export complex. *The EMBO journal* 32, 473-486.

Chang, M., French-Cornay, D., Fan, H. Y., Klein, H., Denis, C. L., Jaehning, J. A. (1999) A complex containing RNA polymerase II, Paf1p, Cdc73p, Hpr1p, and Ccr4p plays a role in protein kinase C signaling. *Molecular and cellular biology* 19, 1056-1067.

Chaudhary, K., Deb, S., Moniaux, N., Ponnusamy, M. P., Batra, S. K. (2007) Human RNA polymerase II-associated factor complex: dysregulation in cancer. *Oncogene* 26, 7499-7507.

Chávez, S., Beilharz, T., Rondón, A. G., Erdjument-Bromage, H., Tempst, P., Svejstrup, J. Q., Lithgow, T., Aguilera, A. (2000) A protein complex containing Tho2, Hpr1, Mft1 and a novel protein, Thp2, connects transcription elongation with mitotic recombination in Saccharomyces cerevisiae. *The EMBO journal* 19, 5824-5834.

Chen, F. X., Woodfin, A. R., Gardini, A., Rickels, R. A., Marshall, S. A., Smith, E. R., Shiekhattar, R., Shilatifard, A. (2015) PAF1, a Molecular Regulator of Promoter-Proximal Pausing by RNA Polymerase II. *Cell* 162, 1003-1015.

Chen, H. T., Warfield, L., Hahn, S. (2007) The positions of TFIIF and TFIIE in the RNA polymerase II transcription preinitiation complex. *Nature structural & molecular biology* 14, 696-703.

Chen, M., Manley, J. L. (2009) Mechanisms of alternative splicing regulation: insights from molecular and genomics approaches. *Nature reviews. Molecular cell biology* 10, 741-754.

Chen, Y., Yamaguchi, Y., Tsugeno, Y., Yamamoto, J., Yamada, T., Nakamura, M., Hisatake, K., Handa, H. (2009) DSIF, the Paf1 complex, and Tat-SF1 have nonredundant, cooperative roles in RNA polymerase II elongation. *Genes & development* 23, 2765-2777.

Cheng, H., Dufu, K., Lee, C. S., Hsu, J. L., Dias, A., Reed, R. (2006) Human mRNA export machinery recruited to the 5' end of mRNA. *Cell* 127, 1389-1400.

Cheung, A. C., Cramer, P. (2012) A movie of RNA polymerase II transcription. *Cell* 149, 1431-1437.

Chiang, P. W., Fogel, E., Jackson, C. L., Lieuallen, K., Lennon, G., Qu, X., Wang, S. Q., Kurnit, D. M. (1996) Isolation, sequencing, and mapping of the human homologue of the yeast transcription factor, SPT5. *Genomics* 38, 421-424.

Cho, E. J., Kobor, M. S., Kim, M., Greenblatt, J., Buratowski, S. (2001) Opposing effects of Ctk1 kinase and Fcp1 phosphatase at Ser 2 of the RNA polymerase II C-terminal domain. *Genes & development* 15, 3319-3329.

Cho, E. J., Takagi, T., Moore, C. R., Buratowski, S. (1997) mRNA capping enzyme is recruited to the transcription complex by phosphorylation of the RNA polymerase II carboxy-terminal domain. *Genes & development* 11, 3319-3326.

Cho, H., Kim, T. K., Mancebo, H., Lane, W. S., Flores, O., Reinberg, D. (1999) A protein phosphatase functions to recycle RNA polymerase II. *Genes & development* 13, 1540-1552.

Choong, M. L., Tan, L. K., Lo, S. L., Ren, E. C., Ou, K., Ong, S. E., Liang, R. C., Seow, T. K., Chung, M. C. (2001) An integrated approach in the discovery and characterization of a novel nuclear protein over-expressed in liver and pancreatic tumors. *FEBS letters* 496, 109-116.

Chu, X. *et al.* (2013) Structural insights into Paf1 complex assembly and histone binding. *Nucleic acids research* 41, 10619-10629.

Chu, Y., Simic, R., Warner, M. H., Arndt, K. M., Prelich, G. (2007) Regulation of histone modification and cryptic transcription by the Bur1 and Paf1 complexes. *The EMBO journal* 26, 4646-4656.

Cléry, A., Blatter, M., Allain, F. H. (2008) RNA recognition motifs: boring? Not quite. *Current opinion in structural biology* 18, 290-298.

Conaway, R. C., Conaway, J. W. (2011) Function and regulation of the Mediator complex. *Curr Opin Genet Dev* 21, 225-230.

Connelly, S., Manley, J. L. (1988) A functional mRNA polyadenylation signal is required for transcription termination by RNA polymerase II. *Genes & development* 2, 440-452.

Corden, J. L., Cadena, D. L., Ahearn, J. M., Jr., Dahmus, M. E. (1985) A unique structure at the carboxyl terminus of the largest subunit of eukaryotic RNA polymerase II. *Proceedings of the National Academy of Sciences of the United States of America* 82, 7934-7938.

Davis, C. A., Ares, M. (2006) Accumulation of unstable promoter-associated transcripts upon loss of the nuclear exosome subunit Rrp6p in Saccharomyces cerevisiae. *Proceedings of the National Academy of Sciences of the United States of America* 103, 3262.

Deka, P., Bucheli, M. E., Moore, C., Buratowski, S., Varani, G. (2008) Structure of the yeast SR protein Npl3 and Interaction with mRNA 3'-end processing signals. *Journal of molecular biology* 375, 136-150.

Dermody, J. L. *et al.* (2008) Unphosphorylated SR-like protein Npl3 stimulates RNA polymerase II elongation. *PloS one* 3, e3273.

Dichtl, B., Blank, D., Sadowski, M., Hübner, W., Weiser, S., Keller, W. (2002) Yhh1p/Cft1p directly links poly(A) site recognition and RNA polymerase II transcription termination. *The EMBO journal* 21, 4125-4135.

Dieci, G., Fiorino, G., Castelnuovo, M., Teichmann, M., Pagano, A. (2007) The expanding RNA polymerase III transcriptome. *Trends in genetics : TIG* 23, 614-622.

Domínguez-Sánchez, M. S., Barroso, S., Gómez-González, B., Luna, R., Aguilera, A. (2011) Genome Instability and Transcription Elongation Impairment in Human Cells Depleted of THO/TREX. *PLoS genetics* 7, e1002386.

Dufu, K., Livingstone, M. J., Seebacher, J., Gygi, S. P., Wilson, S. A., Reed, R. (2010) ATP is required for interactions between UAP56 and two conserved mRNA export proteins, Aly and CIP29, to assemble the TREX complex. *Genes & development* 24, 2043-2053.

Eckmann, C. R., Rammelt, C., Wahle, E. (2011) Control of poly(A) tail length. *Wiley interdisciplinary reviews. RNA* 2, 348-361.

Fairbanks, G., Steck, T., Wallach, D. (1971) Electrophoretic Analysis of the Major Polypeptides of the Human Erythrocyte Membrane. *Biochemistry* 10, 2606-2617.

Faller, M., Guo, F. (2008) MicroRNA biogenesis: there's more than one way to skin a cat. *Biochimica et biophysica acta* 1779, 663-667.

Fasken, M. B., Stewart, M., Corbett, A. H. (2008) Functional significance of the interaction between the mRNA-binding protein, Nab2, and the nuclear pore-associated protein, Mlp1, in mRNA export. *The Journal of biological chemistry* 283, 27130-27143.

Fischer, T., Rodríguez-Navarro, S., Pereira, G., Rácz, A., Schiebel, E., Hurt, E. (2004) Yeast centrin Cdc31 is linked to the nuclear mRNA export machinery. *Nature cell biology* 6, 840-848.

Fischer, T., Strässer, K., Rácz, A., Rodriguez-Navarro, S., Oppizzi, M., Ihrig, P., Lechner, J., Hurt, E. (2002) The mRNA export machinery requires the novel Sac3p-Thp1p complex to dock at the nucleoplasmic entrance of the nuclear pores. *The EMBO journal* 21, 5843-5852.

Fischl, H., Howe, F. S., Furger, A., Mellor, J. (2017) Paf1 Has Distinct Roles in Transcription Elongation and Differential Transcript Fate. *Mol Cell* 65, 685-698.e688.

Flach, J., Bossie, M., Vogel, J., Corbett, A., Jinks, T., Willins, D. A., Silver, P. A. (1994) A yeast RNA-binding protein shuttles between the nucleus and the cytoplasm. *Molecular and cellular biology* 14, 8399-8407.

Gallardo, M., Luna, R., Erdjument-Bromage, H., Tempst, P., Aguilera, A. (2003) Nab2p and the Thp1p-Sac3p complex functionally interact at the interface between transcription and mRNA metabolism. *The Journal of biological chemistry* 278, 24225-24232.

Geisberg, J. V., Moqtaderi, Z., Fan, X., Ozsolak, F., Struhl, K. (2014) Global analysis of mRNA isoform half-lives reveals stabilizing and destabilizing elements in yeast. *Cell* 156, 812-824.

Germain, H. *et al.* (2010) MOS11: a new component in the mRNA export pathway. *PLoS genetics* 6, e1001250-e1001250.

Ghosh, A., Shuman, S., Lima, C. D. (2008) The structure of Fcp1, an essential RNA polymerase II CTD phosphatase. *Mol Cell* 32, 478-490.

Ghosh, A., Shuman, S., Lima, Christopher D. (2011) Structural Insights to How Mammalian Capping Enzyme Reads the CTD Code. *Molecular Cell* 43, 299-310.

Gibson, D. G., Young, L., Chuang, R. Y., Venter, J. C., Hutchison, C. A., 3rd, Smith, H. O. (2009) Enzymatic assembly of DNA molecules up to several hundred kilobases. *Nature methods* 6, 343-345.

Gilbert, W., Siebel, C. W., Guthrie, C. (2001) Phosphorylation by Sky1p promotes Npl3p shuttling and mRNA dissociation. *RNA (New York, N.Y.)* 7, 302-313.

Glover-Cutter, K., Kim, S., Espinosa, J., Bentley, D. L. (2008) RNA polymerase II pauses and associates with pre-mRNA processing factors at both ends of genes. *Nature structural & molecular biology* 15, 71-78.

Glover-Cutter, K., Larochelle, S., Erickson, B., Zhang, C., Shokat, K., Fisher, R. P., Bentley, D. L. (2009) TFIIH-associated Cdk7 kinase functions in phosphorylation of C-terminal domain Ser7 residues, promoter-proximal pausing, and termination by RNA polymerase II. *Molecular and cellular biology* 29, 5455-5464.

Gómez-González, B., García-Rubio, M., Bermejo, R., Gaillard, H., Shirahige, K., Marín, A., Foiani, M., Aguilera, A. (2011) Genome-wide function of THO/TREX in active genes prevents R-loop-dependent replication obstacles. *The EMBO journal* 30, 3106-3119.

González-Aguilera, C., Tous, C., Gómez-González, B., Huertas, P., Luna, R., Aguilera, A. (2008) The THP1-SAC3-SUS1-CDC31 complex works in transcription elongation-mRNA export preventing RNA-mediated genome instability. *Molecular biology of the cell* 19, 4310-4318.

González, A., Larroy, C., Biosca, J. A., Ariño, J. (2008) Use of the TRP1 auxotrophic marker for gene disruption and phenotypic analysis in yeast: a note of warning. *FEMS Yeast Research* 8, 2-5.

Green, D. M., Marfatia, K. A., Crafton, E. B., Zhang, X., Cheng, X., Corbett, A. H. (2002) Nab2p is required for poly(A) RNA export in Saccharomyces cerevisiae and is regulated by arginine methylation via Hmt1p. *The Journal of biological chemistry* 277, 7752-7760.

Grohmann, D., Werner, F. (2011) Cycling through transcription with the RNA polymerase F/E (RPB4/7) complex: structure, function and evolution of archaeal RNA polymerase. *Res Microbiol* 162, 10-18.

Gromadzka, A. M., Steckelberg, A.-L., Singh, K. K., Hofmann, K., Gehring, N. H. (2016) A short conserved motif in ALYREF directs cap- and EJC-dependent assembly of export complexes on spliced mRNAs. *Nucleic acids research* 44, 2348-2361.

Grummt, I. (2003) Life on a planet of its own: regulation of RNA polymerase I transcription in the nucleolus. *Genes & development* 17, 1691-1702.

Grünberg, S., Warfield, L., Hahn, S. (2012) Architecture of the RNA polymerase II preinitiation complex and mechanism of ATP-dependent promoter opening. *Nature structural & molecular biology* 19, 788-796.

Guttman, M. *et al.* (2009) Chromatin signature reveals over a thousand highly conserved large non-coding RNAs in mammals. *Nature* 458, 223-227.

Gwizdek, C., Iglesias, N., Rodriguez, M. S., Ossareh-Nazari, B., Hobeika, M., Divita, G., Stutz, F., Dargemont, C. (2006) Ubiquitin-associated domain of Mex67 synchronizes recruitment of the mRNA export machinery with transcription. *Proc Natl Acad Sci U S A* 103, 16376-16381.
Häcker, S., Krebber, H. (2004) Differential export requirements for shuttling serine/arginine-type mRNA-binding proteins. *The Journal of biological chemistry* 279, 5049-5052.
Hackmann, A., Wu, H., Schneider, U.-M., Meyer, K., Jung, K., Krebber, H. (2014) Quality control of spliced mRNAs requires the shuttling SR proteins Gbp2 and Hrb1. *Nature Communications* 5, 3123.
Hall, T. M. (2005) Multiple modes of RNA recognition by zinc finger proteins. *Current opinion in structural biology* 15, 367-373.
Hantsche, M., Cramer, P. (2016) The Structural Basis of Transcription: 10 Years After the Nobel Prize in Chemistry. *Angewandte Chemie (International ed. in English)* 55, 15972-15981.
Hartzog, G. A., Wada, T., Handa, H., Winston, F. (1998) Evidence that Spt4, Spt5, and Spt6 control transcription elongation by RNA polymerase II in Saccharomyces cerevisiae. *Genes & development* 12, 357-369.
He, F., Jacobson, A. (2001) Upf1p, Nmd2p, and Upf3p regulate the decapping and exonucleolytic degradation of both nonsense-containing mRNAs and wild-type mRNAs. *Molecular and cellular biology* 21, 1515-1530.
Hector, R. E., Nykamp, K. R., Dheur, S., Anderson, J. T., Non, P. J., Urbinati, C. R., Wilson, S. M., Minvielle-Sebastia, L., Swanson, M. S. (2002) Dual requirement for yeast hnRNP Nab2p in mRNA poly(A) tail length control and nuclear export. *The EMBO journal* 21, 1800-1810.
Hobeika, M., Brockmann, C., Gruessing, F., Neuhaus, D., Divita, G., Stewart, M., Dargemont, C. (2009) Structural requirements for the ubiquitin-associated domain of the mRNA export factor Mex67 to bind its specific targets, the transcription elongation THO complex component Hpr1 and nucleoporin FXFG repeats. *The Journal of biological chemistry* 284, 17575-17583.
Hobeika, M., Brockmann, C., Iglesias, N., Gwizdek, C., Neuhaus, D., Stutz, F., Stewart, M., Divita, G., Dargemont, C. (2007) Coordination of Hpr1 and ubiquitin binding by the UBA domain of the mRNA export factor Mex67. *Molecular biology of the cell* 18, 2561-2568.
Hooks, K. B., Delneri, D., Griffiths-Jones, S. (2014) Intron Evolution in Saccharomycetaceae. *Genome Biology and Evolution* 6, 2543-2556.
Huertas, P., Aguilera, A. (2003) Cotranscriptionally formed DNA:RNA hybrids mediate transcription elongation impairment and transcription-associated recombination. *Mol Cell* 12, 711-721.
Hurt, E., Hannus, S., Schmelzl, B., Lau, D., Tollervey, D., Simos, G. (1999) A novel in vivo assay reveals inhibition of ribosomal nuclear export in ran-cycle and nucleoporin mutants. *The Journal of cell biology* 144, 389-401.
Hurt, E., Luo, M.-j., Röther, S., Reed, R., Sträßer, K. (2004) Cotranscriptional recruitment of the serine-arginine-rich (SR)-like proteins Gbp2 and Hrb1 to nascent mRNA via the TREX complex. *Proceedings of the National Academy of Sciences* 101, 1858.
Iglesias, N., Stutz, F. (2008) Regulation of mRNP dynamics along the export pathway. *FEBS letters* 582, 1987-1996.
Iglesias, N., Tutucci, E., Gwizdek, C., Vinciguerra, P., Von Dach, E., Corbett, A. H., Dargemont, C., Stutz, F. (2010) Ubiquitin-mediated mRNP dynamics and surveillance prior to budding yeast mRNA export. *Genes & development* 24, 1927-1938.
Jacobsen, J. O. B., Allen, M. D., Freund, S. M. V., Bycroft, M. (2016) High-resolution NMR structures of the domains of Saccharomyces cerevisiae Tho1. *Acta Crystallogr F Struct Biol Commun* 72, 500-506.
Jaehning, J. A. (2010) The Paf1 complex: platform or player in RNA polymerase II transcription? *Biochimica et biophysica acta* 1799, 379-388.
Jamai, A., Puglisi, A., Strubin, M. (2009) Histone Chaperone Spt16 Promotes Redeposition of the Original H3-H4 Histones Evicted by Elongating RNA Polymerase. *Molecular Cell* 35, 377-383.

Jimeno, S., Luna, R., García-Rubio, M., Aguilera, A. (2006) Tho1, a novel hnRNP, and Sub2 provide alternative pathways for mRNP biogenesis in yeast THO mutants. *Molecular and cellular biology* 26, 4387-4398.
Jimeno, S., Rondón, A. G., Luna, R., Aguilera, A. (2002) The yeast THO complex and mRNA export factors link RNA metabolism with transcription and genome instability. *The EMBO journal* 21, 3526-3535.
Johnson, S. A., Cubberley, G., Bentley, D. L. (2009) Cotranscriptional recruitment of the mRNA export factor Yra1 by direct interaction with the 3' end processing factor Pcf11. *Mol Cell* 33, 215-226.
Jones, J. C., Phatnani, H. P., Haystead, T. A., MacDonald, J. A., Alam, S. M., Greenleaf, A. L. (2004) C-terminal repeat domain kinase I phosphorylates Ser2 and Ser5 of RNA polymerase II C-terminal domain repeats. *The Journal of biological chemistry* 279, 24957-24964.
Kang, G. J. *et al.* (2020) SARNP, a participant in mRNA splicing and export, negatively regulates E-cadherin expression via interaction with pinin. *Journal of cellular physiology* 235, 1543-1555.
Kastner, B., Will, C. L., Stark, H., Lührmann, R. (2019) Structural Insights into Nuclear pre-mRNA Splicing in Higher Eukaryotes. *Cold Spring Harbor perspectives in biology* 11,
Katahira, J., Strässer, K., Podtelejnikov, A., Mann, M., Jung, J. U., Hurt, E. (1999) The Mex67p-mediated nuclear mRNA export pathway is conserved from yeast to human. *The EMBO journal* 18, 2593-2609.
Kelly, S. M., Corbett, A. H. (2009) Messenger RNA export from the nucleus: a series of molecular wardrobe changes. *Traffic (Copenhagen, Denmark)* 10, 1199-1208.
Keren, H., Lev-Maor, G., Ast, G. (2010) Alternative splicing and evolution: diversification, exon definition and function. *Nature reviews. Genetics* 11, 345-355.
Kim, M., Ahn, S. H., Krogan, N. J., Greenblatt, J. F., Buratowski, S. (2004) Transitions in RNA polymerase II elongation complexes at the 3' ends of genes. *The EMBO journal* 23, 354-364.
Kim, M., Suh, H., Cho, E. J., Buratowski, S. (2009) Phosphorylation of the yeast Rpb1 C-terminal domain at serines 2, 5, and 7. *The Journal of biological chemistry* 284, 26421-26426.
Kim, S. J. *et al.* (2018) Integrative structure and functional anatomy of a nuclear pore complex. *Nature* 555, 475-482.
Köhler, A., Hurt, E. (2007) Exporting RNA from the nucleus to the cytoplasm. *Nature reviews. Molecular cell biology* 8, 761-773.
Köhler, A., Pascual-García, P., Llopis, A., Zapater, M., Posas, F., Hurt, E., Rodríguez-Navarro, S. (2006) The mRNA export factor Sus1 is involved in Spt/Ada/Gcn5 acetyltransferase-mediated H2B deubiquitinylation through its interaction with Ubp8 and Sgf11. *Molecular biology of the cell* 17, 4228-4236.
Köhler, A., Schneider, M., Cabal, G. G., Nehrbass, U., Hurt, E. (2008) Yeast Ataxin-7 links histone deubiquitination with gene gating and mRNA export. *Nature cell biology* 10, 707-715.
Kornberg, R. D. (2005) Mediator and the mechanism of transcriptional activation. *Trends in biochemical sciences* 30, 235-239.
Kress, T. L., Krogan, N. J., Guthrie, C. (2008) A single SR-like protein, Npl3, promotes pre-mRNA splicing in budding yeast. *Mol Cell* 32, 727-734.
Krishnamurthy, S., He, X., Reyes-Reyes, M., Moore, C., Hampsey, M. (2004) Ssu72 Is an RNA polymerase II CTD phosphatase. *Mol Cell* 14, 387-394.
Krogan, N. J. *et al.* (2006) Global landscape of protein complexes in the yeast Saccharomyces cerevisiae. *Nature* 440, 637-643.
Krogan, N. J. *et al.* (2003) The Paf1 complex is required for histone H3 methylation by COMPASS and Dot1p: linking transcriptional elongation to histone methylation. *Mol Cell* 11, 721-729.
Krogan, N. J. *et al.* (2002) RNA polymerase II elongation factors of Saccharomyces cerevisiae: a targeted proteomics approach. *Molecular and cellular biology* 22, 6979-6992.
Kuehner, J. N., Pearson, E. L., Moore, C. (2011) Unravelling the means to an end: RNA polymerase II transcription termination. *Nature reviews. Molecular cell biology* 12, 283-294.

Kulak, N. A., Pichler, G., Paron, I., Nagaraj, N., Mann, M. (2014) Minimal, encapsulated proteomic-sample processing applied to copy-number estimation in eukaryotic cells. *Nature methods* 11, 319-324.
Kyburz, A., Sadowski, M., Dichtl, B., Keller, W. (2003) The role of the yeast cleavage and polyadenylation factor subunit Ydh1p/Cft2p in pre-mRNA 3'-end formation. *Nucleic acids research* 31, 3936-3945.
Laemmli, U. K. (1970) Cleavage of Structural Proteins during the Assembly of the Head of Bacteriophage T4. *Nature* 227, 680-685.
Lee, D. C., Aitchison, J. D. (1999) Kap104p-mediated nuclear import. Nuclear localization signals in mRNA-binding proteins and the role of Ran and Rna. *The Journal of biological chemistry* 274, 29031-29037.
Lee, M. S., Henry, M., Silver, P. A. (1996) A protein that shuttles between the nucleus and the cytoplasm is an important mediator of RNA export. *Genes & development* 10, 1233-1246.
Lei, E. P., Krebber, H., Silver, P. A. (2001) Messenger RNAs are recruited for nuclear export during transcription. *Genes & development* 15, 1771-1782.
Liao, S. M., Zhang, J., Jeffery, D. A., Koleske, A. J., Thompson, C. M., Chao, D. M., Viljoen, M., van Vuuren, H. J., Young, R. A. (1995) A kinase-cyclin pair in the RNA polymerase II holoenzyme. *Nature* 374, 193-196.
Libri, D., Graziani, N., Saguez, C., Boulay, J. (2001) Multiple roles for the yeast SUB2/yUAP56 gene in splicing. *Genes & development* 15, 36-41.
Lidschreiber, M., Leike, K., Cramer, P. (2013) Cap completion and C-terminal repeat domain kinase recruitment underlie the initiation-elongation transition of RNA polymerase II. *Molecular and cellular biology* 33, 3805-3816.
Lindstrom, D. L., Squazzo, S. L., Muster, N., Burckin, T. A., Wachter, K. C., Emigh, C. A., McCleery, J. A., Yates, J. R., 3rd, Hartzog, G. A. (2003) Dual roles for Spt5 in pre-mRNA processing and transcription elongation revealed by identification of Spt5-associated proteins. *Molecular and cellular biology* 23, 1368-1378.
Liu, X., Bushnell, D. A., Wang, D., Calero, G., Kornberg, R. D. (2010) Structure of an RNA polymerase II-TFIIB complex and the transcription initiation mechanism. *Science (New York, N.Y.)* 327, 206-209.
Liu, Y., Warfield, L., Zhang, C., Luo, J., Allen, J., Lang, W. H., Ranish, J., Shokat, K. M., Hahn, S. (2009) Phosphorylation of the transcription elongation factor Spt5 by yeast Bur1 kinase stimulates recruitment of the PAF complex. *Molecular and cellular biology* 29, 4852-4863.
Livak, K. J., Schmittgen, T. D. (2001) Analysis of relative gene expression data using real-time quantitative PCR and the 2(-Delta Delta C(T)) Method. *Methods (San Diego, Calif.)* 25, 402-408.
Logan, J., Falck-Pedersen, E., Darnell, J. E., Jr., Shenk, T. (1987) A poly(A) addition site and a downstream termination region are required for efficient cessation of transcription by RNA polymerase II in the mouse beta maj-globin gene. *Proc Natl Acad Sci U S A* 84, 8306-8310.
López, M. C., Sánchez, M., Fermiñán, E., Domínguez, A. (1998) Disruption of six Saccharomyces cerevisiae genes from chromosome IV and basic phenotypic analysis of deletion mutants. *Yeast (Chichester, England)* 14, 1199-1208.
Lunde, B. M. *et al.* (2010) Cooperative interaction of transcription termination factors with the RNA polymerase II C-terminal domain. *Nature structural & molecular biology* 17, 1195-1201.
Lykke-Andersen, S., Jensen, T. H. (2007) Overlapping pathways dictate termination of RNA polymerase II transcription. *Biochimie* 89, 1177-1182.
Malik, S., Roeder, R. G. (2010) The metazoan Mediator co-activator complex as an integrative hub for transcriptional regulation. *Nature reviews. Genetics* 11, 761-772.
Malone, E. A., Fassler, J. S., Winston, F. (1993) Molecular and genetic characterization of SPT4, a gene important for transcription initiation in Saccharomyces cerevisiae. *Molecular & general genetics : MGG* 237, 449-459.
Mandel, C. R., Bai, Y., Tong, L. (2008) Protein factors in pre-mRNA 3'-end processing. *Cellular and molecular life sciences : CMLS* 65, 1099-1122.

Mani, R., St Onge, R. P., Hartman, J. L. t., Giaever, G., Roth, F. P. (2008) Defining genetic interaction. *Proc Natl Acad Sci U S A* 105, 3461-3466.
Mao, X., Schwer, B., Shuman, S. (1995) Yeast mRNA cap methyltransferase is a 50-kilodalton protein encoded by an essential gene. *Molecular and cellular biology* 15, 4167-4174.
Marfatia, K. A., Crafton, E. B., Green, D. M., Corbett, A. H. (2003) Domain analysis of the Saccharomyces cerevisiae heterogeneous nuclear ribonucleoprotein, Nab2p. Dissecting the requirements for Nab2p-facilitated poly(A) RNA export. *The Journal of biological chemistry* 278, 6731-6740.
Maris, C., Dominguez, C., Allain, F. H. (2005) The RNA recognition motif, a plastic RNA-binding platform to regulate post-transcriptional gene expression. *The FEBS journal* 272, 2118-2131.
Martinez-Rucobo, F. W., Cramer, P. (2013) Structural basis of transcription elongation. *Biochimica et biophysica acta* 1829, 9-19.
Martinez-Rucobo, F. W., Kohler, R., van de Waterbeemd, M., Heck, A. J., Hemann, M., Herzog, F., Stark, H., Cramer, P. (2015) Molecular Basis of Transcription-Coupled Pre-mRNA Capping. *Mol Cell* 58, 1079-1089.
Martinez-Rucobo, F. W., Sainsbury, S., Cheung, A. C., Cramer, P. (2011) Architecture of the RNA polymerase-Spt4/5 complex and basis of universal transcription processivity. *The EMBO journal* 30, 1302-1310.
Masuda, S., Das, R., Cheng, H., Hurt, E., Dorman, N., Reed, R. (2005) Recruitment of the human TREX complex to mRNA during splicing. *Genes & development* 19, 1512-1517.
Matheson, K., Parsons, L., Gammie, A. (2017) Whole-Genome Sequence and Variant Analysis of W303, a Widely-Used Strain of Saccharomyces cerevisiae. *G3 (Bethesda)* 7, 2219-2226.
Mayer, A., Lidschreiber, M., Siebert, M., Leike, K., Söding, J., Cramer, P. (2010) Uniform transitions of the general RNA polymerase II transcription complex. *Nature structural & molecular biology* 17, 1272-1278.
Mayer, A., Schreieck, A., Lidschreiber, M., Leike, K., Martin, D. E., Cramer, P. (2012) The spt5 C-terminal region recruits yeast 3' RNA cleavage factor I. *Molecular and cellular biology* 32, 1321-1331.
Mbogning, J., Nagy, S., Pagé, V., Schwer, B., Shuman, S., Fisher, R. P., Tanny, J. C. (2013) The PAF complex and Prf1/Rtf1 delineate distinct Cdk9-dependent pathways regulating transcription elongation in fission yeast. *PLoS genetics* 9, e1004029-e1004029.
McCracken, S. *et al.* (1997) 5'-Capping enzymes are targeted to pre-mRNA by binding to the phosphorylated carboxy-terminal domain of RNA polymerase II. *Genes & development* 11, 3306-3318.
Meinel, D. M. (2013) Genome wide recruitment of TREX reveals a direct interaction with the Rpb1 CTD. Dissertation, LMU München, Fakultät für Chemie und Pharmazie
Meinel, D. M. *et al.* (2013) Recruitment of TREX to the transcription machinery by its direct binding to the phospho-CTD of RNA polymerase II. *PLoS genetics* 9, e1003914.
Meinel, D. M., Sträßer, K. (2015) Co-transcriptional mRNP formation is coordinated within a molecular mRNP packaging station in S. cerevisiae. *BioEssays : news and reviews in molecular, cellular and developmental biology* 37, 666-677.
Mischo, H. E., Proudfoot, N. J. (2013) Disengaging polymerase: terminating RNA polymerase II transcription in budding yeast. *Biochimica et biophysica acta* 1829, 174-185.
Moehle, E. A., Ryan, C. J., Krogan, N. J., Kress, T. L., Guthrie, C. (2012) The yeast SR-like protein Npl3 links chromatin modification to mRNA processing. *PLoS genetics* 8, e1003101.
Moore, M. J. (2005) From birth to death: the complex lives of eukaryotic mRNAs. *Science (New York, N.Y.)* 309, 1514-1518.
Morris, D. P., Greenleaf, A. L. (2000) The splicing factor, Prp40, binds the phosphorylated carboxyl-terminal domain of RNA polymerase II. *The Journal of biological chemistry* 275, 39935-39943.
Mosimann, C., Hausmann, G., Basler, K. (2006) Parafibromin/Hyrax activates Wnt/Wg target gene transcription by direct association with beta-catenin/Armadillo. *Cell* 125, 327-341.

Mosley, A. L., Pattenden, S. G., Carey, M., Venkatesh, S., Gilmore, J. M., Florens, L., Workman, J. L., Washburn, M. P. (2009) Rtr1 is a CTD phosphatase that regulates RNA polymerase II during the transition from serine 5 to serine 2 phosphorylation. *Mol Cell* 34, 168-178.

Mueller, C. L., Jaehning, J. A. (2002) Ctr9, Rtf1, and Leo1 are components of the Paf1/RNA polymerase II complex. *Molecular and cellular biology* 22, 1971-1980.

Mueller, C. L., Porter, S. E., Hoffman, M. G., Jaehning, J. A. (2004) The Paf1 complex has functions independent of actively transcribing RNA polymerase II. *Mol Cell* 14, 447-456.

Mühlbacher, W., Sainsbury, S., Hemann, M., Hantsche, M., Neyer, S., Herzog, F., Cramer, P. (2014) Conserved architecture of the core RNA polymerase II initiation complex. *Nature Communications* 5, 4310.

Nedea, E. *et al.* (2003) Organization and function of APT, a subcomplex of the yeast cleavage and polyadenylation factor involved in the formation of mRNA and small nucleolar RNA 3'-ends. *The Journal of biological chemistry* 278, 33000-33010.

Ng, H. H., Robert, F., Young, R. A., Struhl, K. (2003) Targeted recruitment of Set1 histone methylase by elongating Pol II provides a localized mark and memory of recent transcriptional activity. *Mol Cell* 11, 709-719.

Nilsen, T. W., Graveley, B. R. (2010) Expansion of the eukaryotic proteome by alternative splicing. *Nature* 463, 457-463.

Noble, C. G., Hollingworth, D., Martin, S. R., Ennis-Adeniran, V., Smerdon, S. J., Kelly, G., Taylor, I. A., Ramos, A. (2005) Key features of the interaction between Pcf11 CID and RNA polymerase II CTD. *Nature structural & molecular biology* 12, 144-151.

Nojima, T., Hirose, T., Kimura, H., Hagiwara, M. (2007) The interaction between cap-binding complex and RNA export factor is required for intronless mRNA export. *The Journal of biological chemistry* 282, 15645-15651.

Orphanides, G., Wu, W. H., Lane, W. S., Hampsey, M., Reinberg, D. (1999) The chromatin-specific transcription elongation factor FACT comprises human SPT16 and SSRP1 proteins. *Nature* 400, 284-288.

Ozdilek, B. A., Thompson, V. F., Ahmed, N. S., White, C. I., Batey, R. T., Schwartz, J. C. (2017) Intrinsically disordered RGG/RG domains mediate degenerate specificity in RNA binding. *Nucleic acids research* 45, 7984-7996.

Pascual-García, P., Govind, C. K., Queralt, E., Cuenca-Bono, B., Llopis, A., Chavez, S., Hinnebusch, A. G., Rodríguez-Navarro, S. (2008) Sus1 is recruited to coding regions and functions during transcription elongation in association with SAGA and TREX2. *Genes & development* 22, 2811-2822.

Pei, Y., Shuman, S. (2002) Interactions between fission yeast mRNA capping enzymes and elongation factor Spt5. *The Journal of biological chemistry* 277, 19639-19648.

Pemberton, L. F., Rosenblum, J. S., Blobel, G. (1997) A distinct and parallel pathway for the nuclear import of an mRNA-binding protein. *The Journal of cell biology* 139, 1645-1653.

Penheiter, K. L., Washburn, T. M., Porter, S. E., Hoffman, M. G., Jaehning, J. A. (2005) A posttranscriptional role for the yeast Paf1-RNA polymerase II complex is revealed by identification of primary targets. *Mol Cell* 20, 213-223.

Pérez-Martínez, L., Öztürk, M., Butter, F., Luke, B. (2020) Npl3 stabilizes R-loops at telomeres to prevent accelerated replicative senescence. *EMBO Rep* 21, e49087-e49087.

Piruat, J. I., Aguilera, A. (1998) A novel yeast gene, THO2, is involved in RNA pol II transcription and provides new evidence for transcriptional elongation-associated recombination. *The EMBO journal* 17, 4859-4872.

Ponting, C. P. (2002) Novel domains and orthologues of eukaryotic transcription elongation factors. *Nucleic acids research* 30, 3643-3652.

Proudfoot, N. J. (1989) How RNA polymerase II terminates transcription in higher eukaryotes. *Trends in biochemical sciences* 14, 105-110.

Proudfoot, N. J. (2016) Transcriptional termination in mammals: Stopping the RNA polymerase II juggernaut. *Science (New York, N.Y.)* 352, aad9926.

Puig, O., Caspary, F., Rigaut, G., Rutz, B., Bouveret, E., Bragado-Nilsson, E., Wilm, M., Séraphin, B. (2001) The tandem affinity purification (TAP) method: a general procedure of protein complex purification. *Methods (San Diego, Calif.)* 24, 218-229.

Qiu, H., Hu, C., Gaur, N. A., Hinnebusch, A. G. (2012) Pol II CTD kinases Bur1 and Kin28 promote Spt5 CTR-independent recruitment of Paf1 complex. *The EMBO journal* 31, 3494-3505.

Qiu, H., Hu, C., Hinnebusch, A. G. (2009) Phosphorylation of the Pol II CTD by KIN28 enhances BUR1/BUR2 recruitment and Ser2 CTD phosphorylation near promoters. *Mol Cell* 33, 752-762.

Ralser, M., Kuhl, H., Ralser, M., Werber, M., Lehrach, H., Breitenbach, M., Timmermann, B. (2012) The Saccharomyces cerevisiae W303-K6001 cross-platform genome sequence: insights into ancestry and physiology of a laboratory mutt. *Open biology* 2, 120093.

Rigaut, G., Shevchenko, A., Rutz, B., Wilm, M., Mann, M., Séraphin, B. (1999) A generic protein purification method for protein complex characterization and proteome exploration. *Nature biotechnology* 17, 1030-1032.

Riordan, D. P., Herschlag, D., Brown, P. O. (2011) Identification of RNA recognition elements in the Saccharomyces cerevisiae transcriptome. *Nucleic acids research* 39, 1501-1509.

Rodríguez-Navarro, S., Fischer, T., Luo, M. J., Antúnez, O., Brettschneider, S., Lechner, J., Pérez-Ortín, J. E., Reed, R., Hurt, E. (2004) Sus1, a functional component of the SAGA histone acetylase complex and the nuclear pore-associated mRNA export machinery. *Cell* 116, 75-86.

Rodriguez, C. R., Cho, E. J., Keogh, M. C., Moore, C. L., Greenleaf, A. L., Buratowski, S. (2000) Kin28, the TFIIH-associated carboxy-terminal domain kinase, facilitates the recruitment of mRNA processing machinery to RNA polymerase II. *Molecular and cellular biology* 20, 104-112.

Rodriguez, C. R., Takagi, T., Cho, E. J., Buratowski, S. (1999) A Saccharomyces cerevisiae RNA 5'-triphosphatase related to mRNA capping enzyme. *Nucleic acids research* 27, 2181-2188.

Rogowska-Wrzesinska, A., Larsen, P. M., Blomberg, A., Görg, A., Roepstorff, P., Norbeck, J., Fey, S. J. (2001) Comparison of the proteomes of three yeast wild type strains: CEN.PK2, FY1679 and W303. *Comparative and functional genomics* 2, 207-225.

Rondón, A. G., Gallardo, M., García-Rubio, M., Aguilera, A. (2004) Molecular evidence indicating that the yeast PAF complex is required for transcription elongation. *EMBO Rep* 5, 47-53.

Rougemaille, M., Villa, T., Gudipati, R. K., Libri, D. (2008) mRNA journey to the cytoplasm: attire required. *Biology of the cell* 100, 327-342.

Russell, J., Zomerdijk, J. C. (2005) RNA-polymerase-I-directed rDNA transcription, life and works. *Trends in biochemical sciences* 30, 87-96.

Saguez, C., Schmid, M., Olesen, J. R., Ghazy, M. A. E.-H., Qu, X., Poulsen, M. B., Nasser, T., Moore, C., Jensen, T. H. (2008) Nuclear mRNA Surveillance in THO/sub2 Mutants Is Triggered by Inefficient Polyadenylation. *Molecular Cell* 31, 91-103.

Sakharkar, M. K., Chow, V. T., Chaturvedi, I., Mathura, V. S., Shapshak, P., Kangueane, P. (2004) A report on single exon genes (SEG) in eukaryotes. *Frontiers in bioscience : a journal and virtual library* 9, 3262-3267.

Sambrook, J. F., Russell, D., *Molecular Cloning: A Laboratory Manual (3-Volume Set)*. (2001), vol. 1.

Santos-Pereira, J. M., Herrero, A. B., Garcia-Rubio, M. L., Marin, A., Moreno, S., Aguilera, A. (2013) The Npl3 hnRNP prevents R-loop-mediated transcription-replication conflicts and genome instability. *Genes & development* 27, 2445-2458.

Schumann, S., Baquero-Perez, B., Whitehouse, A. (2016) Interactions between KSHV ORF57 and the novel human TREX proteins, CHTOP and CIP29. *The Journal of general virology* 97, 1904-1910.

Schwalb, B., Michel, M., Zacher, B., Frühauf, K., Demel, C., Tresch, A., Gagneur, J., Cramer, P. (2016) TT-seq maps the human transient transcriptome. *Science (New York, N.Y.)* 352, 1225.

Semlow, D. R., Blanco, M. R., Walter, N. G., Staley, J. P. (2016) Spliceosomal DEAH-Box ATPases Remodel Pre-mRNA to Activate Alternative Splice Sites. *Cell* 164, 985-998.

Sen, R., Barman, P., Kaja, A., Ferdoush, J., Lahudkar, S., Roy, A., Bhaumik, S. R. (2019) Distinct Functions of the Cap-Binding Complex in Stimulation of Nuclear mRNA Export. *Molecular and cellular biology* 39,

Senger, B., Simos, G., Bischoff, F. R., Podtelejnikov, A., Mann, M., Hurt, E. (1998) Mtr10p functions as a nuclear import receptor for the mRNA-binding protein Npl3p. *The EMBO journal* 17, 2196-2207.

Sheldon, K. E., Mauger, D. M., Arndt, K. M. (2005) A Requirement for the Saccharomyces cerevisiae Paf1 complex in snoRNA 3' end formation. *Mol Cell* 20, 225-236.

Shen, E. C., Stage-Zimmermann, T., Chui, P., Silver, P. A. (2000) 7The yeast mRNA-binding protein Npl3p interacts with the cap-binding complex. *The Journal of biological chemistry* 275, 23718-23724.

Shi, M., Zhang, H., Wu, X., He, Z., Wang, L., Yin, S., Tian, B., Li, G., Cheng, H. (2017) ALYREF mainly binds to the 5' and the 3' regions of the mRNA in vivo. *Nucleic acids research* 45, 9640-9653.

Shi, X., Finkelstein, A., Wolf, A. J., Wade, P. A., Burton, Z. F., Jaehning, J. A. (1996) Paf1p, an RNA polymerase II-associated factor in Saccharomyces cerevisiae, may have both positive and negative roles in transcription. *Molecular and cellular biology* 16, 669-676.

Shibagaki, Y., Itoh, N., Yamada, H., Nagata, S., Mizumoto, K. (1992) mRNA capping enzyme. Isolation and characterization of the gene encoding mRNA guanylytransferase subunit from Saccharomyces cerevisiae. *Journal of Biological Chemistry* 267, 9521-9528.

Shuman, S. (2001) Structure, mechanism, and evolution of the mRNA capping apparatus. *Progress in nucleic acid research and molecular biology* 66, 1-40.

Simic, R., Lindstrom, D. L., Tran, H. G., Roinick, K. L., Costa, P. J., Johnson, A. D., Hartzog, G. A., Arndt, K. M. (2003) Chromatin remodeling protein Chd1 interacts with transcription elongation factors and localizes to transcribed genes. *The EMBO journal* 22, 1846-1856.

Sørensen, B. B. *et al.* (2017) The Arabidopsis THO/TREX component TEX1 functionally interacts with MOS11 and modulates mRNA export and alternative splicing events. *Plant molecular biology* 93, 283-298.

Soucek, S., Corbett, A. H., Fasken, M. B. (2012) The long and the short of it: the role of the zinc finger polyadenosine RNA binding protein, Nab2, in control of poly(A) tail length. *Biochimica et biophysica acta* 1819, 546-554.

Squazzo, S. L., Costa, P. J., Lindstrom, D. L., Kumer, K. E., Simic, R., Jennings, J. L., Link, A. J., Arndt, K. M., Hartzog, G. A. (2002) The Paf1 complex physically and functionally associates with transcription elongation factors in vivo. *The EMBO journal* 21, 1764-1774.

Steinmetz, E. J., Brow, D. A. (2003) Ssu72 protein mediates both poly(A)-coupled and poly(A)-independent termination of RNA polymerase II transcription. *Molecular and cellular biology* 23, 6339-6349.

Stewart, M. (2019) Polyadenylation and nuclear export of mRNAs. *The Journal of biological chemistry* 294, 2977-2987.

Strässer, K., Bassler, J., Hurt, E. (2000) Binding of the Mex67p/Mtr2p heterodimer to FXFG, GLFG, and FG repeat nucleoporins is essential for nuclear mRNA export. *The Journal of cell biology* 150, 695-706.

Strässer, K., Hurt, E. (2000) Yra1p, a conserved nuclear RNA-binding protein, interacts directly with Mex67p and is required for mRNA export. *The EMBO journal* 19, 410-420.

Strässer, K., Hurt, E. (2001) Splicing factor Sub2p is required for nuclear mRNA export through its interaction with Yra1p. *Nature* 413, 648-652.

Strässer, K. *et al.* (2002) TREX is a conserved complex coupling transcription with messenger RNA export. *Nature* 417, 304-308.

Sugiura, T., Sakurai, K., Nagano, Y. (2007) Intracellular characterization of DDX39, a novel growth-associated RNA helicase. *Experimental cell research* 313, 782-790.

Swanson, M. S., Malone, E. A., Winston, F. (1991) SPT5, an essential gene important for normal transcription in Saccharomyces cerevisiae, encodes an acidic nuclear protein with a carboxy-terminal repeat. *Molecular and cellular biology* 11, 3009-3019.

Sydow, J. F., Brueckner, F., Cheung, A. C., Damsma, G. E., Dengl, S., Lehmann, E., Vassylyev, D., Cramer, P. (2009) Structural basis of transcription: mismatch-specific fidelity mechanisms and paused RNA polymerase II with frayed RNA. *Mol Cell* 34, 710-721.

Takagaki, Y., Manley, J. L. (2000) Complex protein interactions within the human polyadenylation machinery identify a novel component. *Molecular and cellular biology* 20, 1515-1525.

Tardiff, D. F., Abruzzi, K. C., Rosbash, M. (2007) Protein characterization of Saccharomyces cerevisiae RNA polymerase II after in vivo cross-linking. *Proceedings of the National Academy of Sciences* 104, 19948.

Taylor, R. G., Walker, D. C., McInnes, R. R. (1993) E. coli host strains significantly affect the quality of small scale plasmid DNA preparations used for sequencing. *Nucleic acids research* 21, 1677-1678.

Thomas, B. J., Rothstein, R. (1989) Elevated recombination rates in transcriptionally active DNA. *Cell* 56, 619-630.

Tietjen, J. R. *et al.* (2010) Chemical-genomic dissection of the CTD code. *Nature structural & molecular biology* 17, 1154-1161.

Topisirovic, I., Svitkin, Y. V., Sonenberg, N., Shatkin, A. J. (2011) Cap and cap-binding proteins in the control of gene expression. *Wiley interdisciplinary reviews. RNA* 2, 277-298.

Tran, E. J., Zhou, Y., Corbett, A. H., Wente, S. R. (2007) The DEAD-box protein Dbp5 controls mRNA export by triggering specific RNA:protein remodeling events. *Mol Cell* 28, 850-859.

Tsukamoto, T., Shibagaki, Y., Imajoh-Ohmi, S., Murakoshi, T., Suzuki, M., Nakamura, A., Gotoh, H., Mizumoto, K. (1997) Isolation and characterization of the yeast mRNA capping enzyme beta subunit gene encoding RNA 5'-triphosphatase, which is essential for cell viability. *Biochemical and biophysical research communications* 239, 116-122.

Tuck, A. C., Tollervey, D. (2013) A transcriptome-wide atlas of RNP composition reveals diverse classes of mRNAs and lncRNAs. *Cell* 154, 996-1009.

Valverde, R., Edwards, L., Regan, L. (2008) Structure and function of KH domains. *The FEBS journal* 275, 2712-2726.

Vinciguerra, P., Iglesias, N., Camblong, J., Zenklusen, D., Stutz, F. (2005) Perinuclear Mlp proteins downregulate gene expression in response to a defect in mRNA export. *The EMBO journal* 24, 813-823.

Vitaliano-Prunier, A., Babour, A., Hérissant, L., Apponi, L., Margaritis, T., Holstege, F. C., Corbett, A. H., Gwizdek, C., Dargemont, C. (2012) H2B ubiquitylation controls the formation of export-competent mRNP. *Mol Cell* 45, 132-139.

Wahle, E. (1995) Poly(A) tail length control is caused by termination of processive synthesis. *The Journal of biological chemistry* 270, 2800-2808.

Wahle, E., Rüegsegger, U. (1999) 3'-End processing of pre-mRNA in eukaryotes. *FEMS microbiology reviews* 23, 277-295.

Wang, D., Bushnell, D. A., Westover, K. D., Kaplan, C. D., Kornberg, R. D. (2006) Structural basis of transcription: role of the trigger loop in substrate specificity and catalysis. *Cell* 127, 941-954.

Wen, Y., Shatkin, A. J. (1999) Transcription elongation factor hSPT5 stimulates mRNA capping. *Genes & development* 13, 1774-1779.

Wier, A. D., Mayekar, M. K., Héroux, A., Arndt, K. M., VanDemark, A. P. (2013) Structural basis for Spt5-mediated recruitment of the Paf1 complex to chromatin. *Proceedings of the National Academy of Sciences* 110, 17290.

Will, C. L., Lührmann, R. (2011) Spliceosome structure and function. *Cold Spring Harbor perspectives in biology* 3, (7):a003707.

Wilmes, G. M. *et al.* (2008) A genetic interaction map of RNA-processing factors reveals links between Sem1/Dss1-containing complexes and mRNA export and splicing. *Mol Cell* 32, 735-746.

Wong, C., Sridhara, S., Bardwell, J. C., Jakob, U. (2000) Heating greatly speeds Coomassie blue staining and destaining. *BioTechniques* 28, 426-428, 430, 432.
Wood, A., Schneider, J., Dover, J., Johnston, M., Shilatifard, A. (2003) The Paf1 complex is essential for histone monoubiquitination by the Rad6-Bre1 complex, which signals for histone methylation by COMPASS and Dot1p. *The Journal of biological chemistry* 278, 34739-34742.
Wood, W. B. (1966) Host specificity of DNA produced by Escherichia coli: bacterial mutations affecting the restriction and modification of DNA. *Journal of molecular biology* 16, 118-133.
Workman, J. L. (2006) Nucleosome displacement in transcription. *Genes & development* 20, 2009-2017.
Wyers, F. *et al.* (2005) Cryptic pol II transcripts are degraded by a nuclear quality control pathway involving a new poly(A) polymerase. *Cell* 121, 725-737.
Xiao, T., Kao, C. F., Krogan, N. J., Sun, Z. W., Greenblatt, J. F., Osley, M. A., Strahl, B. D. (2005) Histone H2B ubiquitylation is associated with elongating RNA polymerase II. *Molecular and cellular biology* 25, 637-651.
Xu, Y., Bernecky, C., Lee, C.-T., Maier, K. C., Schwalb, B., Tegunov, D., Plitzko, J. M., Urlaub, H., Cramer, P. (2017) Architecture of the RNA polymerase II-Paf1C-TFIIS transcription elongation complex. *Nature Communications* 8, 15741.
Yamada, T., Yamaguchi, Y., Inukai, N., Okamoto, S., Mura, T., Handa, H. (2006) P-TEFb-Mediated Phosphorylation of hSpt5 C-Terminal Repeats Is Critical for Processive Transcription Elongation. *Molecular Cell* 21, 227-237.
Yao, W., Roser, D., Köhler, A., Bradatsch, B., Bassler, J., Hurt, E. (2007) Nuclear export of ribosomal 60S subunits by the general mRNA export receptor Mex67-Mtr2. *Mol Cell* 26, 51-62.
Youdell, M. L., Kizer, K. O., Kisseleva-Romanova, E., Fuchs, S. M., Duro, E., Strahl, B. D., Mellor, J. (2008) Roles for Ctk1 and Spt6 in regulating the different methylation states of histone H3 lysine 36. *Molecular and cellular biology* 28, 4915-4926.
Zander, G., Hackmann, A., Bender, L., Becker, D., Lingner, T., Salinas, G., Krebber, H. (2016) mRNA quality control is bypassed for immediate export of stress-responsive transcripts. *Nature* 540, 593-596.
Zarnack, K., Balasubramanian, S., Gantier, M. P., Kunetsky, V., Kracht, M., Schmitz, M. L., Sträßer, K. (2020) Dynamic mRNP Remodeling in Response to Internal and External Stimuli. *Biomolecules* 10,
Zenkin, N., Yuzenkova, Y., Severinov, K. (2006) Transcript-assisted transcriptional proofreading. *Science (New York, N.Y.)* 313, 518-520.
Zhang, D. W., Rodríguez-Molina, J. B., Tietjen, J. R., Nemec, C. M., Ansari, A. Z. (2012) Emerging Views on the CTD Code. *Genet Res Int* 2012, 347214.
Zhang, Z., Fu, J., Gilmour, D. S. (2005) CTD-dependent dismantling of the RNA polymerase II elongation complex by the pre-mRNA 3'-end processing factor, Pcf11. *Genes & development* 19, 1572-1580.
Zhou, K., Kuo, W. H., Fillingham, J., Greenblatt, J. F. (2009) Control of transcriptional elongation and cotranscriptional histone modification by the yeast BUR kinase substrate Spt5. *Proc Natl Acad Sci U S A* 106, 6956-6961.
Zhu, B., Mandal, S. S., Pham, A. D., Zheng, Y., Erdjument-Bromage, H., Batra, S. K., Tempst, P., Reinberg, D. (2005) The human PAF complex coordinates transcription with events downstream of RNA synthesis. *Genes & development* 19, 1668-1673.

9 List of figures

10 List of tables

11 Abbreviations

Table 20: Abbreviations

Abbreviation	Description
AA	Amino acid
bp	Base pair
CBP	Calmodulin binding protein
CBC	cap-binding complex
ChIP	Chromatin immunoprecipitation
CPF	cleavage and polyadenylation factor
CF	cleavage factor
CT	Cycle threshold
CTD	carboxy-terminal domain of RNAPII
CTR	C-terminal region of Spt5
E. coli	*Escherichia coli*
EtOH	ethanol
FISH	Fluorescence *in situ* hybridization
FTpA	FLAG-TEV-prot A tag
GMP	Guanine monophosphate
GTP	Guanine triphosphate
HRP	Horseradisch peroxidase
KH	K homology
LB	lysogeny broth
M	Mol
MDa	Megadalton
miRNA	micro RNA
MPC	Magnetic particle collector
mRNA	messenger ribonucleic acid
mRNP	messenger ribonucleoprotein particle
m^7G	n7 methylated guanosine
NGN	NusG N-terminal
NPC	nuclear pore complex
NTP	Nucleoside triphosphate
NTR	Non-transcribed region
Nup	nucleoporin
OE	overexpression
PAB	poly(A)-binding protein
PCR	polymerase chain reaction
PIC	Pre-initiation complex
poly(A)	Poly-adenylation
RBP	RNA binding protein
RNAPII	RNA polymerase II
RNP	ribonucleoprotein
RRM	RNA recognition motif
rRNA	Ribosomal ribonucleic acid
RT	Room temperature
(RT)-qPCR	(Reverse transcription)- quantitative polymerase chain reaction
S	Serine
SS	splice site
S. cerevisiae	*Saccharomyces cerevisiae*
SDS-PAGE	sodium dodecyl sulfate polyacrylamide gel electrophoresis
snRNP	small nuclear RNP
snRNA	small nuclear RNA

snoRNA	Small nucleolar RNA
SR	serine-arginine
TAP	tandem affinity purification
TBST	tris-buffered saline tween
TEV	Tobacco etch virus
TF	Transcription factor
TREX	transcription and export
tRNA	transfer-RNA
TSS	Transcription start site
WB	Western blot
YPD	Yeast extract, peptone, dextrose
ZnF	zinc finger domain

12 Danksagung

Nun liegt diese Arbeit geschrieben vor mir und es ist Zeit einmal Danke an all die Menschen zu sagen, die mich dabei auf die verschiedensten Arten unterstützt haben.

Mein erster Dank gilt Prof. Dr. Katja Sträßer für die Möglichkeit meine Arbeit in ihrem Labor unter ihrer Anleitung und Betreuung anfertigen zu dürfen. Während dieser vergangenen Zeit durfte ich nicht nur wissenschaftlich, sondern auch menschlich wachsen.

Prof. Dr. Albrecht Bindereif danke ich für die Übernahme des Zweitgutachters sowie den Denkanstößen, die ich während meiner Zeit im RTG bekommen habe.

Mein Dank gilt natürlich auch dem ganzen Labor! Zum einem Cornelia die meine Arbeit Korrektur gelesen hat und dabei noch so manch einen Fehler ausgemerzt hat. Peter danke ich für den technischen Support und Wolle der immer eine offene Tür für mich hatte. Egal ob mein PC gestreikt hat, ich Fragen zur Klonierung oder Proteinaufreinigung hatte oder ich Hilfe bei sonst einem Gerät brauchte. Bei Heike möchte ich mich für ihre Unterstützung im Labor bedanken, da sie besonders während meiner Schwangerschaft, so manch eine Aufgabe übernommen hat, die man dann besser nicht mehr durchführen sollte. Besonderer Dank gilt auch den Doktorranden die mich in dieser Zeit begleitet haben. Ich möchte mich bei euch für die tolle Zusammenarbeit und die konstruktiven Gespräche bedanken, dafür dass ihr mit mir die Höhen und die Tiefen durchgemacht habt, für so manch eine Spätschicht aber eben auch das ein oder andere Feierabendbier. Ihr alle wart ein Grund warum ich morgens gerne ins Labor gekommen bin.

Zum Schluss möchte ich mich bei meiner Familie bedanken, die mich immer dazu ermutigt hat meinen eigenen Weg zu gehen - insbesondere für die letzten Jahre, in denen sie mir Freiräume für diese Arbeit geschaffen hat. Mein besonderer Dank gilt Philipp und Rike. Rike du hast im letzten Jahr in vielen Momenten auch mal hintenanstehen müssen und kamst trotzdem am Ende des Tages mit einem riesen Lächeln auf mich zu. Philipp du hast mich sowohl privat als auch wissenschaftlich immer unterstützt und mir durch manch einen Tiefpunkt geholfen, indem du mir immer wieder neue Wege aufgezeigt hast und diese dann mit mir beschritten hast.

DANKE an ALLE für eure vielfältige Unterstützung!

13 Eidesstattliche Erklärung

Ich erkläre: Ich habe die vorgelegte Dissertation selbstständig und ohne unerlaubte fremde Hilfe und nur mit den Hilfen angefertigt, die ich in der Dissertation angegeben habe. Alle Textstellen, die wörtlich oder sinngemäß aus veröffentlichten Schriften entnommen sind, und alle Angaben, die auf mündlichen Auskünften beruhen, sind als solche kenntlich gemacht. Ich stimme einer evtl. Überprüfung meiner Dissertation durch eine Antiplagiat-Software zu. Bei den von mir durchgeführten und in der Dissertation erwähnten Untersuchungen habe ich die Grundsätze guter wissenschaftlicher Praxis, wie sie in der „Satzung der Justus-Liebig-Universität Gießen zur Sicherung guter wissenschaftlicher Praxis“ niedergelegt sind, eingehalten.

Gießen, den: ..... Unterschrift: .....

(Vorname, Nachname)